

DEVELOPMENT OF *EUCALPYTUS TERETICORNIS* COMPOSITE (BARKS AND LEAVES) ADSORBENT FOR ADSORPTION OF CHROMIUM (VI) AND LEAD (II) IONS FROM SIMULATED WASTEWATER

BY

ZIKRAH, ISMAIL AHUOIZA AMINU

DEPARTMENT OF CHEMICAL ENGINEERING
AHMADU BELLO UNIVERSITY,

ZARIA, NIGERIA

DECEMBER, 2016

DEVELOPMENT OF *EUCALPYTUS TERETICORNIS* COMPOSITE (BARKS AND LEAVES) ADSORBENT FOR ADSORPTION OF CHROMIUM (VI) AND LEAD (II) IONS FROM SIMULATED WASTEWATER

BY

Zikrah Ismail Ahuoiza AMINU, B.Eng (Fut) Minna, 2008
M.Sc/Eng/25147/2012-2013

A DISSERTATION SUBMITTED TO THE SCHOOL OF POSTGRADUATE STUDIES, AHMADU BELLO UNIVERSITY, ZARIA

IN PARTIAL FULFILLMENT OF THE REQUIREMENTS FOR THE AWARD

OF A

MASTER DEGREE IN CHEMICAL ENGINEERING

DEPARTMENT OF CHEMICAL ENGINEERING,
FACULTY OF ENGINEERING
AHMADU BELLO UNIVERSITY,
ZARIA, NIGERIA

DECEMBER, 2016

Declaration

I Zikrah, Ismail Ahuoiza Aminu hereby declare that the work in this dissertationentitled **Development of *Eucalpytus tereticornis* Composite (Barks and Leaves)Adsorbent for Adsorption of Chromium (VI) and Lead (II) Ions from Simulated Wastewater**has been carried out by me in the Department of Chemical Engineering, Ahmadu Bello University Zaria, Nigeria under the supervision of Dr. M.S. Galadima, Dr. M.T. Isa and Dr. A.O. Ameh of the Department of Chemical Engineering, Ahmadu Bello University, Zaria. The information derived from the literature has been duly acknowledged in the text and a list of reference provided. No part of this dissertation was previously presented for another degree or diploma at this or any other Institution.

Zikrah, Ismail Aminu. _____ _____

Signature Date

Certification

This Dissertation entitled **Development of *Eucalpytus tereticornis* Composite (Barks and Leaves)Adsorbent for Adsorption of Chromium (VI) and Lead (II) Ions from Simulated Wastewater**meets the regulations governing the award of the degree of Msc Chemical Engineering Ahmadu Bello University, and is approved for its contribution to knowledge and literary presentation.

Dr. M.S. Galadima _____ _____
Chairman, Supervisory Committee Signature Date

Dr. M.T. Isa _____ _____
Member, Supervisory Committee Signature Date

Dr. A.O. Ameh _____ _____
Member, Supervisory Committee Signature Date

Dr. S. M. Waziri _____ _____
Head, Department of Chemical Engineering, A.B.U Zaria Signature Date

Professor K. Bala _____ _____Dean,
School of Postgraduate Studies, A.B.U Zaria, Nigeria Signature Date

Dedication

This project work is dedicated to Al-mighty Allah; the creator of all creation.

Acknowledgement

All praise belong to Allah, Lord of the Worlds. Peace and blessing be on the most exalted messenger, our leader; Muhammad (S.A.W), his family and companions (sahabah).

Firstly, I would like to express my gratitude to my supervisors: Dr M.S. Galadima, Dr. M.T Isa and Dr.A.O Amehfor their advice, support, guidance and encouragement throughout the course of this work. This work would not have been possible without their supervision. I am very much indebted to them more than they know. God bless you all.

My heartfelt gratitude is very much extended to my beloved husband Engr. M.S Ismail for his valuable advice, prayer and financial support during the course of this research. It would have been difficult indeed to have made progress without his support.

Furthermore, my gratitude goes to my family: Mallam and Mallama Bello Aminu, my beautiful children: Majidah, Fadilah and Fawziya, my brother and his wife AminuYahya and nephew Mubarak Lawal. Thank you for your love, support, endurance and patience. I am truly blessed to have you as my family.

Special thanks to Petroleum Technology Development Fund (PTDF) Chair and Chemical Engineering Department, Department of Water Resource and Environmental Engineering, Department of Chemistry and Institute of Agricultural Research for providing research facilities. It is also a pleasure to convey my gratitude to Mr Ilu and Mallam Musa for laying a very good foundation for this work.

Many thanks go to my fellow postgraduate colleagues: AbdullahiBello,GbengaOseke,Katherine Adze and Sani Ismail for their support.

Finally, I would like to thank everybody who played a very important role towards the completion of this work, as well as expressing my apology that I could not mention all the names one by one.

Table of Contents

Cover Page	i
Title Page	ii
Declaration	iii
Certification	iv
Dedication	v
Acknowledgement	vi
Table of Contents	vii
List of Figures	xi
List of Tables	xiv
List of Plates	xvi
List of Appendices	xvii
Abbreviation	xvii
Abstract	xix
CHAPTER ONE	**1**
INTRODUCTION	1
1.1 Background of Study	1
1.2 Research Problem	3
1.3 Justification	3
1.4 Aim and Objectives	3

1.5 Research Scope 4

CHAPTER TWO 5

LITERATURE REVIEW 5

2.1 Heavy Metals and its Toxicities 5

2.2 Conventional Processes for Removal of Heavy Metal 7

2.2.1 Chemical precipitation 7

2.2.2 Ion exchange 8

2.2.3 Photocatalysis 8

2.2.4 Electrodialysis 8

2.2.5 Membrane filtration 9

2.2.6 Adsorption 9

2.3 Types of Adsorption 10

2.3.1 Physical adsorption 10

2.3.2 Chemical adsorption 10

2.4 Factors Affecting Adsorption Process 11

2.5 Adsorption Phenomenon 11

2.6 Adsorption with Non-Conventional Adsorbent 13

2.7 Chemically Modified Adsorbents 17

2.8 Response Surface Methodology (RSM) 20

2.9 Equilibrium Isotherm Models 23

2.9.1 Langmuir adsorption isotherm 24

2.9.2 Freundlich adsorption isotherms 26

2.9.3 Temkin adsorption isotherm 27

2.10 Kinetic Models of Adsorption 28

2.10.1 Pseudo-first order kinetics 28

2.10.2 Pseudo seconder kinetic model 29

2.10.3 Second order-kinetic model 29

2.10.4 Elovich kinetic model 30

CHAPTER THREE 31

MATERIALS AND METHODS 31

3.1 Materials 31

3.1.1 Chemicals and reagents 31

3.2 Methods 32

3.2.1 Sample collection and identification 32

3.2.2 Adsorbent preparation 33

3.2.3 Simulated wastewater preparation 34

3.2.4: Design of experiment of adsorption Cr (VI) and Pb (II) ions on *E. tereticornis* parts 34

3.2.5: Batch experimental procedure for adsorption of Cr (VI) and Pb (II) ions from simulated wastewater using *E.tereticornis* barks. 36

3.2.6: Batch experimental procedure for adsorption of Cr (VI) and Pb (II) ions from simulated wastewater using *E.tereticornis* leaves. 36

3.2.7: Batch experimental procedure for adsorption of Cr (VI) and Pb (II) from simulated wastewater using composite of *E.tereticornis* barks and leaves adsorbent 37

3.2.8: Adsorption isotherm studies and kinetics for composite of *E. tereticornis* barks and leaves adsorbent for Cr (VI) and Pb (II) ions adsorption 37

CHAPTER FOUR

RESULTS AND DISCUSSION 38

4.1:Preamble 38

4.2:Characterization of the Adsorbents 38

4.2.1:FTIR analysis of *Eucalyptus tereticornis* leaves 38

4.2.2:SEM Micrograph analysis *Eucalpytus tereticornis* parts 42

4.3:Comparative Studies for Chromium (VI) and Lead (II) Ions Adsorption using *Eucalyptus tereticornis* Composite of Barks and Leaves Adsorbents 74

4.4:Adsorption Isotherm and Kinetic Modeling 75

4.4.1:Adsorption isotherm 75

4.4.2:Kinetic Modeling 80

CHAPTER FIVE 84

CONCLUSION AND RECOMMENDATIONS 84

5.1:Conclusions 84

5.2:Recommendations 85

REFERENCES 86

APPENDICES 93

List of Figures

Figure 3.1: Block diagram methodology of *Eucalpytus tereticornis* composite (barks and leaves) adsorbents for chromium (VI) and lead (II) ions adsorption 32

Figure 3.2: Image of raw and grinded *Eucalpytus tereticornis* leaves adsorbent 33

Figure 3.3: Image of raw and grinded *Eucalpytus tereticornis* barks adsorbent 33

Figure 4.1: FTIR spectra of *Eucalyptus tereticornis* leaves before treatment with nitric acid 39

Figure 4.2: FTIR spectra of *Eucalyptus tereticornis* leaves after treatment with nitric acid 40

Figure 4.3: FTIR spectra of *Eucalpytus Tetreticornis* barks before treatement with nitric acid 41

Figure 4.4:FTIR spectra of *Eucalpytus tereticornis* barks after treatedwith nitric acid 42

Figure 4.5: Effect of contact time against adsorption capacity of chromium (VI) ions at room temperature (30^oC). 46

Figure 4.6: Effect of adsorbent dosage against adsorption capacity of chromium (VI) ion at constant room temperature (30^oC). 47

Figure 4.7: Effect of contact time against adsorption capacity of lead (II) ion at room temperature (30^oC). 49

Figure 4.8: Effect of adsorbent dose against adsorption capacity of lead (II) ion at room temperature (30^oC) 49

Figure 4.9: Parity plot of the actual and predicted value of chromium (VI) ion adsorption on *E. tereticornis* leaves adsorbent 52

Figure 4.10: Parity plot of actual and predicted value of lead (II) ion adsorption on *E. tereticornis* leaves adsorbent 52

Figure 4.11: 3D Response surface plot of chromium (VI) ion adsorption on *E.tererticornis* leaves 53

Figure 4.12: 3D Response surface plot of lead (II) ion adsorption *on E. tereticornis* leaves 54

Figure 4.13: Effect of contact time against adsorption capacity of chromium (VI) at room temperature. 56

Figure 4.14: Effects of adsorbent dose against adsorption capacity of chromium (VI) at room temperature 57

Figure 4.15: Effects of contact time against adsorption capacity of lead (II) ion at room temperature. 58

Figure 4.16: Effects of adsorbent dose against adsorption capacity of lead (II) ion at temperature 59

Figure: 4.17: Parity plot of the actual and predicted value of chromium (VI) ion adsorption on *E. tereticornis* barks (ETB) adsorbent. 61

Figure: 4.18: Parity plot of the actual and predicted value of lead (II) ion adsorption on *E.tereticornis* barks (ETB) adsorbent

62

Figure 4.19: 3D Response surface plots of chromium (VI) ion adsorption on *E. tereticornis* barks (ETB) adsorbent. 63

Figure 4.20: 3D Response surface plots of lead (II) ion adsorption on *E. tereticornis* barks (ETB) adsorbent 63

Figure 4.21: Effect of contact time against chromium (VI) ion adsorption on composite *Eucalyptus tereticornis* barks and leaves adsorbent 66

Figure: 4.22: Effect of formulation ratio against chromium (VI) ion adsorption on composite *Eucalyptus tereticornis* 67

Figure 4.23: Effect of contact time against lead adsorption on composite of *Eucalyptus tereticornis* barks and leaves adsorbent 69

Figure 4.24: Effect of contact time against lead adsorption on composite of *Eucalyptus tereticornis* barks and leaves adsorbent 70

Figure: 4.25: Parity plots of actual and predicted value of chromium (VI) ion adsorption on composite of *Eucalpytus tereticornis* barks and leaves adsorbent 72

Figure 4.26: Parity plots of the actual and predicted value of lead (II) ion adsorption on composite of *Eucalpytus tereticornis* barks and leaves adsorbent 72

Figure 4.27: 3D Response surface plot of chromium (VI) ion adsorption on composite of *Eucalpytus tereticornis* barks and leaves adsorbent 73

Figure 4.28: 3D Response surface plot of lead (II) ion adsorption on composite of *Eucalpytus tereticornis* barks and leaves adsorbent. 74

Figure 4.29: Chromium (VI) ion adsorption on *E.tereticornis* composite Langmuir plot 75

Figure 4.31: Chromium (VI) ion adsorption on composite of *E.tereticornis* Freundlich plot 76

Figure 4.32: Lead (II) ion adsorption on composite of *E. terticornis* Langmuir plot 77

Figure 4.33: Lead (II) ion adsorption on composite of *E. tereticornis* barks and leaves adsorbent for Freundlich plot 78

Figure 4.34: Lead (II) ion adsorption on of composite *E. tereticornis* barks and leaves adsorbent for Temkin plot 78

Figure 4.35: Chromium (VI) ion adsorption on composite of *E. tereticornis* barks and leaves adsorbent for pseudo second kinetic model 80

Figure 4.36: Chromium (VI) ion adsorption on composite of *E. terticornis* barks and leaves adsorbent for seconder kinetic model 80

Figure 4.37: Chromium (VI) ion adsorption on composite of *E. tereticornis* barks and leaves adsorbent for elovich kinetics 81

Figure 4.38: Lead (II) ion adsorption on composite of *E. tereticornis* barks and leaves adsorbent for pseudo second order kinetics 82

Figure 4.39: Lead (II) ion adsorption on composite of *E.tereticornis* barks and leaves for second order kinetics 82

Figure 4.40: Lead (II) ion adsorption on composite of *E .tereticornis* barks and leaves adsorbent for second order kinetics 83

List of Tables 6

Table 2.1: Classification of Heavy Metals Based on Toxicity (Thakur, 2006).

Table 2.2: The MCL Standards for the Most Hazardous Heavy Metals (Babel and Kurniawan, 2003). 7

Table 2.3: Comparison between Physiosorption and Chemisorption (Satya *et al*., 2003). 11

Table 2.4:The Main Advantages and Disadvantages of The Various Physiochemical Methods for Treatment of Heavy Metal in Wastewater (Barakat *Et Al.,* 2004) 13

Table 2.5: Type of Isotherm According to Value of R_L 26

Table 2.6: Adsorption Isotherm Equations. 28

Table 3.1: List of Equipment 31

Table 3.3: Design Summary for Adsorption of Cr (VI) and Pb (II) Ions on *Eucalpytus tereticornis* Barks and Leaves Adsorbent 34

Table 3.4: Experimental Runs of *E. tereticornis* Barks and Leaves Adsorbents for Adsorption of Cr (VI) and Pb (II) Ions from Simulated Wastewater 35

Table 3.5: Design Summary for Adsorption of Cr (VI) and Pb (II) Ions on the Composite of *E.tereticornis* Barks and Leaves Adsorbent from Simulated Wastewater 35

Table 3.6: Experimental Runs of *E. tereticornis* Barks and Leaves Composite for Adsorption of Cr (VI) and Pb (II) Ions 35

Table 4.1: Result Of Sample Identification 38

Table 4.2:Experimental Design Matrix For Chromium (VI) And Lead (II) Adsorption Capacity (AC) Using *Eucalyptus Tereticornis* Leave (ETL). 45

Table 4.3: Inverse Transformation of Chromium Adsorption Capacity Using *Eucalpytus tereticornis* Leaves (ETL) Adsorbent 46

Table 4.4: Inverse Transformation of Lead (II) Ion Adsorption Capacity Using *Eucalpytus Tereticornis* Leaves 48

Table 4.5: Summary of ANOVA Results for Cr (VI) And Pb (II) Ions Adsorption on *E. Tereticorni*s Leaves (ETL) Adsorbent 50

Table 4.6: Experimental Design Matrix for Chromium (VI) and Ion Adsorption Capacity (AC) Using *Eucalyptus tereticornis* Barks (ETB) Adsorbent 55

Table 4.7: Experimental Design Matrix for Lead (II) Ions Adsorption Capacity (AC) Using *Eucalyptus tereticornis* Barks (ETB) Adsorbent 58

Table 4.8: Summary of ANOVA Results for Cr (VI) And Pb (II) Adsorption on *E.tereticornis* Barks (ETB) Adsorbent 60

Table 4.9: Adsorption of Chromium (VI) on Composite of *Eucalpytus tereticornis* Barks and Leaves Adsorbent 65

Table 4.10: Adsorption of Lead (II) on Composite of *Eucalpytus tereticornis* Barks and Leaves Adsorbent 68

Table 4.11: Summary of ANOVA Results for Adsorption Capacities of Cr (VI) and Pb (II) Ions on *Eucalpytus tereticornis* Composite (ETC) Barks and Leaves Adsorbent 71

Table 4.12: Chromium (VI) Ion Adsorption Isotherm Parameter Values 77

Table 4.13: Lead (II) Ion Adsorption Isotherm Value 79

Table 4.14: Evaluated Constants Obtained from the Tested Kinetic Model forComposite of Chromium (VI) Ion Adsorption 81

Table 4.15: Evaluated Constants Obtained from the Tested Kinetic Model forComposite of Lead (II) Ion Adsorption 83

List of Plates

Plate 3.1: Image of raw and grinded *Eucalpytus tereticornis* leaves adsorbent 33

Plate 3.2: Image of raw and grinded *Eucalpytus tereticornis* barks adsorbent 43

Plate 4.1: SEM micrograph of *E. tereticornis* leaves before after treatment at 900 times magnification respectively.

Plate 4.2: SEM micrograph of *E. tereticornis* barks and after treatment with nitric acid at 1000 times' magnifications respectively. 43

Plate 4.3: Spent *E.tereticornis* composite after chromium (VI) and lead (II) ions adsorption 44

List of Abbreviation

Co Initial solute concentration in the aqueous phase	mg/L
Ce Equilibrium or final metal concentration	mg/L
K_1 Rate constant of the pseudo first- order equation per min	
K_2 Rate constant of the pseudo second- order equation	mg/g.min
Adsorption capacity	mg/g
K_L Langmuir equation constant	L/g
K_PIntraparticle rate constant	$mg/gmin^{0.5}$
N Adsorption intensitydimensionless	
qe Amount of adsorbate at equilibrium	mg/g
b Monolayer capacity from Langmuir model	mg/g
qt Amount adsorbed at time t	
RL Dimensionless separation factor of equilibrium	
ETB *Eucalpytus tereticornis* Barks	
ETL *Eucalyptus tereticornis* Leaves	
ETC *Eucalyptus tereticornis* Composite	
MCL Maximum Contaminant Level	mg/g

Abstract

The research titled Development of *Eucalpytus tereticornis* composite for chromium (VI) and lead (II) ions adsorption from simulated wastewater was aimed to establish the efficacy of *Eucalpytus tereticornis* composite as an adsorbent applied in the adsorption of Cr^{6+} and Pb^{2+} ions from simulated solution of respective ions. The adsorbent was pretreated with 0.5M of Nitric acid to remove the adsorbent colouration and soluble organic compound. Characterization of the adsorbent was done by the application of Fourier transform infrared (FTIR) and Scanning electronic microscopy (SEM) to determine the functional group and morphology of the adsorbent respectively. Model was developed using RSM to study the interactive effect of contact time and adsorbent dosage on the response (adsorption capacity).batch adsorption test was carried on simulated solution using barks, leaves and composite.it was revealed that adsorption capacity barks on Cr6+ was in the range of 0.80 mg/g to 21.6mg/g. The result on Pb2+ was 2.29 mg/g to 54.05mg/g. The leaves adsorbent showed adsorption capacity for Cr6+ in the range of 0.99mg/g to 28.6mg/g and that of Pb2+ was in the range of 4.330mg/g to 40.65mg/g.The barks to leaves composite ratio in the range of (0.1-0.9) showed the adsortption capacity of Cr6+ in the range of 6.00mg/gto 100mg/g ,while for Pb2+ was in the range of 1.01mg/g to 26.2mg/g. It was revealed that barks to leaves ratio of 0.7 g/g was capable of adsorbing 100mg/g and 26.2 mg/g for Cr6+ and Pb2+ respectively from simulated solution of 100mg/l within the experimental error. Finally, equilibrium data for the adsorption of chromium (VI) and lead (II) ions on *Eucalyptus tereticornis* composite were tested with various adsorption isotherm models such as Langmuir, Freundlich and Temkin with their generalized equation. The Langmuir isotherm model described the adsorption data best with the highest correlation values R^2= 0.9987 for chromium (VI) and R^2 0.9793 for lead (II) ions.

Different kinetic models such as Pseudo second order, Second order and Elovichnetic model were used to evaluate the mechanism of adsorption of chromium (VI) and lead (II) ions. The kinetics of adsorption of chromium on ETC was well described by the Pseudo-second-order kinetic model with correlation value R^2 =0.9961 and that of lead (II) ion followed Elovich kinetic model with highest correlation value R^2 = 0.8914.

CHAPTER ONE

INTRODUCTION

1.1 Background of Study

Heavy metals are excessively released into the environment due to rapid industrialization and have created a major global concern (Wang*et al.*,2008). Chromium, lead, cadmium, zinc, copper, nickel and mercury are often detected Gin industrial wastewater, which originate from metal plating, mining activities, smelting, battery manufacture, tanneries, petroleum refining, paint manufacture, pesticides, pigment manufacture, printing and photographic industries(Kadirvelu *et al.*,2001). Unlike organic wastes, heavy metals are non-biodegradable and they can be accumulated in living tissues, causing various diseases and disorders; as a result of the degree of disorder caused by heavy metal, their removal from wastewater before being discharge is of great interest. There are several methods of wastewater treatment such as chemical precipitation, ion-exchange, electro flotation, membrane separation, reverse osmosis, electro dialysisand solventextraction.

Adsorption is one of the physiochemical treatment processes found to be effective in removing heavy metals from aqueous solutions according to Bailey *et al.*,(1999).An adsorbent can be considered as cheap or low-cost if it is abundant in nature, requires little processing or is a by-productfrom another industry. Plant wastes are inexpensive as they have no or very low economic value. Most of the adsorption studies have been focused on untreated plant wastes such assago waste (Quek *et al.,* 1998), peanut hull pellets (Johnson *et al.,* 2002), and grape stalk wastes (Karunasagar *et al.,* 2005),papaya wood (Saeed *et al.,* 2005), maize leaf (Babarinde *et al.,* 2006),rice husk ash and neem bark (Bhattacharya *et al.,* 2006),saltbush (Atriplex canescens) leaves (Sawalha *et al.,* 2007).

However, the application of untreated plant wastes as adsorbents for industrial wastewater treatment can lead to the blockage of adsorption site during the adsorption process due to release of soluble organic compounds contained in the plant materials (Gaballah *et al.*, 1997; Nakajima and Sakaguchi, 1990).

The *Eucalyptus*, a native genus from Zaria Nigeria,belongs to *Myrtaceae* family and comprises about 90 species (Batish *et al.*, 2008)**.**More than 300 species of this genus contain volatile oils in their leaves. *E. tereticornis* has been most successful in summer rainfall conditions with a moderate to fairly severe dry season.

In this present study, *Eucalpytus tereticornis* powder treated with nitric acid to eliminate colouration and contamination during adsorption process was used as an adsorbent for adsorption lead (II) and chromium (VI) ions from simulated wastewater. In addition, there has been an intensive studies on the use of low cost adsorbent developed from agricultural, plant and biological materials for the adsorption of heavy metals from wastewater. However, there is no known report in the literature regarding the use of Response Surface Methodology (RSM) to ascertain the optimum conditions necessary for efficient adsorption of chromium (VI) and lead (II) ions using *Eucalyptus tereticornis* adsorbent from simulated wastewater.

Therefore, Response surface methodology (RSM) is a collection of mathematical and statistical techniques useful for analyzing the effects of several independent variables on the response, (Montgomery, 1997 and Lee *et al*., 2000).

RSM generates an experimental design for model preparation. An experimental design is a specific set of experiments defined by a matrix composed of the different level combinations of low and high variables studied.

1.2 Research Problem

Despite several works in the use of plant parts for the adsorption of heavy metals from wastewater, report regarding the optimization of process parameters on the use of *Eucalyptus tereticornis* barks, leaves and its composite for the adsorption of chromium (VI) and lead (II) ions are lacking. Also, the conventional method in the design of experiment known as one factor variable is time consuming with low efficiency.

1.5 Justification

Adsorbent developed from *Eucalpytus tereticornis* parts (barks and leaves) are abundant and cheap. In addition, if the adsorbents are found highly efficient for heavy metals adsorption, not only the industries, but the living organisms and the surrounding environment will be also benefited from the decrease or elimination of potential toxicity caused by heavy metal.The outcome of this study will enhance indigenous technology through the use of local materials and serve as means of converting waste materials to wealth.

1.6 Aim and Objectives

The aim of this study is to develop*Eucalyptus tereticornis* composite barks and leaves adsorbentfor chromium (VI) and lead (II) ions adsorption from simulated wastewater.

The specific objectives of the study are to:

i. Prepare and employ low cost adsorbents from plant wastes *Eucalyptus tereticornis* to treat simulatedwastewater.
ii. Develop model equations using response surface methodology (RSM) to study the interactive effect of independent variables on the response.
iii. Evaluate the adsorption capacity of the prepared adsorbents for adsorption of chromium (VI) and lead (II) ions from simulated wastewater.

iv. Determine the effects of operating conditions such as adsorbent dosage and contact time on the chromium (VI) and lead (II) adsorption in the batch process using design expert to design the experiment

v. Identify the applicable adsorption isotherms and kinetic models for each adsorbent.

1.5 Research Scope

The scope of this research will cover**:**

i. The use of *Eucalyptus tereticornis* leave and bark for adsorbent production.

ii. Investigation the effectof chromium (VI) and lead (II) ions adsorption from simulated wastewater using the developed adsorbent from *Eucalyptus tereticornis* barks and leaves

iii. Use of Design Expert software to design and calculate the adsorption capacity result obtained from batch adsorption test.

iv. Scan Electronic Microscopic machine (SEM) will be used to determine the morphology of the adsorbent.

v. Surface characterization of the adsorbents with the aid of Fourier Transform Infrared (FTIR) to determine the active functional group responsible for heavy metal uptakes.

vi. Characterization of raw wastewater and treated wastewater with the help of Atomic Adsorption Spectrophotometer (AAS) to determine the initial and final concentration of chromium (VI) and lead (II) ions.

vii. The results will be evaluated using the equilibrium adsorption isotherm and kinetic models.

CHAPTER TWO

LITERATURE REVIEW

2.1 Heavy Metals and its Toxicities

Lead (II) and chromium (VI) ions are toxic metal contaminants in water. According to Nigeria standard, the maximum discharge limits for lead (II) and chromium (VI) ions in wastewater are 0.5 mg /l and 1.0 mg /l respectively. Maximum limit in drinking water is 0.05 mg /l for both metals. Infact there is no safe level of these metals in drinking water and even a very dilute content can cause adverse health effects. Lead (II) ion is toxic to living organisms and if released into the environment can bioaccumulate and enter the food chain. Lead (II) ion is known to cause mental retardation, reduces haemoglobin production necessary for oxygen transport and it interferes with normal cellular metabolism. Lead (II) ion has damaging effects on body nervous system. It reduces intelligence quotient (IQ) level in children. Strong exposure of hexavalent chromium causes cancer in the digestive tract and lungs and may cause gastric pain, nausea, vomiting, severe diarrhoea, and haemorrhage (Mohanty *et al.,* 2005).

The conventional methods for treatment of lead (II) and chromium (VI) ions in wastewater include: precipitation, ion exchange, reverse osmosis, evaporation, electrodialysis, adsorption and removal of chromium by using various conventional and non-conventional adsorbents. These methods are economically unfavourable or technically complicated, and are used only in special cases of wastewater treatment (Kratochvil *et al.,* 1998; Sharma, 2003).

Heavy metals are defined as metals with a specific weight usually more than 5.0 g/cm^3, which is five times higher than water (Liu *et al.,* 2003). The toxicity of heavy metals occurs even in low concentrations of about 1.0-10 mg/l. of the 90 naturally occurring elements, 21 are non-metals, 16 are light metals and the remaining 53 are heavy metals.

Most heavy metals are transition elements with incompletely filled d-orbitals. These d-orbitals provide heavy metal cations with the ability to form complex compounds, which may or may not be redox-active. Out of 53 heavy metals, 30 elements are now believed to be essential to life. They can be divided into the 6 structural elements, 5 macro minerals and 19 trace elements (Florence, 1989). Virtually, all metals can exhibit toxicity above certain threshold concentrations, which for highly toxic metal species may be extremely low. The toxicity caused by heavy metals is generally a result of strong coordinating abilities (Gadd, 1992). Certain metals are known to be toxic for centuries. Based on the physiological effect and toxicity, heavy metals are classified as shown in Table 2.1

Table 2.1: Classification of Heavy Metals Based on Toxicity (Thakur, 2006).

Metal	Toxicity
Fe, Mo, Mn	Low toxicity
Zn, Ni, Cu, V, Co, W, Cr	Average toxicity
As, Ag, Sb, Cd, Hg, Pb, U	High toxicity

Heavy metals cause serious health effects, including reduced growth and development, cancer, organ damage, nervous system damage, and in extreme cases, death. Exposure to some metals, such as mercury and lead, may also cause development of autoimmunity, in which a person's immune system attacks its own cells. This can lead to joint diseases such as rheumatoid arthritis, and diseases of the kidneys, circulatory system, nervous system, and damaging of fetal brain. At higher doses, heavy metals can cause irreversible brain damage. Children may receive higher doses of metals from food than adults, since they consume more food for their body weight than adults. Wastewater regulations were established to minimize human and environmental exposure to hazardous chemicals. This includes limits on the types and concentration of

heavy metals that may be present in the discharged wastewater. The Maximum Contaminant Level (MCL) standard for the most hazardous heavy metals established by United State of Environmental Protection Agency (USEPA) (Babel and Kurniawan, 2003) are summarized in Table 2.2.

Table 2.2: The MCL Standards for the Most Hazardous Heavy Metals (Babel and Kurniawan, 2003).

Heavy metal	Toxicities	MCL (mg/L)
Arsenic	Skin manifestations, visceral cancers, vascular disease	0.0500
Cadmium	Kidney damage, renal disorder, human carcinogen	0.0100
Chromium	Headache, diarrhea, nausea, vomiting, cancer	0.0500
Copper	Liver damage, Wilson disease, insomnia	0.2500
Nickel	Dermatitis, nausea, chronic asthma, coughing, human	0.2000
Zinc	Depression, lethargy, neurological signs and increased thirst	0.8000
Lead	Damage the fetal brain, diseases of the kidneys.	0.0060
Mercury	Rheumatoid arthritis and diseases of the kidneys.	0.0003

2.2 Conventional Processes for Removal of Heavy Metal

The conventional processes for removing heavy metals from wastewater include many processes such as chemical precipitation, flotation, adsorption, ion exchange, and electrochemical deposition.

2.2.1 Chemical precipitation

Chemical precipitation is the most widely used for heavy metals adsorption from inorganic effluent. Precipitation of metals is achievedby the addition of coagulants such as alum, lime, iron salts and other organic polymers.

The large amount of sludge containing toxic compounds produced during the process is the main disadvantage (Aziz *et al.,* 2008). Lime precipitation can be employed to effectively treat inorganic effluent with a metal concentration of higher than 1000 mg/L. Other advantages of using lime precipitation include the simplicity of the process, inexpensive equipment requirement, and convenient and safe operations. However, chemical precipitation requires a large amount of chemicals to reduce metals to an acceptable level for discharge. Other drawbacks are its excessive sludge production that

requires further treatment, slow metal precipitation, poor settling, the aggregation of metal precipitates, and the long-term environmental impacts of sludge disposal (Aziz *et al.,* 2008).

2.2.2 Ion exchange

Ion exchange is another method used successfully in the industry for the removal of heavy metals from effluent. An ion exchanger is a solid capable of exchanging either cations or anions from the surrounding materials. Commonly used matrices for ion exchange are synthetic organic ion exchange resins. The disadvantage of this method is that it cannot handle concentrated metal solution as the matrix gets easily fouled by organics and other solids in the wastewater. Moreover ion exchange is nonselective and is highly sensitive to the pH of the solution (Kurniawan *et al.,* 2006).

2.2.3 Photocatalysis

In recent years, photocatalytic process in aqueous suspension of semiconductor has received considerable attention in view of solar energy conversion. This photocatalytic process was achieved for rapid and efficient destruction of environmental pollutants. Upon illumination of semiconductor– electrolyte interface with light energy greater than the semiconductor band gap, electron–hole (e-/h+)pairs are formed in the conduction and the valence band of the semiconductor, respectively (Herrmann, 1999).

2.2.4 Electrodialysis

Electrodialysis (ED) is a membrane separation in which ionized species in the solution are passed through an ion exchange membrane by applying an electric potential. The membranes are thin sheets of plastic materials with either anionic or cationic characteristics. When a solution containing ionic species passes through the cell compartments, the anions migrate toward the anode and the cations toward the cathode, crossing the anion exchange and cation-exchange membranes (Chen, 2004).

2.2.5 Membrane filtration

Membrane filtration has received considerable attention for the treatment of inorganic effluent, since it is capable of removing not only suspended solid and organic compounds, but also inorganic contaminants such as heavy metals. Depending on the size of the particle that can be retained, various types of membrane filtration such as ultrafiltration, nanofiltration and reverse osmosis can be employed for heavy metal removal from wastewater. Ultrafiltration (UF) utilizes permeable membrane to separate heavy metals, macromolecules and suspended solids from inorganic solution on the basis of the pore size (5–20 nm) and molecular weight of the separating compounds (1000– 100,000 Da). These unique specialties enable UF to allow the passage of water and low-molecular weight solutes, while retaining the macromolecules, which have a size larger than the pore size of the membrane (Vigneswaran *et al.*, 2004).

2.2.6 Adsorption

Sorption is transfer of ions from water to the soil i.e. from solution phase to the solid phase. Sorption actually describes a group of processes, which includes adsorption and precipitationof wastewater laden with heavy metals. Basically, adsorption is a mass transfer process by which a substance is transferred from the liquid phase to the surface of a solid, and becomes bound by physical or chemical interactions (Babel and Kurniawan, 2003). Various low-cost adsorbents, derived from agricultural waste, industrial by-product, natural material, or modified biopolymers, have been recently developed and applied for the removal of heavy metals from metal contaminated wastewater. In general, there are three main steps involved in pollutant sorption onto solid sorbent.

(i) The transport of the pollutant from the bulk solution to the sorbent surface;

(ii) Adsorption on the particle surface; and

(iii) Transport within the sorbent particle. Technical applicability and cost-effectiveness are the key factors that play major roles in the selection of the most suitable adsorbent to treat inorganic effluent.

2.3 Types of Adsorption

At molecular level, adsorption is due to attractive interactions between a surface and the species being adsorbed.

2.3.1 Physical adsorption

It is a result of intermolecular forces of attraction between molecules of the adsorbent and the adsorbate. In this case the molecular attractive forces that retain the adsorbent on the surface are purely physical are called Vander waal forces. This is a readily reversible phenomenon. The energy of interaction between the adsorbate and adsorbent has the same order of magnitude, but is usually greater than the energy of condensation of the adsorptive. Therefore, no activation energy is needed.

2.3.2 Chemical adsorption

It is a result of chemical interaction between the solid and the adsorbed substance. It is also called activated adsorption. It is irreversible. It is particularly important in catalysis. Therefore, the energy of chemisorptions considered like chemical reaction. It may be exothermic or endothermic processes ranging from very small to very large magnitudes. The elementary step in chemisoption often involves large activation energy (Activated adsorption) (Satya *et al*., 2003).

Table 2.3 provides vivid comparison between physical and chemical adsorption processes.

Table 2.3:Comparison between Physiosorption and Chemisorption (Satya *et al*., 2003).

Physiosorption	Chemisorption
1. Low heat of adsorption usually in the range of 20-40 kJ mol^{-1}	High heat of adsorption in the range of 40-400 kJ mol^{-1}
2. Force of attraction are Van der Waal's forces	Forces of attraction are chemical bond forces
3. It usually takes place at low temperature and decreases with increasing temperature	It takes place at high temperature
4. It is reversible	It is irreversible
5. It is related to the ease of liquefaction of the gas	The extent of adsorption is generally not related to liquefaction of the gas
6. It is not very specific	It is highly specific
7. It forms multi-molecular layers	It forms monomolecular layers
8. It does not require any activation energy	It requires activation energy

2.4 Factors Affecting Adsorption Process

The extent of adsorption depends upon the following factors:

1. Nature of adsorbate and adsorbent.
2. The surface area of adsorbent.
3. Activation of adsorbent.
4. Experimental conditions. e.g. temperature, concentration and time.

2.5Adsorption Phenomenon

Adsorption is a surface phenomenon with common mechanism for organic and inorganic pollutants removal. When a solution containing solute comes into contact with

a solid with a highly porous surface structure, liquid–solid intermolecular forces of attraction cause some of the solute molecules from the solution to be concentrated or deposited at the solid surface. The solute retained (on the solid surface) in processes is called adsorbate, whereas, the solid on which it is retained is called as an adsorbent. This surface accumulation of adsorbate on adsorbent is called adsorption. This creation of an adsorbed phase having a composition different from that of the bulk fluid phase forms the basis of separation by adsorption technology.

In a bulk material, all the bonding requirements (be they ionic, covalent, or metallic) of the constituent atoms of the material are filled by other atoms in the material. However, atoms on the surface of the adsorbent are not wholly surrounded by other adsorbent atoms and therefore can attract adsorbates. The exact nature of the bonding depends on the details of the species involved, but the adsorption process is generally classified as physicsorption (characteristic of weak Van Der Waals forces) or chemisorption (characteristic of covalent bonding). It may also occur due to electrostatic attraction.As the adsorption progress, an equilibrium of adsorption of the solute between the solution and adsorbent is attained (where the adsorption of solute is from the bulk onto the adsorbent is minimum). The adsorption amount (qe, mg/g) of the molecules at the equilibrium step was determined according to Equation 2.1(Oliveria *et al.,* 2005).

$$qe = \frac{(Co - C\ e)V}{m} \qquad (2.1)$$

Where v is the solution volume (L); m is the mass of monolithic adsorbents (g); and Co and Ce are the initial and equilibrium adsorbate concentrations, respectively.

Table 2.4explains the advantages and disadvantages of physiochemical methods for heavy metals treatment in wastewater.

Table 2.4: TheMain Advantages and Disadvantages of the Various Physiochemical Methods for Treatment of Heavy Metal in Wastewater (Barakat *et al.*, 2004)

Treatment method	Advantages	Disadvantages	References
Chemical precipitation	Low capital cost, simple operation	Sludge generation, extra operational cost for sludge disposal	Kurniawan *et al*,. 2006.
Membrane filtration	Small space requirement, low pressure, high separation selectivity	High operational cost due to membrane fouling	Kurniawan *et al*,. 2006
Electrodialysis	High separation	selectivity High operational cost due to membrane fouling and energy consumption	Mohammadi *et al*,. 2005.
Photocatalysis	Removal of metals and organicpollutant simultaneously, less harmful byproducts.	Long duration time, limitedapplications	Barakat *et al*.,2004; Kajitvichyanukula*et al*.,2005.
Adsorption with new adsorbents	Low-cost, easy operating conditionsand high metal binding capacities	Low selectivity, production of waste Products	Babel and Kurniawan, 2003

2.6 Adsorption with Non-Conventional Adsorbent

Removal of chromium from industrial effluent was investigated using *Eucalyptus tereticornis* bark (Indu and Dinesh, 2011) with various parameters including amount of biomass, pH of solution and contact time. Biomass (2%) was able to remove 88% and

91.5% of chromium at pH 4.0 and pH 5.0, respectively from solution amended with 50 mg of Cr^{6+} l/L. Maximum chromium removal capacities of treated bark biomass were 70% and 94% from tannery effluent and chrome plating effluent, respectively in column mode. The adsorption parameters were determined using both Langmuir and Freundlich isotherms model. Calorific values of native bark biomass, tannery effluent and chrome plating effluent treated biomass were 2,227, 3,885 and 4,003 kcal/kg, respectively with increases in chromium laden biomass. The results revealed that chromium loaded bark biomass can be disposed off by incineration or used in furnace as a fuel.

Phussadee *et al.,* (2008) investigated powdered activated carbon (PAC) prepared from *Eucalyptus camaldulensis dehn.* Bark was tested for its adsorption capacity for Cu (II) and Pb (II). The experiment was conducted to investigate the effect of pH, contact time, initial metal concentration, and temperature. The best adsorption of both Cu (II) and Pb (II) occurred at pH 5, where the adsorption reached equilibrium within 45 min for the whole range of initial heavy metal concentrations (0.1–10 mmol/L). The adsorption kinetics was found to follow the pseudo-second order model where equilibrium adsorption capacities and adsorption rate constants increased with initial heavy metal concentrations.

The adsorption isotherm followed Langmuir better than Freundlich models within the temperature range (25–60°C).The maximum adsorption capacities (q_m) occurred at 60°C, where *q*m for Cu(II) and Pb(II) were 0.85 and 0.89 mmol/g, respectively. The enthalpies of Cu (II) and Pb(II) adsorption were 43.26 and 58.77 kJ/mol, respectively. The positive enthalpy of adsorption indicated an endothermic nature of the adsorption.

Abdel *et al.,* (2008).Studied the *Eucalyptuscamaldulenis* tree leaves were used to study adsorption of several cations (Cu^{2+}, Zn^{2+}, Cd^{2+} and Pb^{2+}) from wastewater within various experimental conditions. The dried leaves of *Eucalyptus camaldulenis* were

used at different adsorbent/metal ion ratios. The influence of pH, contact time, metal concentration, and adsorbent loading weight on the removal process was investigated. Batch adsorption studies were carried out at room temperature. The adsorption efficiencies were found to be pH dependent, increasing by increasing the pH in the range from 2.5 to 8.5. The equilibrium time was attained after 90-120 minutes and the maximum removal percentage was achieved at an adsorbent loading weight of 1.5 g/50ml mixed ions solution. The removal order was found to be Pb (II)> Cu (II) >Cd (II)> Zn (II).This study is one of the first reports of removal of the highly toxic Cu^{2+}, Zn^{2+}, $Cd^{2+}$and Pb^{2+}in mixed systems based on the adsorption by natural materials. The potential of application for the treatment of solutions containing these heavy metals in multi-metal solutions is indicated.

Mangifera indica(Mango) seed and seed shell powders were studied for their possible application in the removal of Cu (II) from wastewater. The adsorption of Cu (II) on the powder of Mango seeds and seed shell was found maximum at pH 6 and followed Freundlich type adsorption Isotherm The overall process was spontaneous and exothermic in nature. The total adsorption on each adsorbent increased with the increase in temperature between 30-50 0C and then decreased up to 60^0C. Moreover, it was found that the seed shell of *Mangifera indica* had higher sorption capacity than that of the seed powder for Cu (II). The presence of Ca (II), Mg (II), and K(I) decreased the percent adsorption of Cu(II) on these adsorbents (Ali *et al.*, 1997).

Sawdust, an inexpensive material has been utilized as an adsorbent for the removal of Cu (II) from wastewater. The effect of contact time, pH concentration, temperature, dose and particle size of the adsorbent and salinity on the removal of Cu (II) has been studied. The equilibrium nature of copper (II) adsorption at different temperatures (30-50^0C) has been described by the Freundlich and Langmuir isotherms and a tentative

mechanism has also been proposed. The thermodynamic parameters such as free energy, entropy and enthalpy changes for the adsorption of Cu (II) have also been computed and discussed. The kinetics and the factors controlling the adsorption process have also been studied. In order to widen the applicability of the removal technique, the optimized method was applied for the removal of Cu (II) from Ganga river water (Ajmal *et al*, 1998).The removal efficiency was found to be 63%. In the river water sample, the adsorption capacity was slightly decreased, probably due to the presence of other major cations like calcium and magnesium.

The fruit peel of orange (*Citrus reticulate*) is a low cost adsorbent, which is abundantly available in India as waste material. The ability of fruit peels of orange to remove Zn (II), Ni (II), Cu (II), and Pb(II) was studied. The adsorption was found in the order Ni (II)>Cu (II)>Pb (II)>Zn (II).The extent of removal of Ni (II) was found to be dependent on sorbent dose, initial concentration, pH and temperature. The adsorption followed first order Kinetics. The process was found to be endothermic showing monolayer adsorption of Ni (II) with a maximum adsorption of 96% at 50^0C for an initial concentration of 50 mg/l at pH 6. Thermodynamic parameters were also computed(Ajmal *et al*., 2000).

Mohsen, (2007). Studied the potential adsorption of lead removal from various aqueous solutions. Parameters such as pH, temperature of the solution, particle size of okra wastes and the concentrations of adsorbent and adsorbate were studied to optimize the conditions to be utilized on a commercial scale for the decontamination of effluents using a batch adsorption technique. Adsorption parameters were determined using both Langmuir and Freundlich isotherms. The optimum pH for lead removal was between 4 and 6, the percentage of lead removal at equilibrium increases with increasing the amount of okra wastes and temperature. Better adsorption at higher temperatures. The

removal of Pb^{2+} ions attained 99%., this means that Pb^{2+} can be effectively removed from aqueous solutions by okra wastes. The mechanisms for adsorption of Pb^{2+} ions on to okra wastes involved ion exchange or the formation of hydroxyl complexes. The results obtained could be useful for the application of agricultural wastes for heavy metal removal from industrial wastewater.

Despite the usefulness of plant waste as an adsorbent for wastewater treatment, the non - modification of plant wastes as adsorbents can cause low adsorption capacity by the blockage of active site during adsorption process due to release of soluble organic compounds contained in the plant materials. Therefore, plant wastes need to be chemically treated or modified before being applied to the decontamination of heavy metals. Also, pretreatment of plant wastes can extract soluble organic compounds and enhance chelating efficiency (Gaballah *et al.*, 1994).

Pretreatment methods using different kinds of modifying agents have been used such as base solutions (sodium hydroxide, calcium hydroxide, and sodium carbonate), mineral and organic acid solutions (hydrochloric acid, nitric acid, sulfuric acid, tartaric acid, citric acid, and thioglycolic acid), organic compounds (ethylenediamine, formaldehyde, epichlorohydrin, and methanol), oxidizing agent (hydrogen peroxide), and dye (Reactive Orange 13). For the purpose of removing soluble organic compounds, eliminating coloration of the aqueous solutions and increasing efficiency of metal adsorption have been performed by many researchers (Gupta *et al.*, 2003; Taty-Costodes *et al.*, 2003).

2.7Chemically Modified Adsorbents

Abia *et al.*, (2003) carried out an experiment on determining the optimal concentration of thioglycolic acid ($HSCH_2COOH$) for the removal of Cd^{2+}, Cu^{2+}, and Zn^{2+}ions by

cassava waste. Cassava waste consists of ligands such as hydroxyl, sulfur, cyano, and amino which could bind heavy metal ions. It was noticed that absorptivity of the cassava waste was greatly improved as the concentration of modifying agent (thioglycolic acid) was increased from 0.5 to 1.0 M due to the increase in sulfhydryl groups,−SH. Adsorption was reported to take place on the cell wall of the biomass. Optimum adsorptions of all three heavy metals were achieved in less than 30 min. The order of maximum adsorption capacity among the three heavy metal ions after treating cassava waste with 1.0 M thioglycolic acid is as follows: $Zn^{2+} > Cu^{2+} > Cd^{2+}$. The authors however did not conduct a detailed experiment on the kinetic model of adsorption.

Horsfall and Abia, (2003) investigated the effect of modifying agent concentration on the adsorption of Zn^{2+} and Cd^{2+} ions onto thioglycolic acid for treating cassava waste. Cassava waste treated with 0.5 M and untreated adsorbent showed lowest removal of Cd^{2+} and Zn^{2+} ions compared to 1.0 M thioglycolic acid but the time to reach equilibrium remained similar for treated and untreated adsorbent. It was discovered that treated cassava waste sustains a much higher adsorption capacity for Zn^{2+} and Cd^{2+} ions compared to untreated sample. The adsorption capacities of treated cassava waste were reported to be 647.48 mg Cd/g and 559.74 mg Zn/g, as compared to only 86.68 mg Cd/g and 55.82 mg Zn/g when using untreated cassava waste.

The increase in adsorption capacity of Zn and Cd after acid treatment could be related to the formation of micro porosity, which leads to enhanced thiol (−SH) groups on the adsorbent surface.

The relative release of exchanging hydrogen atoms of the thiol groups with heavy metal ions results in improved level of adsorption. Desorption studies showed that untreated

cassava waste showed better recovery of Zn^{2+} and Cd^{2+}. The authors suggest that the low recovery of heavy metal ions by acid treated cassava waste was due to enhancement in binding sites after acid treatment, which enables the metal ions to bind strongly to the adsorbent surface.

Srivastava *et al.*,(1994) studied adsorption of Pb and zinc (Zn) onto lignin. The lignin was extracted from black liquor, a waste product of the paper industry. Waste black liquor can be purchased for $1.00/ton, and the lignin can be processed for approximately $60/ton, as compared to activated carbon at $100/ton. The adsorption capacity for lignin at 30°C was found to be 1587 mg/g for Pb and 73 mg/g for Zn, which increased to 1865 and 95 mg/g, respectively, at 40°C. The high adsorption capacity of lignin is in part due to polyhydric phenols and other functional groups on the surface. Ion-exchange may also play a role in the adsorption of metals by lignin.

Kumar and Bandyopadhyay (2006) reported that rice husk treated with sodium carbonate, sodium hydroxide, and epichlorohydrin enhanced the adsorption capacity for heavy metals. The sorption of Cd (II) from aqueous solution by rice husk, a surplus agricultural byproduct was investigated. Some simple and low-cost chemical modifications resulted in increasing the sorption capacity of raw rice husk (RRH) from 8.58 mg/g to 11.12, 20.24, 16.18 mg/g and reducing the equilibrium time from 10 h of RRH to 2, 4 and 1 h for epichlorohydrin treated rice husk (ERH), NaOH treated rice husk (NRH), sodium bicarbonate treated rice husk (NCRH), respectively. The effect of pH, sorption kinetics and isotherms were studied in batch experiments. Good correlation coefficient was obtained for pseudo second-order kinetic model, which agreed with chemisorption as the rate-limiting mechanism. Sorption isotherm test showed that equilibrium sorption data were better represented by Langmuir model than the

Freundlich model. The highly efficient low cost and the rapid uptake of Cd (II) by NCRH indicated that it could be an excellent alternative for the removal of heavy metal by sorption process.

Bhattacharya *et al.,* (2006). Studied rice husk ash with pretreatment for Zn^{+2} removals. It was found that 96.8% of Zn^{+2} removal were obtained at a pH value of 5. The Langmuir and Freundlich adsorption isotherm models were used to represent the experimental data. Both of the models were fitted well. The adsorption capacity was obtained as 14.30 mg/g at optimum pH 5.0.

2.8 Response Surface Methodology (RSM)

RSM is a collection of mathematical and statistical techniques useful for developing, improving and optimizing processes and can be used to evaluate the relative significance of several affecting factors even in the presence of complex interactions.

Before applying the RSM, it is necessary to choose an experimental design that will define the number of experimental runs that should be carried out in the experimental feasible region. Several experimental designs exist that reduce the number of experiments. Thus, if it is desired to detect the significant variables which influence the response, first-order experimental design like Factorial design, or Plackett-Burman design can be used.

On the other hand, to maximize a response function or to optimize a process, second-order experimental designs such as three level factorial designs, Box-Behnken Design (BBD) and Central Composite Design (CCD) can be used (Baş and Boyaci, 2007).

Basically, this optimization process involves three major steps, which are, performing the statistically designed experiments, estimating the coefficients in a mathematical model and predicting the response and checking the adequacy of the model.

The optimum values of the selected variables were obtained by solving the regression equation and by analyzing the response surface contour plots. The variability in dependent variables was explained by the multiple coefficient of determination, R^2 and the model equation was used to predict the optimum value and subsequently to elucidate the interaction between the factors within the specified range.

Application of RSM using Central Composite Design for second order models for optimizing the operational parameters in separation technology have been discussed by various authors. The Central composite experimental design in response surface methodology was used for designing the experiments as well as for full response surface estimation. Recently many statistical experimental design methods have been employed in chemical process optimization. Experimental design technique is a very useful tool for this purpose as it provides statistical models, helps in understanding the interactions among parameters. The experimental data points were used to obtain the empirical model from Central composite design.

The previous literature review on the heavy metal removal under Response Surface Methodology with the aid of Central Composite Design (CCD) is given as follows.

Deepa and Suresha, (2014**) s**tudied the biosorption of Pb (II) by using the leaves *Araucaria cookii* from aqueous solution and industrial effluent. The batch studies were performed to evaluate the different parameters like pH, contact time, metal ion concentration, adsorbent mass and size variation. Characterization of biosorbent was carried out by Fourier Transform Infrared (FTIR) and Scanning Electron Micrograph (SEM). Experimental results shows that at pH 5 the biosorption efficiency reached a maximum removal of 98.52% with a contact time of 60 min and an initial ion concentration 200 mg/L. Kinetic models are described and fitted good with Pseudo-second order reaction. Langmuir and Freundlich isotherms were also applied and

evaluated. The Central Composite experimental Design (CCD) in Response Surface Methodology was used to design the experiment and the optimum conditions. The result showed that the model and experimental data was favourable in the removal of Lead (II) in the industrial waste water and can be used as low cost biosorbent.

Bhatti *et al*., (2011) investigated the optimized process variables, electrolysis voltage and treatment time for the electrocoagulation removal of hexavalent chromium. Response surface methodology (RSM) with central composite design (CCD) was used to achieve energy efficient removal of Cr (VI). Predictive models using ANOVA and multiple response optimizations revealed that optimal Cr (VI) removal efficiency occurred at 11 V and 18.6 min treatment time to give 50% Cr (VI) removal efficiency with a consumption of 15.46KWh/m^3 energy.

Biswajit, *et al*., (2013) studied adsorption of chromium (VI) ions from aqueous solution by alluvial soil of Bhagirathi River, which was investigated under batch mode. The removal of hexavalent chromium was optimized by using Response Surface Methodology. The influence of various process parameters such as initial chromium (VI) concentration, solution pH, sorbent dose and contact time on the removal process were investigated. A total of 29 sorption experimental runs were carried out employing the detailed conditions designed by Response Surface Methodology based on the Box-Behnken Design. The analysis of variance (ANOVA) depicted that the quadratic model was suitable for all the responses. Contour and response surface plots were used to determine the interaction effects of main factors and optimum conditions of process, respectively. From the experimental result, maximum chromium (VI) removal of 93 % was obtained at the optimum condition of initial chromium (VI) concentration (10 mg/L), pH (2), adsorbent dose (1.5 g) and contact time (62.5 min). The experimental removal efficiency (93 %) agreed very well with the predicted one (91.79 %), indicating

the suitability of the model employed and the success of response surface methodology in optimizing the conditions of the removal of chromium (VI) ions from aqueous solution.

RSM has been used to optimize the process variables such as initial metal ion concentration, adsorbent dosage and pH of the solution on the performance of percentage removal of Cr (VI) ions and adsorption capacity of SDCCB. Various isotherm and kinetic models have been fitted with experimental data to describe the solute interaction and behaviour of rate controlled mechanism with the adsorbent in batch studies (Alhaji *et al.*, 2015).

SDCCB is an effective, economic and eco-friendly adsorbent for the removal of nearly 95% of Cr (VI) from aqueous solutions. The mathematical model development and optimization for adsorption of Cr (VI) using statistical design of experiments appears to be a useful tool to predict and understanding the interaction effects between process variables. The isotherm models for the experimental data followed is in the order of Freundlich > Langmuir > Temkin Isotherm for adsorption of Cr (VI) ions and adsorption kinetics fit suitably in a pseudo second order kinetic model. The activation parameters evaluated points out that the adsorption of Cr (VI) on SDCCB surface is an endothermic chemisorption process.

2.9Equilibrium Isotherm Models

Analysis of the isotherm data is important to develop an equation which accurately represents the results and which could be used for design purposes and to optimize an operating procedure. The most common isotherms applied in solid/liquid systems are the theoretical equilibrium isotherm; Langmuir and Freundlich (two parameter models) (Ho and Wang 2004; Basha *et al*., 2008). Simplicity and easy interpretability are some

of the reasons for extensive use of these models. At the same time, linear regression has been frequently used to evaluate the model parameters.

2.9.1 Langmuir adsorption isotherm

Langmuir is the simplest type of theoretical isotherms. Langmuir adsorption isotherm describes quantitatively the formation of a monolayer of adsorbate on the outer surface of the adsorbent, and after that no further adsorption takes place. Thereby, the Langmuir represents the equilibrium distribution of adsorbate between the solid and liquid phases. The Langmuir adsorption is based on the view that every adsorption site is identical and energetically equivalent (thermodynamically, each site can hold one adsorbate molecule).

The Langmuir isotherm assume that the ability of molecule to bind and adsorbe is independent of whether or not neighbouring sites are occupied. This mean, there will be no interactions between adjacent molecules on the surface and immobile adsorption. Also mean, transmigration of the adsorbate in the plane of the surface is prevented. In this case, the Langmuir isotherm is valid for the dynamic equilibrium adsorption desorption processes on completely homogeneous surfaces with negligible interaction between adsorbed molecules that exhibit the form of Equation (2.2)

$$q_e = \frac{q_m b C_e}{1 + b C_e} \tag{2.2}$$

It is linearly re-written as:

$$\frac{C_e}{q_e} = \frac{1}{q_m} Ce + \frac{1}{q_m b} \tag{2.3}$$

Plotting $\frac{C_e}{q_e}$ against Ce

Where Ce= equilibrium concentration in solution

qe= the amount of adsorbate adsorbed for unit mass of adsorbent

q and b are related to standard monolayer adsorption capacity and the Langmuir constant, respectively.

Langmuir model represent one of the first theoretical treatments of non-linear sorption and suggests that uptake occurs on a homogenous surface by monolayer sorption without interaction between adsorbed molecules. The Langmuir isotherm assumes that adsorption sites on the adsorbent surfaces are occupied by the adsorbate in the solution.

Therefore the Langmuir constant (b) represents the degree of adsorption affinity of the adsorbate. The maximum adsorption capacity (q) associated with complete monolayer cover is typically expressed in (mg/g). High value of b indicates for much stronger affinity of adsorbate to adsorption.

A dimensionless separation factor or equilibrium parameter, R_L was proposed by Wang *et al.,* (2008) as an essential feature of the Langmuir Isotherm to predict favourability of adsorption which is defined as:

$$R_L = \frac{1}{1+bC_0} \quad (2.4)$$

Co= reference fluid-phase concentration of adsorbate (mg/l) (initial adsorbate concentration)

b= Langmuir constant (ml/mg)

Value of R_L indicates the shape of the isotherm accordingly as shown in Table 2.5.

Table 2.5: Type of Isotherm According to Value of R_L

R_L Value	Langmuir Isotherm type
$0 < R_L < 1$	Favourable
$R_L > 1$	Unfavourable
$R_L = 1$	Linear
R= 0	Irreversible

2.9.2 Freundlich adsorption isotherms

Freundlich isotherm is commonly used to describe the adsorption characteristics for the heterogeneous surface. It represents an initial surface adsorption followed by a condensation effect resulting from strong adsorbate-adsorbate interaction.The heat of adsorption, in many instances, decreases in magnitude with increasing extent of adsorption. This decline in heat is logarithmic implying that the adsorption sites are distributed exponentially with respect to adsorption energy.

This isotherm does not indicate an adsorption limit when coverage is sufficient to fill a monolayer. It is given by Equation (2.5)

$$q_e = K_f Ce^{1/n} \quad (2.5)$$

The linearized equation is given by Equation (2.6)

$$\log q_{e=} \frac{1}{n} logC_e + logK_f \quad (2.6)$$

K_f= Freundlich constant related to maximum adsorption capacity (mg/g). It is a

Temperature-dependent constant.

n= Freundlich constant related to surface heterogeneity (dimensionless). It gives an indication of how favourable the adsorption processes.

With n= 1, the equation reduces to the linear form of Equation (2.7) $q_e = k \times C_e$

(2.7)

2.9.3 Temkin adsorption isotherm

Temkin isotherm contains a factor that explicitlytakes into account the adsorbent and adsorbate interactions. By ignoring the extremely low and large value of concentrations.

The model assumes that heat of adsorption (function of temperature) of all molecules in the layer would decrease linearly rather than logarithmic with coverage (Tempkin and Pyzhev, 1940). Its equation is given in Equation (2.8)

$$q_e = \frac{RT}{b_T} In(K_T Ce \quad (2.8)$$

The linearized equation is given by Equation (2.9)

$$q_e = \frac{RT}{b_T} InCe + \frac{RT}{b_T} InK_T \quad (2.9)$$

Where A_T =Temkin isotherm equilibrium binding constant (L/g)

b_T = Temkin isotherm constant

R= universal gas constant (8.314J/mol/K)

T= Temperature at 298K.

B = Constant related to heat of sorption (J/mol)

Summarized in Table 2.6 are the adsorption isotherm normal equations and their linearized form.

Table: 2.6: Adsorption Isotherm Equations.

Isotherm	Normal Equation	Linear Form	Plot
Langmuir	$q_e = \frac{q_m b C_e}{1 + bC_e}$	$\frac{C_e}{q_e} = \frac{1}{q_m} Ce + \frac{1}{q_m b}$	$\frac{C_e}{q_e}\ vs. C_e$
Freundlich	$q_e = K_f Ce^{1/n}$	$\log q_{e=} \frac{1}{n} logC_e + logK_f$	$log\ q_e$vs log C_e
Temkin	$q_e = \frac{RT}{b_T} In(K_T Ce)$	$q_e = \frac{RT}{b_T} InCe + \frac{RT}{b_T} InK_T$	$q_e\ vs\ In\ C_e$

2.10 Kinetic Models of Adsorption

Contact time from experimental results can be used to study the rate-limiting step in the adsorption process in terms of the kinetic energy. The overall adsorption process can be controlled either by one or more steps such as pore diffusion, surface diffusion or a combination of more than one step. Lagergen's first order equation, pseudo second order, second order and elovich equation are such examples of kinetic models commonly used to describe these adsorption kinetic models (Ho, 2006)

2.10.1 Pseudo first order kinetics

Lagergren showed that the rate of adsorption of solute on the adsorption is based on the adsorption capacity and follows a pseudo-first-order equation (Ozturk and Kavak, 2005) The non-linear form of pseudo-first-order equation is given by Equation (2.10)

$$\frac{dq_t}{dt} = k_1(q_e - q_t) \qquad (2.10)$$

Where, qe and qt are the amounts of adsorbate adsorbed g/g at equilibrium time and at any instant of time, t respectively, and $k_1 min^{-1}$is the rate constant of the pseudo first-order adsorption operation. The integrated rate law after application of the initial condition of qt= 0 at t= 0, is linearized to Equation (2.11)

$$\log(q_e - q_t) = logq_e - \frac{k_1 t}{2.303} \quad (2.11)$$

Pseudo first order equation refers to the assumption of the rate of change of solute uptake with time which is directly proportional to the difference in the saturation concentration and the amount of solid uptake with time (Ho, 2006).

2.10.2 Pseudo second order kinetic model

The pseudo secondorder kinetics is given by:

$$dqt/dt = K\,(qe - qt)^2 \quad (2.12)$$

Rearranging the above equation, we get in the linear form in Equation (2.13)

$$t/qt = 1/(Kqe^2) + (1/qe)\,t \quad (2.13)$$

If the pseudo second order kinetics is applicable, the plot of (t/qt) versus t gives a linear relationship that allows computation of qe and K.

The pseudo second order model which considers the rate-limiting step as the formation of chemisorptive bond involving sharing or exchange of electrons between the adsorbate and adsorbent applied.

2.10.3 Second order-kinetic model

The second order-kinetic model is shown in Equation (2.13); it is often used for chemical reaction in kinetics and chemical reaction engineering, but can also be applied for adsorption processes (Ho and Mckay, 1999).

$$\frac{1}{C_e} = k_2 t + \frac{1}{C_o}$$

(2.13)

The plot of log ($q_e - q_t$)) versus t, whereas in a true first order log q_e should be equal to the intercept. In such cases, applicability of the second order kinetics should be tested with the rate equation given by Equation (2.14)

$$\frac{dq_t}{dt} = k_2(q_e - q_t)^2$$

(2.14)

Which when integrated and linearized will give Equation (2.15)

$$\frac{t}{q_t} = \frac{1}{h} + \frac{t}{q_e} \quad (2.15)$$

Where h= k_2qe^2

2.10.4 Elovich kinetic model

The Elovich equation was first developed to describe thekinetics of chemisorption of gas onto solids (Kumara *et al.,* 2011). The linear form of the Elovich model is presented by the following equation:

$$q_t = \frac{1}{b} In(ab) + \frac{1}{b} In\ t \quad (2.16)$$

Where a is the initial adsorption rate (mg/gmin) and b is related to the extent of surface coverage and the activation energy for chemisorption (g/mg). A plot of q_t against *Int* gives a straight line with a slope of $\frac{1}{b}$ and an intercept of $\frac{1}{b}$In (ab) with correlation coefficients.

CHAPTER THREE

MATERIALS AND METHODS

3.1 Materials

The materials used in the research are listed as below

3.1.1 Chemicals and reagents

All chemicals and reagents were of analytical grade and used without further purification. Chemical reagents such as potassium dichromate (K_2CrO_7), lead nitrate (Pb (NO3)2), nitric acid (HNO_3), and distilled water were obtained from the Department of Chemical Engineering Store, Ahmadu Bello University Zaria,Nigeria.

Table 3.1 showed the list of the equipment used and their respective models

Table 3.1: List of Equipment

S /	Equipment	Model	Availability
1	FTIR machine	HC 404, PerkinElmer	NARICT. Zaria
2	SEM machine	Pro X Phenom, Netherland	Chem. Eng. ,ABU
3	AAS machine	AAS500 Jasco	Soil Sci. ABU
4	Digital Weighing balance	Adventurer Pro ModelAV264	Chem. Eng. ABU
5	Electric heater	LH 120/14Nabertherm , Bremen, Germany	Chem. Eng. ABU
6	Volumetric Flask	Pyrex	Chem. Eng. ABU
7	Measuring Cylinder	Pyrex	Chem. Eng. ABU
8	pH meter	Bibby Scientific Ltd. Jenway 3510 Model, England.	Chem. Eng. ABU
9	Filter paper		Steve Moris Nig. Chem. Limited
10	Bucket (plastic)		Steve Moris Nig. Chem. Limited
11	Stop watch		Steve Moris Nig. Chem. Limited

3.2 Methods

Figure 3.1 shows the process and methods employed in the research

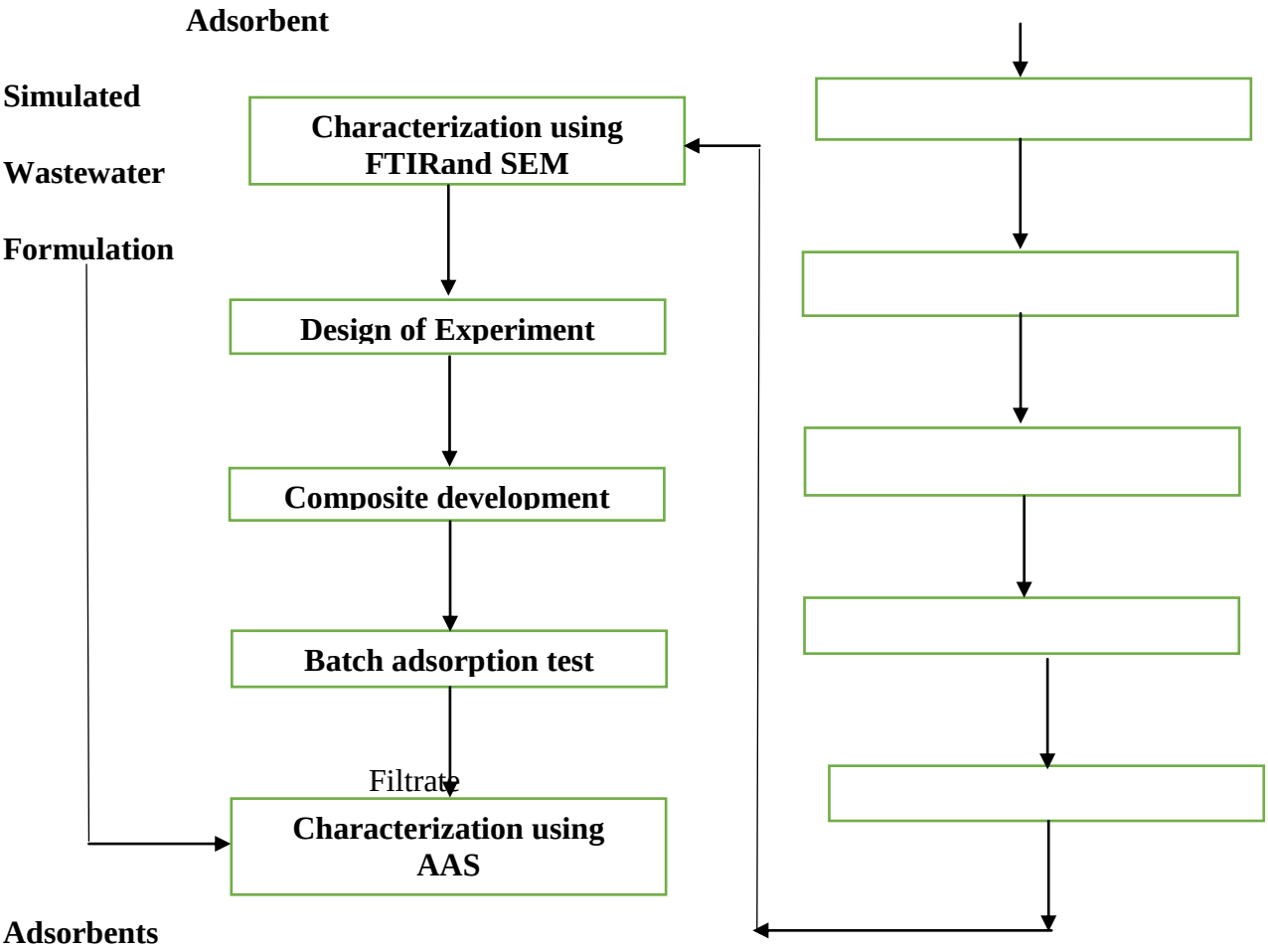
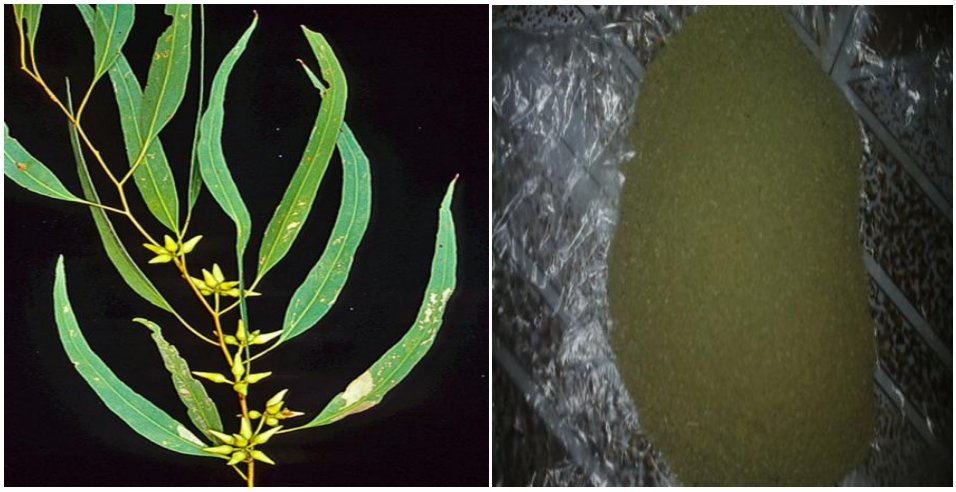


Figure 3.1 Block diagram methodology of *Eucalpytus tereticornis*composite (barks and leaves) adsorbents for chromium (VI) and lead (II) ions adsorption.

3.2.1 Sample collection and identification

The *Eucalyptus tereticornis*parts (barks and leaves) used for adsorbent production were sourced from the Institute of Agricultural Research Ahmadu Bello University-Zaria Kaduna State of Nigeria. The samples were identified at Department of Biological Science in the same University. The images of *Eucalpytus tereticorns*barks and leaves are shown in Plates3.2-3.3.



Raw *E. tereticornis* leaves Grinded *E.tereticornis* leaves

Plate3.1: Image of raw and grinded *Eucalpytus tereticornis* leaves adsorbent



Raw *E. tereticornis* barks Grinded *E. tereticornis* barks

Plate3.2: Image of raw and grinded *Eucalpytus tereticornis* barks adsorbent

3.2.2 Adsorbent preparation

Eucalpytus tereticornis (bark and leaves) were collected from Institute of Agricultural Research, Ahmadu Bello University Zaria, Nigeria (Latitude 11^{o} 05^{l} N, Longitude 7^{o} 43^{l} E) and identified at the Department of Herbarium Biological Science in the same University. These adsorbents were washed with tap water and dried in shadow for five days. Dried adsorbent was ground and sieved to particle size of 1.4mm. The adsorbent were soaked in 0.1 molar HNO_3 for 24 hrs. The choice of acid soaking time was based on the results of previous studies (Suleiman *et al*; 2007).Then after 24 hours, the

adsorbent was thoroughly washed with distilled water to remove any acid that might be present in the adsorbent and sun dried to remove the moisture content. The adsorbent was stored in plastic container at room temperature for further use.

3.2.3 Simulated wastewater preparation

All chemicals used were of analytical reagent grade. 1.6 gram of lead nitrite and 2.827 of potassium dichromate were measured and dissolved in one of distilled water to make 1000ml solution of metal ions in a separate container. This is similar to the procedure employed by Sari and Tuzen, (2009).

3.2.4: Design of experiment of adsorption Cr (VI) and Pb (II) ions on *E. tereticornis* parts

A central composite was employed resulting in a total of 13 experiments using the Design-Expert 6.0.6 version to optimize the chosen key factors namely contact time A, and adsorbent dosage B. These variables each at twolevels, low and high: A (20 – 120 mins) and B (1.0–5.0g). These levels were chosen based on previous literature.

Design summary and experimental runs for the adsorption of chromium (VI) and lead (II) ions on *Eucalpytus tereticornis* barks and leaves adsorbent is given in table 3.3 and 3.4 respectively.

Table 3.3: Design Summaryfor Adsorption ofCr (VI) and Pb (II) Ions on *Eucalpytus tereticornis* Barks and Leaves Adsorbent

Factor	Name	Unit	Low actual	High actual	Low	High
A	Contact time	Min	20.00	120.00	-1.000	+1.000
B	Adsorbent dosage	Gram	1.00	5.00	-1.000	+1.000

Presented in Table 3.4 is experimental runs generated by the Design Expert after computation of the two chosen variables with their low and high values.

Table 3.4: Experimental Runs of *E. tereticornis* Barks and Leaves Adsorbents for Adsorption of Cr(VI) and Pb (II) Ions from Simulated Wastewater

Runs	Contact time (min)	Adsorbent dose (gram)
1	20.000	1.00
2	70.000	3.00
3	70.000	3.00
4	120.00	5.00
5	70.000	5.83
6	120.00	1.00
7	20.000	5.00
8	70.00	3.00
9	140.71	3.00
10	70.000	0.71
11	70.000	3.00
12	0.7100	3.00
13	70.000	3.00

Design Expert software was employed for composite development with minimum to maximum ratio of 0.1 -0.9 of barks to leaves ratio. The summary of the design and experimental runs is presented in Table 3.5 and Table 3.6 respectively.

Table 3.5: Design Summary for Adsorption of Cr (VI) and Pb (II) Ions on the Composite of *E.tereticornis* Barks and Leaves Adsorbent from Simulated Wastewater

Factor	Name	Unit	Low actual	High actual	Low	High
A	Contact time	Min	20.00	120.00	-1.000	+1.000
B	Formulation ratio	%	0.10	0.90	-1.000	+1.000

Table 3.6: Experimental Runs of *E. tereticornis* Barks and Leaves Composite for Adsorption of Cr (VI) And Pb (II) Ions

Runs	Contact time(min)	Formulation ratio (g/g)
1	20.000	0.10
	120.00	0.10
3	20.000	0.90
4	120.00	0.90
5	0.7100	0.50
6	140.71	0.50
7	70.000	0.07
8	70.000	1.07
9	70.000	0.50
10	70.000	0.50
11	70.000	0.50
12	70.00	0.50
13	70.00	0.50

3.2.5: Batch experimental procedure for adsorption of Cr (VI) and Pb (II) ions from simulated wastewater using *E.tereticornis* barks.

Batch experiment was carried out in 500 ml glass conical flasks for adsorption of chromium (VI) and lead (II) ions separately. A specific amount of *E. tereticornis* barks (adsorbent) according to the design formulation was added in 100 ml of Cr (VI) and Pb (II) simulated wastewater solutions, and then stirred for a predetermined period (found out from design formulation) at 30^{0C}. The solutions were vigorously stirred by use of a magnetic stirrer at a constant speed of 150 rpm to reach equilibrium. Afterwards, the resultant solution was filtered using filter paper.

The agitation speed was kept constant for each run to ensure equal mixing. The raw simulated wastewater and the filtrate were analyzed using atomic adsorption spectrophotometer to determine the concentration of metal ions before and after adsorption.

.The amount of metal sorbed was calculated by material balance. Sorption capacity q was determined using the formula:

$$q_e = \frac{V\,(Co - Cf)}{m} \qquad 3.1$$

Where C_0 and C_f are the initial and final concentrations of metal in solution, V is the volume of solution and m is the mass of adsorbent.The procedure was based on previous report in the literature Induand Dinesh,(2011); Suleiman *et al*., (2007).

3.2.6: Batch experimental procedure for adsorption of Cr (VI) and Pb (II) ions from simulated wastewater using *E.tereticornis* leaves.

Batch experimental procedure for adsorption of Cr (VI) and Pb (II) ions from simulated wastewater using *E.tereticornis* leaves was also followed the same batch adsorption process employed in section 3.2.5.

3.2.7 Batch experimental procedure for adsorptionof Cr (VI) and Pb (II) from simulated wastewater using composite of *E.tereticornis*barks and leaves adsorbent

A total mass of 5.0grams being the optimum adsorbent dosage for the two adsorbents when individually used for adsorption of chromium (VI) and lead (II) ions from simulated wastewater serve as the basis for composite development with formulated ratio of 0.1-0.9g/g (barks to leaves ratio) with contact time of 20-120 minutes.

3.2.8 Adsorption isotherm studies and kinetics for composite of *E. tereticornis* barks and leaves adsorbent for Cr (VI) and Pb (II) ions adsorption

Adsorption isotherms experiment was conducted on *E. tereticornis* composite of barks and leaves adsorbent by varying initial concentration of Cr (VI) and Pb (II) ions from 20 to 120 mg/L and pH 5.6 at room temperature (30^{o}C) while maintaining the adsorbent dosage of 5g (this 5g is optimum value obtained in batch adsorption test for individual adsorbent) at 0.1 to 0.9 of barks to leaves ratio

Meanwhile, kinetics study was carried out for *E. tereticornis* composite of barks and leaves with different contact time of Cr (VI) and Pb (II) ranging from 20 to 120 minute at constant initial concentration (100mg/l) and room temperature (30^{o}C) with optimal adsorbent dosage of 5g (barks to leaves ratio).

CHAPTER FOUR

RESULTS AND DISCUSSION

4.1 Preamble

This section contain detailed analysis carried out with their results and discussion. *Eucalpytus* plant was identified as *tereticornis* specie. Other identifications are as presented in Table 4.1

Table 4.1 Result of Sample Identification

Name	Kingdom	Family	Rank	Order	Specie
Eucalyptus	Plantae	Myrtaceae	Angiosperms	Myrtales	*tereticornis*

4.2 Characterization of the Adsorbents

This section covered the FTIR characterization of *Eucalyptus tereticornis* barks and leaves.

4.2.1 FTIR analysis of *Eucalyptus tereticornis* leaves

Figure 4.1 display a number of absorption peaks, indicating the complex nature of the surfaces of *E. tereticornis* leaves (ETL).

The adsorption peaks spectra with labeled peaks are shown in Appendix E. Assignment of absorption bands shows that the functional groups such as OH-, C-H, C=O, C-O and –NH are present in ETL before and after treatment. The presence of cellulose, hemicelluloses and lignin is probably responsible for the appearance of these bands. Agricultural biomass mainly consist of lignin, cellulose, hemicelluloses and some proteins which make them effective adsorbents for heavy metal. The functional groups obtained on the surface of produced *Eucalyptus tereticornis* adsorbent agree with the literature reports.

The spectrum of *Eucalyptus tereticornis* leaves was measured within the range of 400 to 4000cm^{-1}.The broad band at 1656cm^{-1} indicates the presence of –COOH group. The peak at 3419.90 cm^{-1}shows –NH stretching of amides and amines and –OH group of

alcohols, phenols and carboxylic acids. The shift in the band is an indication that pigment and soluble organic compound has been reduced if not totally removed from the adsorbent which might have cause blockage of occupation site during adsorption process. Additionally, the peak 1674.27.1 cm^{-1} for C-O stretching vibrations in ETL before treatment shifted to (1656.91cm^{-1}) after treatment. The surface functional group before treatment ranges from 3406.40, 2929.97, 1656.91 1369.50 and 1369.50 indicates hydroxyl bonding, -OH Stretching of bonding, carboxylic acid, C=O stretching of unsaturated acid, C-O stretching of carbonyl, -OH and stretching of nitro group. IR spectra of studied adsorbent showed the presence of functional groups like carboxyl, amine, alcohol, amide and aldehyde as a result of metal ion attaches to it, and forms chelate compounds. It follows ion exchange mechanism and complexation.The reduction in the peak band after acid treatment on *Eucalyptus tereticornis* parts is similar to that reported byHamadi *et al.*, (2001).This reduction serves an indication that the release of soluble tannins and small molecular weight of phenolic from the bark and leave into water, which causes coloring and contamination might have been probably eliminated.

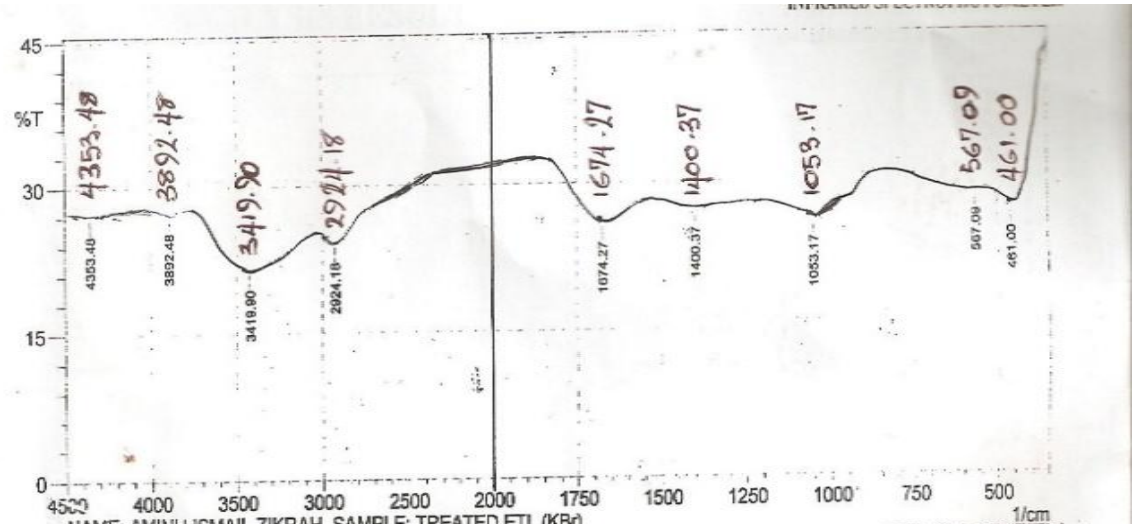


Figure 4.1:FTIR spectra of *Eucalyptustereticornis* leaves before treatment withnitric acid

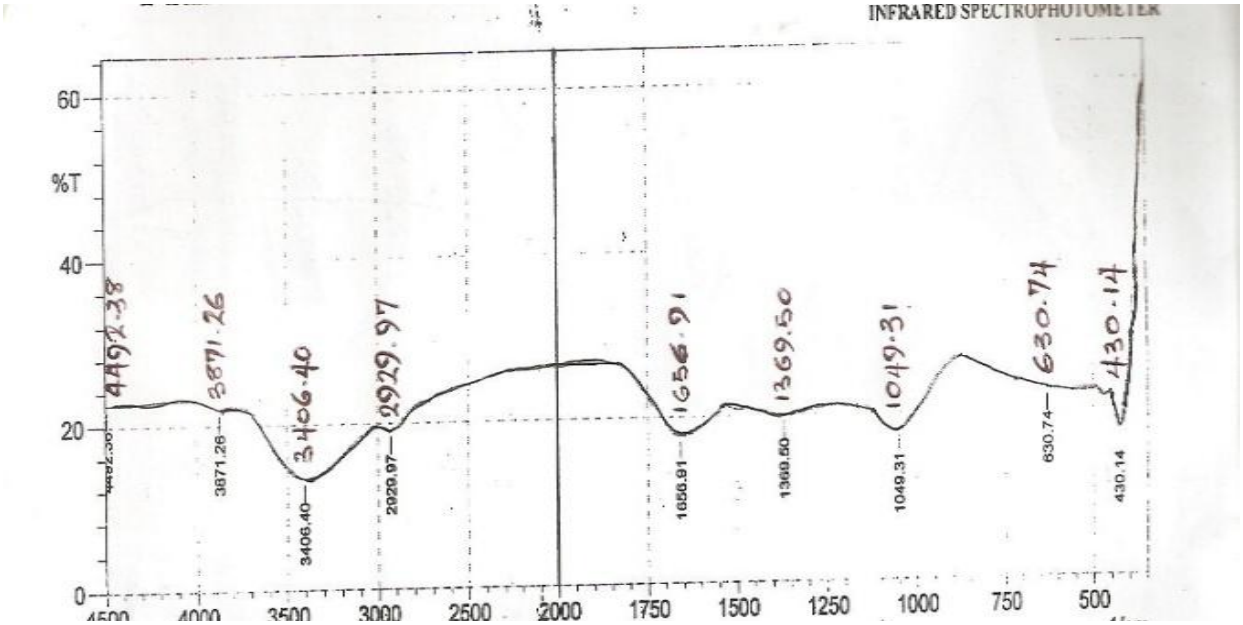


Figure 4.2: FTIR spectra of *Eucalyptus tereticornis* leaves after treatment with nitric acid

In untreated *Eucalyptus tereticornis* bark broad, absorption peaks around 3400.62 cm^{-1} are indicative of the existence of hydroxyl groups which shows presence of phenols and alcohols. Absorbance band at 2266.43cm^{-1} is indicative of COO- in carboxylic acids. Absorbance at 1631.83cm^{-1} shows presence of carbonyl groups C-O of functional groups of cellulose. Peaks observed between 1323.21 and 434.00cm^{-1}indicated as finger print.

In treated *Eucalyptus tereticornis* sample, after treatment peaks around 3425.69 cm^{-1} can be assigned to O–H stretching vibrations due to inter- and intra-molecular hydrogen bonding of polymeric compounds such as alcohols, phenols and carboxylic acids, as in pectin, cellulose and lignin, thus, showing the presence of "free" hydroxyl groups on the adsorbent surface.

The peaks at 2956.97cm^{-1} are attributed to the symmetric and asymmetric C–H stretching vibration of carboxylic acids. The peak at 2127.55 cm^{-1} is due to stretching vibration of bond amine group. The peaks around 1637cm^{-1} are due to the C-C stretching that can be attributed to the carbonyl group C–O bond.

These shifts in band after biomass modification increased the heavy metals uptake and also suggest that the alcohols/phenols and carboxylic acid groups were involved in metal binding. Plant biomasses mainly consist of lignin, cellulose, hemicelluloses and some proteins which make them effective adsorbents for heavy metal uptake.

The hydroxyl group is the main active in metals adsorption by the adsorbent produced from *eucalyptus tereticornis* parts followed by carboxylic group, carbonyl group, and amine and nitro group.

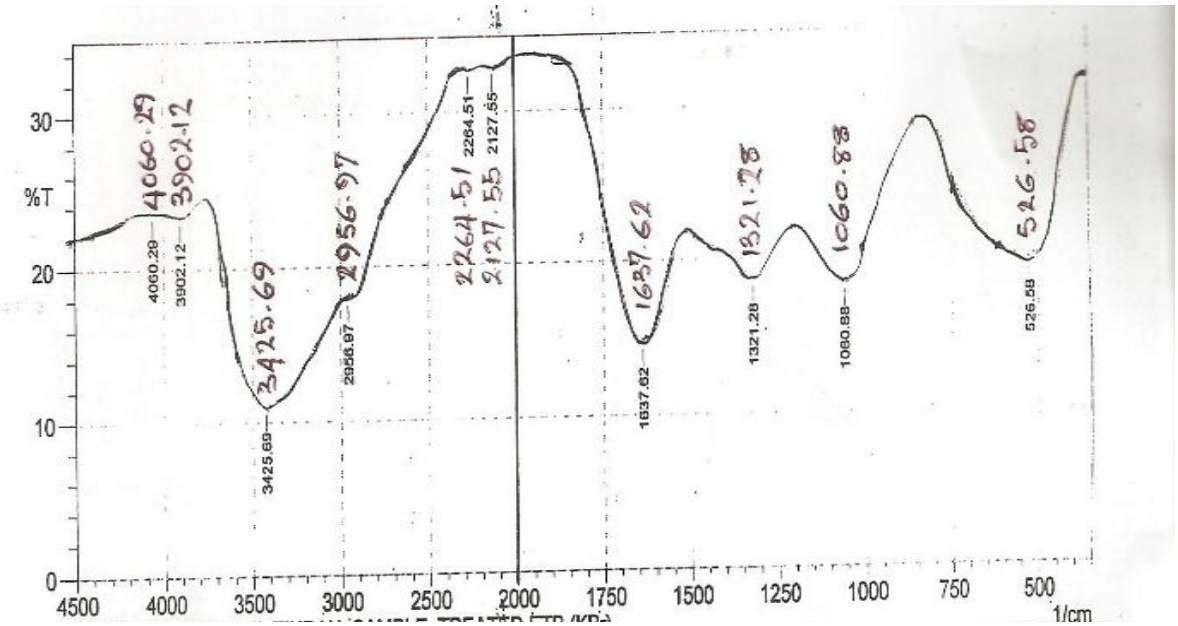


Figure 4.3:FTIR spectra of *Eucalpytus Tetreticornis* barks before treatement with nitric acid

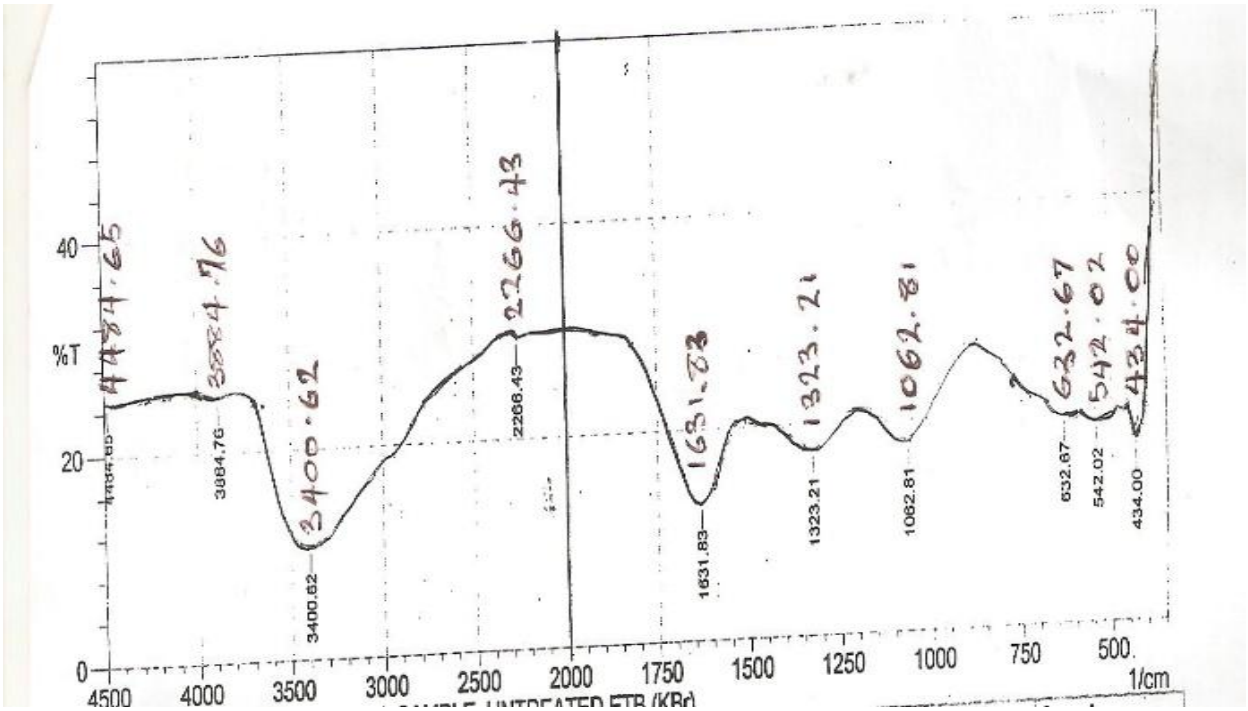
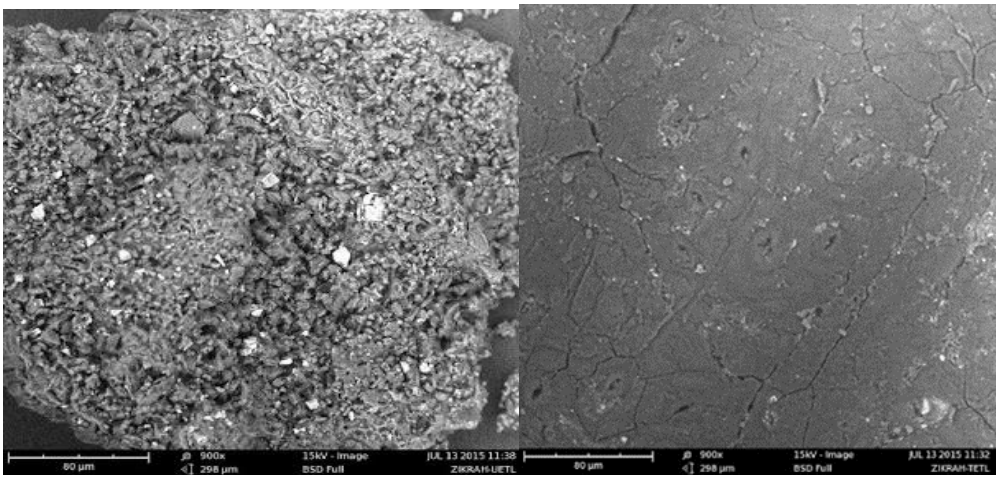


Figure 4.4: FTIR spectra of *Eucalpytus tereticornis* barks after treatedwith nitric acid

The absorption peak around 3425cm^{-1} indicates the existence of free and intermolecular bonded hydroxyl groups. The peaks observed at 2956 cm^{-1}can be assigned to the C-H stretching vibration of the -CH_2 group. The peaks around 1637 cm^{-1}correspond to the carbonyl structure with strong vibrations from a combination of C=O and C=C. The O–H and C–O band absorption peaks are observed to shift to 3400and 1631 cm^{-1}when treated with nitric acid. The result was compared with that reported by Hamadi *et al.*, (2001) and it was found that the same functional group participates in metal binding with a little deviation in the peak band. The detailed information of Fourier Transform Infrared of *Eucalpytus tereticornis* barks and leaves adsorbent peak bands are presented in Appendix E.

4.2.2 SEM Micrograph analysis *Eucalpytus tereticornis* parts

The SEM micrograph of untreated and treated *E.tereticornis* leaves (ETL) leaves with nitric acid at 900 magnification is presented in Plates4.1



UntreatedETL adsorbent Treated ETL adsorbent

Plate 4.1:SEM micrograph of *E. tereticornis* leaves before after treatment at 900 times magnification respectively.

Plates 4.2 presented SEM micrograph of *Eucalpytus tereticornis* barks before and after treatment with nitric acid at 1000 times magnification respectively.



Untreated ETBadsorbent TreatedETB adsorbent

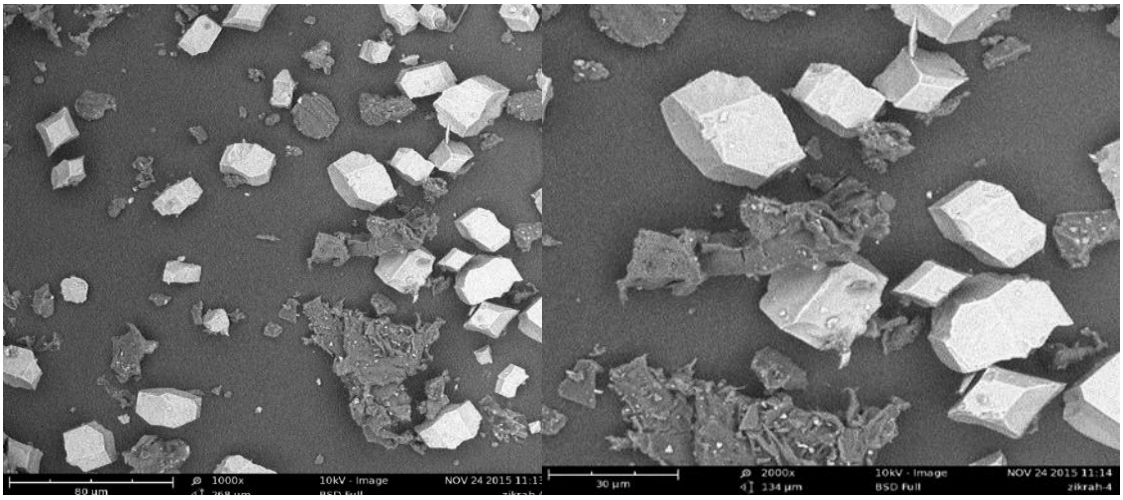
Plate 4.2:SEM micrograph of *E.tereticornis* barks and aftertreatmentwith nitric acid at 1000 times' magnifications respectively.

The SEM analysis in plates4.1 and 4.2 were used to observe the changes in the surface morphology of the adsorbent. Untreated *Eucalyptustereticornis*leaves and bark in plates4.4 and 4.5 revealed coarse nature on the surface of the adsorbent. The fine particle size on the surface of the adsorbent obtained in the treated*Eucalyptustereticornis* leaves and barks hasshown in plate 1 and 2 has also been reported by Swayampakula *et al*, (2009)which probably makes possible for the

adsorption of heavy metal on different part of the adsorbent. The plate illustrate the surface texture and porosity of barks and leaves adsorbent with holes and small openings on the surface which increase the surface contact area and led pores diffusion during adsorption.

The morphological analysis of raw and modified barks and leaves adsorbent in Plates4.1 to 4.4 showed changes of coarse particles size into fine particle size of an adsorbent. The surface area is related to adsorption capacity of an adsorbent. As the surface area increases more binding site are available for adsorbate to adsorbed (Tatycostodes *et al,* 2003).

The SEM micrograph of *Eucalpytus tereticornis* composite adsorbent for chromium (VI) and lead (II) ions adsorption after adsorption test is presented in Plate 4.3.



Chromium (VI) ion Lead (II) ion

Plate 4.3:Spent *E.tereticornis* composite after chromium (VI) and lead (II) ions adsorption

The progressive changes in the surface particles size after adsorption depicted that Chromium (VI) and lead (II) ions have deposited as aggregates in the adsorbent. In this study, the coated white portion in Plate 4.3 showed the deposited of chromium (VI) and lead (II) ions. Similar observation was reported in the work of Depeer and Suresha, (2014).

Experimental adsorption capacity results obtained for chromium (VI) and lead (II) ions on *Eucalpytus tereticornis*is leaves adsorbent given in Table 4.2.

Table 4.2:ExperimentalDesign Matrix for Chromium (VI) and Lead (II) Adsorption Capacity (AC) Using *Eucalyptus tereticornis* Leave (ETL).

Runs	Actual value	Actual value	Adsorption capacity (mg/g)	Adsorption capacity (mg/g)
	Contact time(min)	Adsorbent dose (g)	Lead (Pb)	Chromium (Cr)
1	20.00	5.00	0.0338	1.07
2	70.00	5.83	0.0211	0.99
3	70.00	3.00	0.0769	1.42
4	70.00	3.00	0.0756	1.49
5	70.00	3.00	0.0718	1.33
6	70.00	3.00	0.0564	1.36
7	70.00	0.17	0.8147	28.6
8	20.00	1.00	0.2131	1.13
9	0.170	3.00	0.0821	1.6
10	120.0	5.00	0.0246	1.09
11	70.00	3.00	0.0462	1.36
12	120.0	1.00	0.2308	3.09
13	140.71	3.00	0.0769	1.62

Table 4.2 shows the data generated for chromium (VI) and lead (II) ions adsorption runs on *Eucalyptus tereticornis* leaves, chromium (VI) adsorption response ranges from 0.99-28.6 with a ratio of max to min of 28.889 and lead (II) adsorption response ranges from 0.0211 to 0.8147 with a ratio of max to min of 38.6114 .A ratio greater than 10 usually indicates a transformation is required.This transformation divided into: Square root, Natural log, Base 10 log, Inverse square root, and Inverse, Power, Logit and ArcSin square root.

The inverse transformation of chromium (VI) ion adsorption using *Eucalyptus tereticornis* leaves is presented in Table 4.3.

Table 4.3: Inverse Transformation of Chromium (VI) Adsorption Capacity Using *Eucalpytus tereticornis* Leaves (ETL) Adsorbent

Runs	Contact time(min)	Adsorbent dosage (g)	Adsorption capacity $(mg/g)^{-1}$
1	20.000	5.00	0.930
2	70.000	5.83	1.010
3	70.000	3.00	0.700
4	70.000	3.00	0.690
5	70.000	3.00	0.750
6	70.000	3.00	0.740
7	70.000	0.17	0.035
8	20.000	1.00	0.880
9	0.1700	3.00	0.630
10	120.00	5.00	0.920
11	70.000	3.00	0.740
12	120.00	1.00	0.330
13	140.71	3.00	0.620

The response ranges from 0.99-28.6 with a ratio max to min of 28.889 for adsorption of chromium (VI) ion. A ratio greater than 10 usually indicate that transformation is required.

Therefore, the inverse transformed for adsorption of chromium (VI) ion is given in Table 4.3 used to plot the graph of adsorption capacity against contact time and adsorbent dose as presented in Figures 4.5and 4.6 respectively.

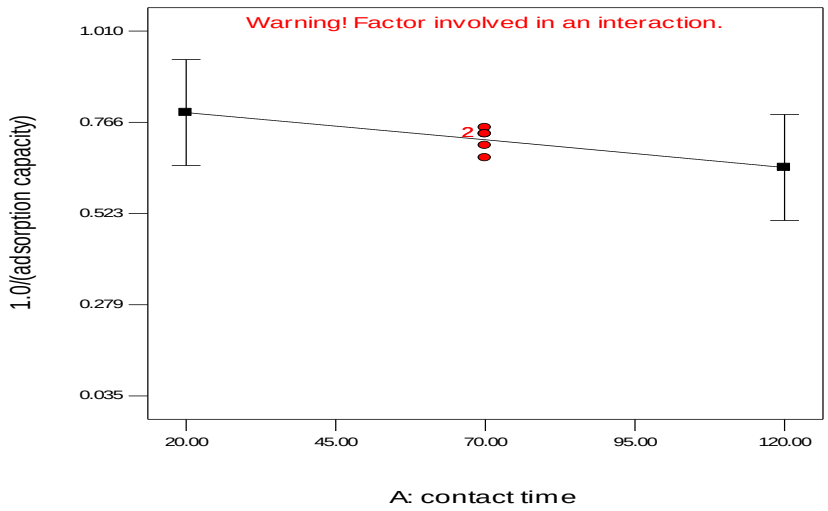


Figure 4.5:Effect of contact time against adsorption capacity of chromium (VI) ions at room temperature ($30^{o}C$).

Adsorption of chromium (VI) was measured at given contact time ranges from 20-120minutes. From Figure 4.4, the plot reveals that the adsorption of chromium (VI) ion is higher at the beginning. This is probably due to larger surface area of the *Eucalyptus tereticornis* leaves being available at beginning for the adsorption of chromium (VI) ions. It is evident from Figure 4.4 that rapid adsorption becomes slower after 20 minutes and the maximum adsorption capacity of chromium (VI) ion in this study was attained at about 20 minutes contact time. Thereafter, further increase in contact time caused ta decrease in adsorption capacity.

Replicate point at the center of regression line is central point or design point is used to determine the effect of the chosen factors and their interactions.

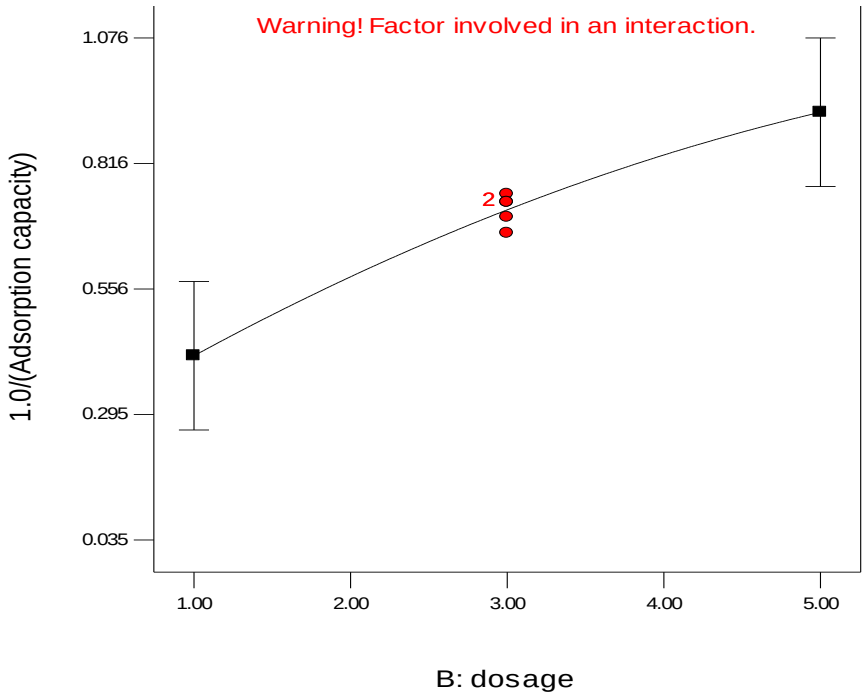


Figure 4.6: Effectof adsorbent dosage against adsorption capacity of chromium(VI) ion at constant room temperature (30^{o}C).

As it can be seen in Figure 4.6, adsorption of Cr (VI) increases as the adsorbent dosage increase from 0.035 g up to 0.93 g due to the limited availability of the number of adsorbing species for a relatively larger number of surface sites on the adsorbent at

higher dosage of adsorbent. It is plausible that with higher dosage of adsorbent there would be greater availability of exchangeable sites from metal ions (Babel and Kurniawan, 2004). Similar observation has been reported by Mashitah, *et al.*, (1999) for the adsorption of copper ions onto Pycnoporous sanguineus biomass.

Response adsorption capacity of lead (II) ion ranges from 0.0211 to 0.8147 with a ratio of maximum to minimum of 38.6114 .A ratio greater than 10 usually indicates a transformation is required. The inverse transformed is given in table 4.4.

Table 4.4: Inverse Transformation of Lead (II) Ion Adsorption Capacity Using *Eucalpytus tereticornis* Leaves

Runs	Contact time(min)	Adsorbent dosage (g)	Adsorption capacity (mg/g)
1	20.000	5.00	29.59
2	70.000	5.83	37.39
3	70.000	3.00	17.73
4	70.000	3.00	13.93
5	70.000	3.00	13.00
6	70.000	3.00	39.06
7	70.000	0.17	1.230
8	20.000	1.00	8.120
9	0.1700	3.00	12.18
10	120.00	5.00	40.65
11	70.000	3.00	21.65
12	120.00	1.00	4.330
13	140.71	3.00	13.00

The inverse transformation value of lead (II) adsorption was used to plot adsorption capacity against contact time and adsorbent dose as presented in the Figures4.6 and 4.7 respectively.

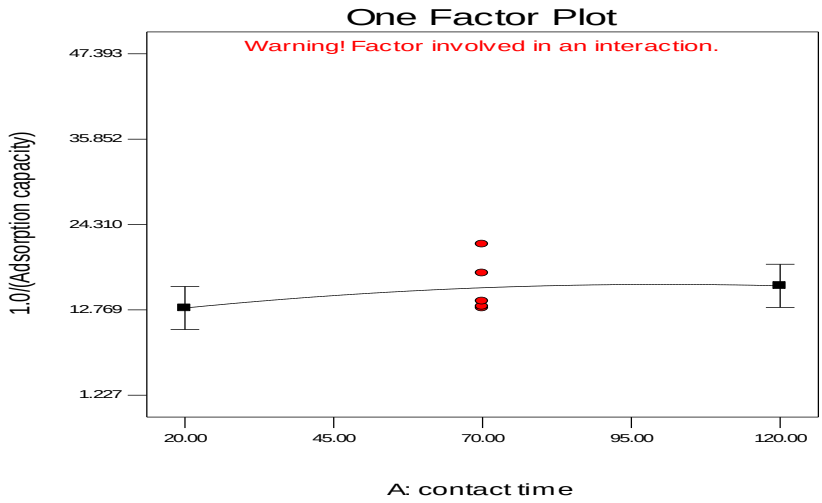


Figure 4.7: Effect of contact time against adsorption capacity of lead (II) ion at roomtemperature (30^{o}C).

It was observed that the adsorption capacity of Pb (II) ion increases with increasing contact time up to 70 min and became constant. These results indicate that the sorption process can be considered very fast because of the largest amount of active adsorption sites within 20 – 60 min. The maximum adsorption attained was at 70 min of adsorption of Pb (II) as indicated in Figure 4.6.

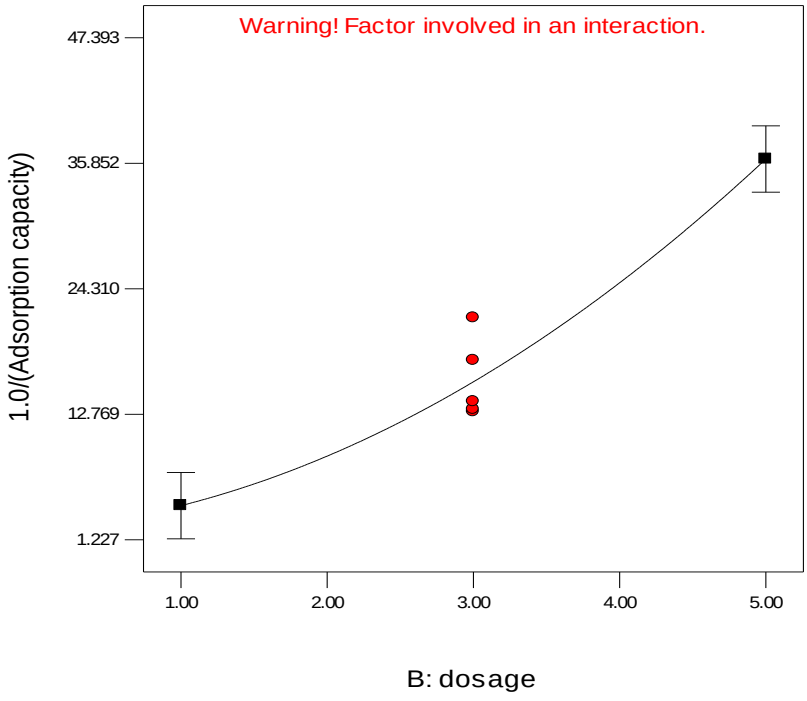


Figure 4.8:Effectof adsorbent dose against adsorption capacity of lead(II) ion at room temperature (30^{o}C)

The effect of the adsorbent dose was studied at room temperature by varyingthe sorbent amounts from 1.0 to 5.0 g/L. Figure 4.8 shows the adsorption of lead (II) ion increases rapidly with increase in the amount of adsorbent dose due to greater availability of the surface area at higher concentration of the adsorbent. The significant increase in uptake was observed when the dose was increased from 2.0 to 5.0 g/L. The maximum adsorption of lead (II) ion was obtained in the adsorbent dose of 5.0 g. Similar result was reported for the removal of Pb (II) by groundnut hull and by using Rice Husk and its ash (Suleiman *et al.*,2009).

A statistical program package Design Expert 6.0.6 was used for regression analysis of the data generated in Tables 4.3 and 4.4 to estimate the response function as a second order polynomial. Analysis of variance for the response surface model of chromium (VI) and lead (II) ions adsorption on *Eucalpytus tereticornis* leaves are presented in Tables 4.5.Model and regression coefficients were considered significant when P-values were lower than 0.05 (Liu *et al*., 2003).

Table 4.5: Summary of ANOVA Results for Cr (VI) and Pb(II) Ions Adsorption on *E. tereticornis* Leaves (ETL) Adsorbent

Parameters	Chromium (VI)	Lead (II)
Model	0.0314	< 0.0001
Standard deviation, S.D	0.16	3.32
Mean	0.69	21.99
Coefficient of variances, C.V	23.75	18.31
Rsquared	0.7750	0.9651
R^2 adjusted	0.6143	0.9401
Adeq. Precision	6.987	20.221

The data obtained in the regression analysis was used to estimating the coefficient of the regression equation. The equations were validated by the analysis of variance (ANOVA) test are presented in Equations 4.1 and 4.2.

$$\text{qCr} = 0.61403 - 5.49043E - 003A + 0.10650B - 3.09621E007A^2\ 0.012519B^2 + 1.35519E - 003AB \quad 4.1$$

$$\text{qPb} = +7.69617 - 0.028678A - 2.03873B - 4.40287E - 004 + 1.188 + 0.037138AB \quad 4.2$$

Where *qCr* and*q*Pb are the predicted adsorption capacities for chromium (VI) and lead (II) ions respectively. The variables *A and B* are the coded values of the test variables, for contact time (min) and dose (g) respectively. For testing the fit of the models, the correlation coefficient, R^2 values were evaluated and it was observed that Equation (4.1), which is the quadratic response surface model for chromium (VI) ion adsorption, had the R^2 (0.7750) value which was not close to 1 and the predicted adsorption capacity were not close to the experimental values and that of Equation (4.2), R^2 was found to be 0.9651 which was close to 1and the predicted adsorption capacity were close to experimental value.

The statistical significance of the two model equations was evaluated by the *F*-test and the analysis of variance (ANOVA). However, the *F*-test and ANOVA for the adsorbents was outlined explicitly in this section. Thus, the response surface model equation for chromium and lead ions adsorption was chosen for investigation using ETL and its detailed ANOVA were summarized in Table 4.5. The detail ANOVA results for the both chromium (VI)and lead (II) ions adsorption were presented in Table D8 to D11. In this work, the model acceptance for lead was made on the basis of 95% confidence level. The ANOVA for the lead ion quadratic model in Table 4.5 revealed that this regression model is statistically significant. In order for a term to be significant at this confidence level, the calculated probability (<0.0001) should be lower than 0.05 (Bhatia *et al*., 2009).

Parity plot for actual and predicted value for chromium (VI) and lead (II) ion adsorption onto *Eucalpytus tereticornis* leaves adsorbent are presented in Figures 4.9 and 4.10 respectively

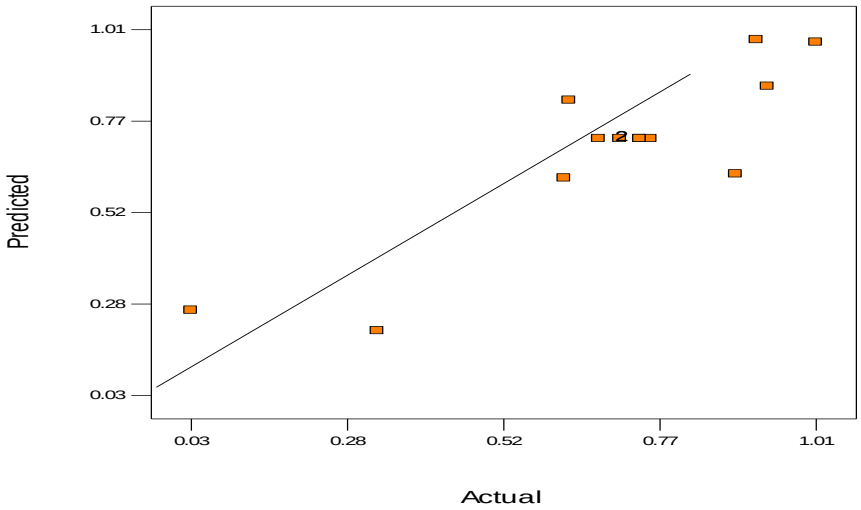


Figure 4.9: Parityplot of the actual and predicted value of chromium (VI) ion adsorptionon *E. tereticornis* leaves adsorbent

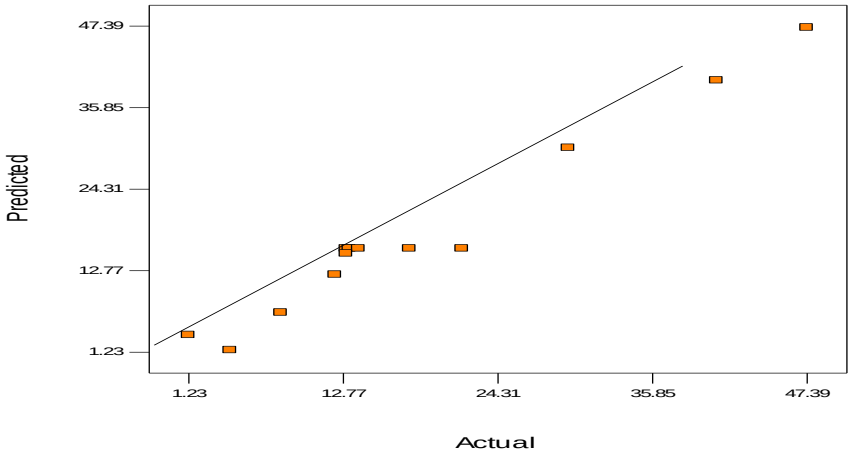


Figure4.10:Parityplot of actual and predicted value of lead (II) ion adsorptionon *E. tereticornis* leaves adsorbent

For a model to be reliable, the response should be predicted with a reasonable accuracy by the model when compared with the experimental data. In this case, the model presented a high correlation coefficient (R^2 = 0.7750 for chromium (VI) and R^2= 0.9651 showed that there is a good agreement between experimental data and predicted values (Figure 4.19 and 4.10), the model equation could be used to directly predict the

adsorption capacity under variable conditions with respect to adsorbent dose and Contact time. The model Equations for Cr (VI) and Pb (II) are statistically significant since the model Prob. >*F* values are less than 0.05 and their R^2 values are 0.7750 and 0.9651 respectively.

The response surface curves for adsorption of chromium (VI) and lead (II) ion from simulated wastewater using *Eucalpytus tereticornis*leaves are presented in Figures 4.11 and 4.12 shows interaction of time and adsorbent dose on adsorption of chromium (VI) and lead (II) ions respectively.

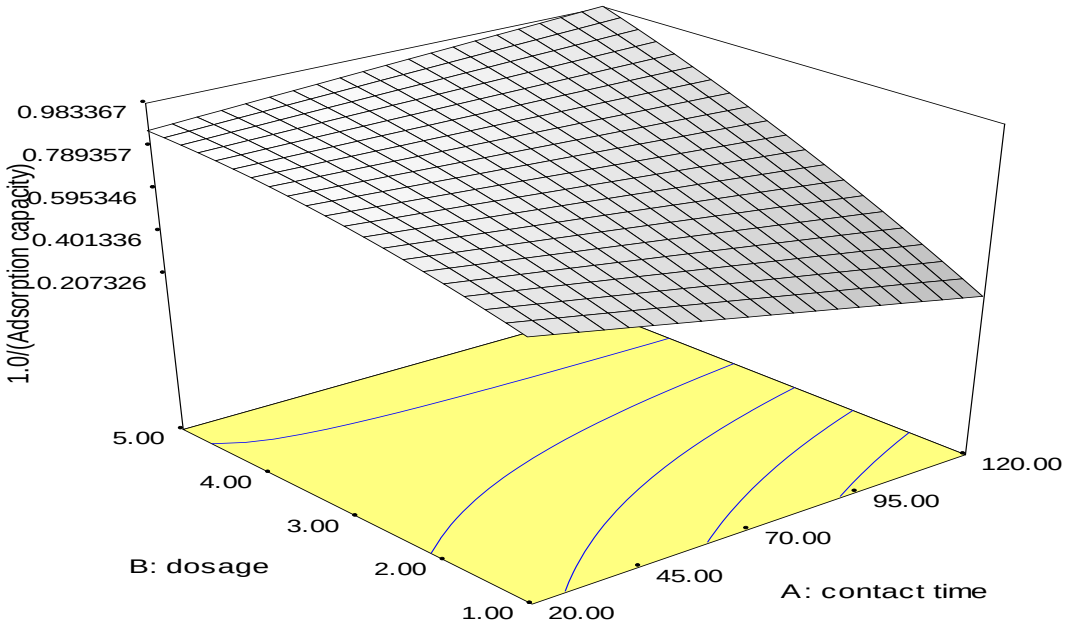


Figure 4.11:3D Response surface plot of chromium (VI) ion adsorption on *E.tererticornis* leaves

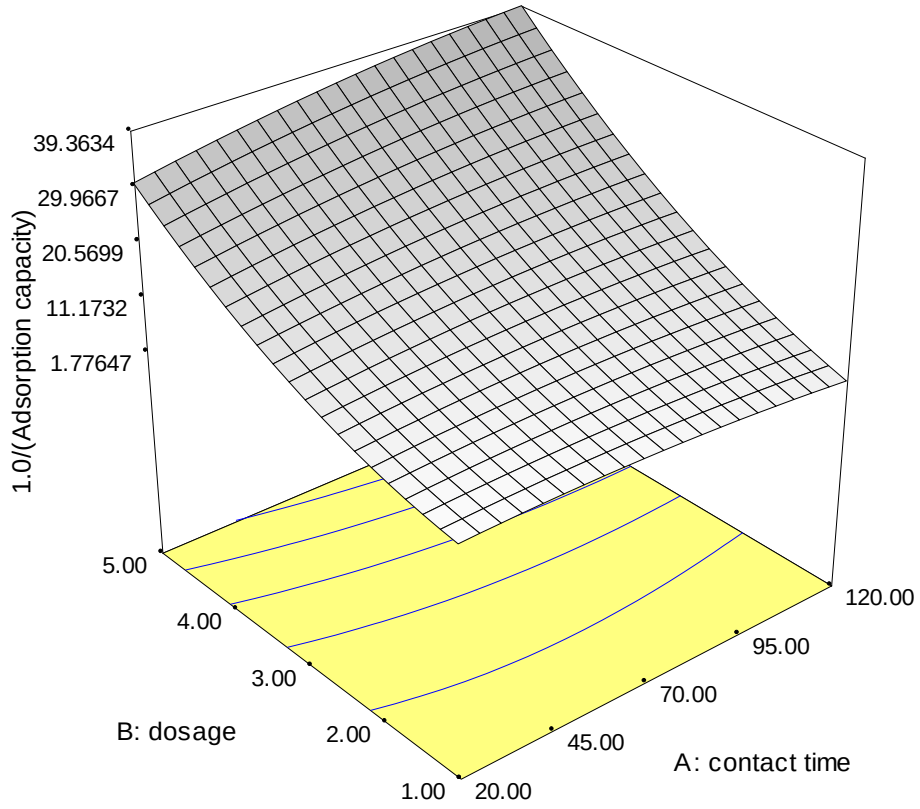


Figure 4.12: 3D Response surface plot of lead (II) ion adsorption *on E. tereticornis* leaves

The three-dimensional response surface plots are generally the graphical representations of the regression equation and are presented in Figures 4.11 and 4.12 for adsorption of chromium (VI) and lead (II) ions from simulated wastewater for which the values of adsorption capacity for different levels of the variables can be predicted. The main goal of response surface is to track efficiently for the optimum values of the variables such that the response is maximized. By analyzing the plots, the best response range can be calculated. Each response plot represents an infinite number of combinations of two test variables with the other maintained constant.

The optimum values of the process parameters were obtained from numerical optimization of chromium (VI) and lead (II) ions adsorption on ETL using the optimization summary in Appendix D9 and D12. The desired goal of numerical

optimization was to maximize the adsorption capacity. The optimum values contact time and adsorbent dose predicted by the model were 120 min and 2.45g for chromium (VI) and 120min and 3.68g for lead (II) ions adsorption respectively. A desirability value of 1.000 was obtained after optimizing the both process parameters. The response surface curves are plotted to understand the interaction of the variables and the optimum level of each variable for maximum response (Rafatullah*et.al.* 2009).

The detailed experimental design matrix for adsorption of chromium (VI) and lead (II) ions on *Eucalpytus tereticornis* barks adsorbent are presented in Tables 4.6 and 4.7

Table 4.6: Experimental Design Matrix for Chromium (VI) and Ion Adsorption Capacity (AC) Using *Eucalyptus tereticornis* Barks (ETB) Adsorbent

Runs	Contact time(min)	Adsorbent dose (g)	Chromium (VI) (mg/g)
1	20.000	5.00	1.19
2	70.000	5.83	1.05
3	70.000	3.00	1.51
4	70.000	3.00	1.51
5	70.000	3.00	1.53
6	70.000	3.00	1.57
7	70.000	0.17	0.80
8	20.000	1.00	2.33
9	0.1700	3.00	0.84
10	120.00	5.00	21.9
11	70.000	3.00	1.47
12	120.00	1.00	3.07
13	140.71	3.00	2.22

The data generated in Table 4.6 showed that chromium response ranges from 0.8-21.9 with a ratio of max to min is 27.375. Therefore, ratio greater than 10 usually indicates a transformation is required. The model was transformed using power transformation and the generated data was used to plot the curves of chromium (VI) adsorption capacity against contact time and adsorbent dose as presented in Figures 4.13 and 4.14 respectively

Figure 4.13 present the plot for adsorption capacity of chromium (VI) ion against contact time.

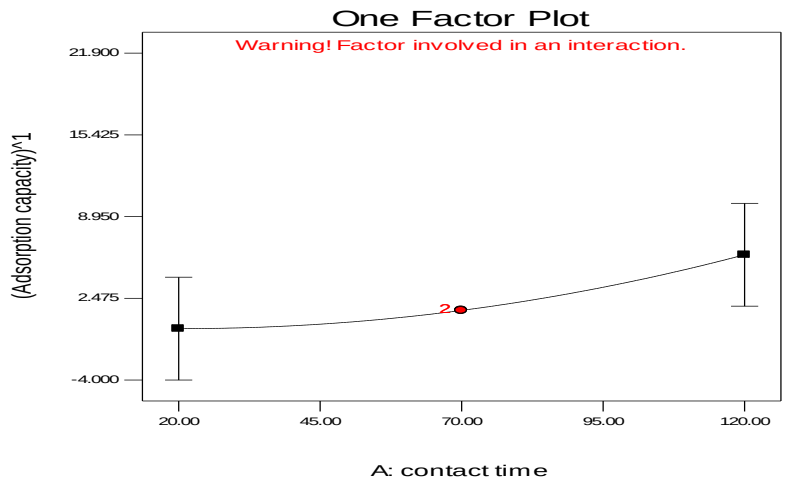


Figure 4.13: Effect of contact time against adsorption capacity of chromium (VI) at room temperature.

Effect of contact time on adsorption was studied and the result is given in Figure 4.13. As the time period for which the adsorbent was kept in the contact with metal solution was increased, adsorption capacity went on increasing up to 120 minute contact time thereby provide more active site for adsorption.

Significance test showed that contact time has impact on adsorption capacity. It was described by previous researchers also that, the contact time had impact on the development of surface area and pore structure of the adsorbent prepared from cassava peel (Sudaryanto *et al.*, 2006).

Figure 4.14 present the plot for adsorption capacity of chromium (VI) ion against adsorbent dosage.

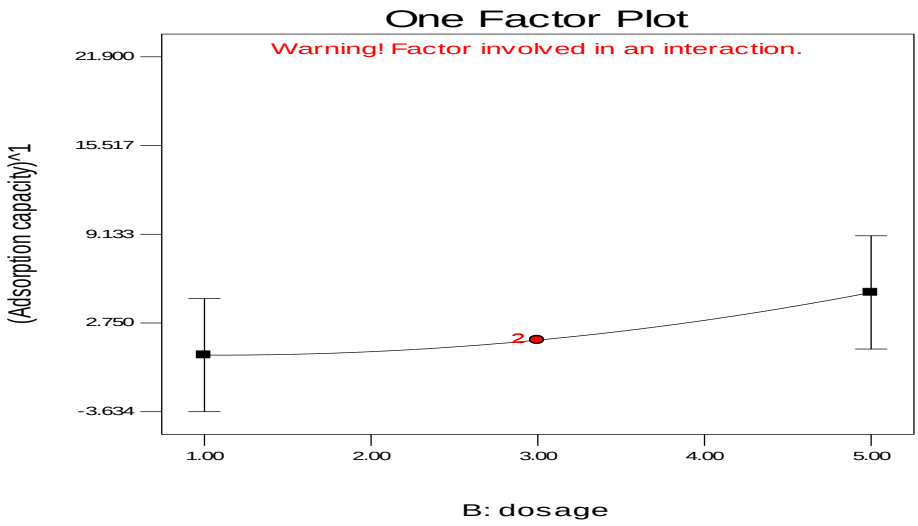


Figure 4.14: Effects of adsorbent dose against adsorption capacity of chromium (VI)at room temperature.

The result obtained in this study described the adsorption of chromium (VI) which increases as the dose of *Eucalyptus tereticornis* barks increase from 1.0 -5.0 g/l which further explaining the large availability of surface area at high concentration of adsorbent dose. Any further addition of adsorbent dose beyond this will not cause changes in the adsorption due to overlapping of adsorption site of adsorbent particles. Similar observation was reported bySiti *et al*., (2013).

Experimental design matrix for adsorption of lead (II) ion on *Eucalyptus tereticornis* barks (ETB) adsorbent is presented in Table 4.7.

Table 4.7: Experimental Design Matrix for Lead (II) Ions Adsorption Capacity (AC) Using *Eucalyptus tereticornis* Barks (ETB) Adsorbent

Runs	Contact time (min)	Adsorbent dose (g)	Lead (II) mg/g	Lead(II) (mg/g)-1
1	20.00	5.00	0.0338	32.47
2	70.00	5.83	0.0264	37.88
3	70.00	3.00	0.0513	19.49
4	70.00	3.00	0.0508	19.69
5	70.00	3.00	0.0656	15.24
6	70.00	3.00	0.0513	19.49
7	70.00	0.17	0.8147	1.230
8	20.00	1.00	0.0769	13.00
9	0.17	3.00	0.0462	21.65
10	120.00	5.00	0.0185	54.05
11	70.00	3.00	0.0513	19.49
12	120.00	1.00	0.1077	2.290
13	140.71	3.00	0.0436	22.94

Adsorption capacity of lead (II) ion response ranges from 0.0185 to 0.8147 with a ratio of max to min is 44.0378 .A ratio greater than 10 usually indicates a transformation is required. The model was transformed using inverse transformation and the new data generated in Table 4.7 was used to plot adsorption capacity against contact time and adsorbent dose as presented in Figures 4.15 and 4.16 respectively.

Figure 4.15present the effect of contact time against adsorption capacity of lead (II) ionat room temperature.

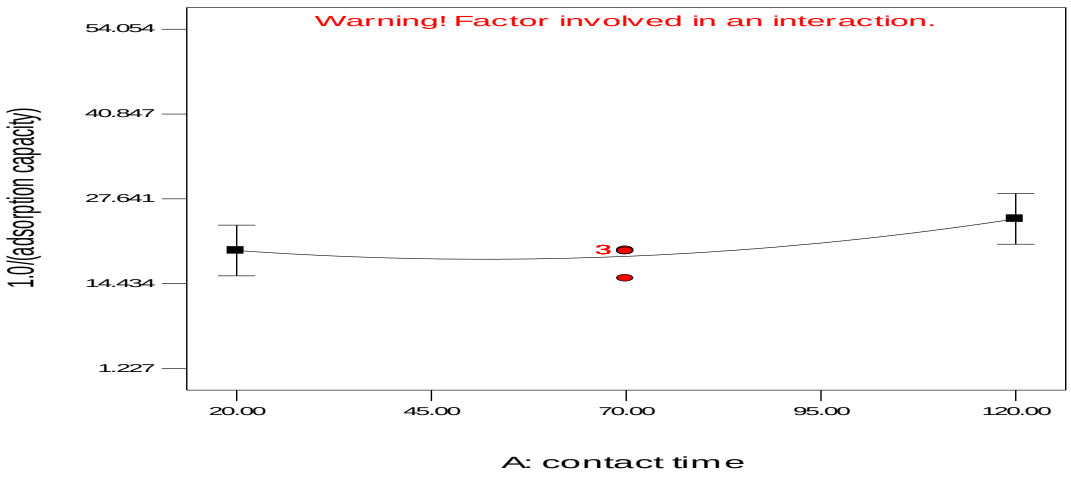


Figure 4.15: Effects of contact time against adsorption capacity of lead (II) ion atroom temperature.

Adsorption of Pb (II) ion on *E. tereticornis*barks was observed at 120min as the optimum contact time during the studies. The range of contact time varies from 20 – 120 minutes but it was revealed from the plot, as contact time increases, there is steady increased in adsorption capacity probably due to more availability of exchangeable site for lead (II) ion uptake. This result is similar to that of the literature reported by (Rafatullah *et al*., 2009).

Figure 4.16 present effect of adsorbent dose against adsorption capacity of lead (II) ion at temperature.

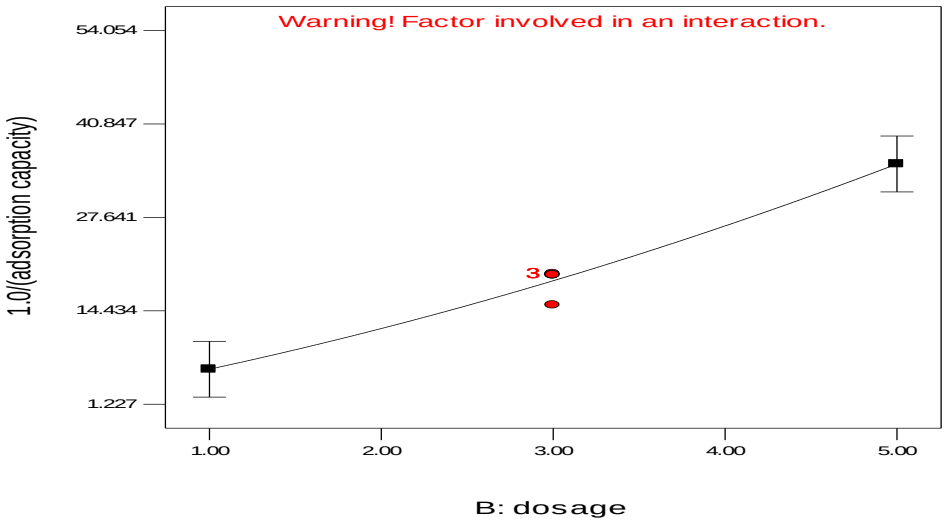


Figure 4.16: Effects of adsorbent dose against adsorption capacity of lead (II)ion at temperature.

From Figure 4.16, Increased in lead (II) ion adsorption with increasedin adsorbent dosage can be explained by the increase in active sites in the higher amount of adsorbent, thus providing easier penetration of metal ions to active sites. Similar observations were reported in the literature (Karimaian, *et al;* 2013; Sari and Tuzen, 2009).

The competence and significance of the model was justified by analysis of model for Cr (VI) and Pb (II) ions adsorption were presented in Table 4.6.

Table 4.8: Summary of ANOVA Results for Cr (VI) and Pb (II) Adsorption on *E.tereticornis* Barks (ETB) Adsorbent

Parameters	Chromium (VI) ion	Lead (II) ion
Model		
Standard deviation, S.D	4.70	8.22
Mean	3.15	20.14
Coefficient of variances, C.V	149.07	40.80
R^2 squared	0.6089	0.8163
R^2 adjusted	0.4123	0.6852
Adeq. Precision	5.959	8.178

The chromium (VI) ion model Model F-value of 2.09 implies the model is not significant and the lead (II) ion model F-value observed was 6.22 enlightening that the model was significant. Values of Prob> F less than 0.05 reflects that the model terms were significant. Here, B was significant model terms. Also the non-significant model term normally demonstrated to be 0.1.In this study, the non-significant lack of fit was more than 0.1 which implies that the non-significant lack of fit is good.

The quadratic model was selected by the software for both responses. Multiple regression analysis was used to correlate the responses of adsorption capacity with the two variables studied using a second order polynomial as shown in Equation (4). The quadratic regression models for adsorption of chromium Cr (VI) and Pb (II) ions can be represented by following Equations of (4.3) and (4.4)respectively.

$$q_{Cr\ =} 10.12806 - 0.17600A - 4.12579B + 6.05201E - 004A^2 + 0.28875B^2 + 0.049925AB \quad 4.3$$

$$q_{Pb=}\ 17.19624 - 0.28630A + 0.013948B + 9.54048E - 004A^2 + 0.46825B^2 + 0.063263AB \quad 4.4$$

Here, in Equation (4.3) and (4.4), A and B represents the coded values for contact time and adsorbent dose.

The ANOVA results for the quadratic model were defined to predict the adsorption capacities of both chromium (VI) and lead (II) ions within the range of variables applied here for preparation of *E. tereticornis* barks. In this study, Adeq. Precision obtained for the adsorption capacities for Cr (VI) and Pb (II) ions were 14.601 and 4.959 respectively which measures signal to noise ratio.

The ratio determined were greater than 4, representing that model can be used to navigate the design space. Finally, detailed ANOVA results of *Eucalpytus tereticornis* barks for chromium (VI) and lead (II) ions adsorption were presented in Appendix D2 and D5

The performance of the model can be observed by the plots of predicted value versus experimental value of adsorption capacity given in Figures.4.17 and 4.18.

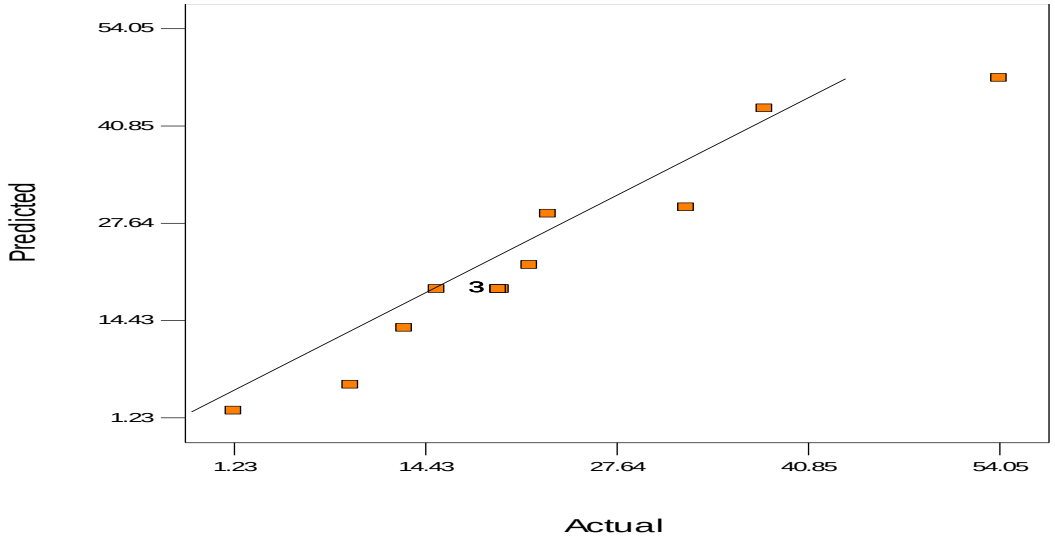


Figure: 4.17: Parity plot of the actual and predicted value of chromium (VI) ion adsorption on *E. tereticornis* barks (ETB) adsorbent.

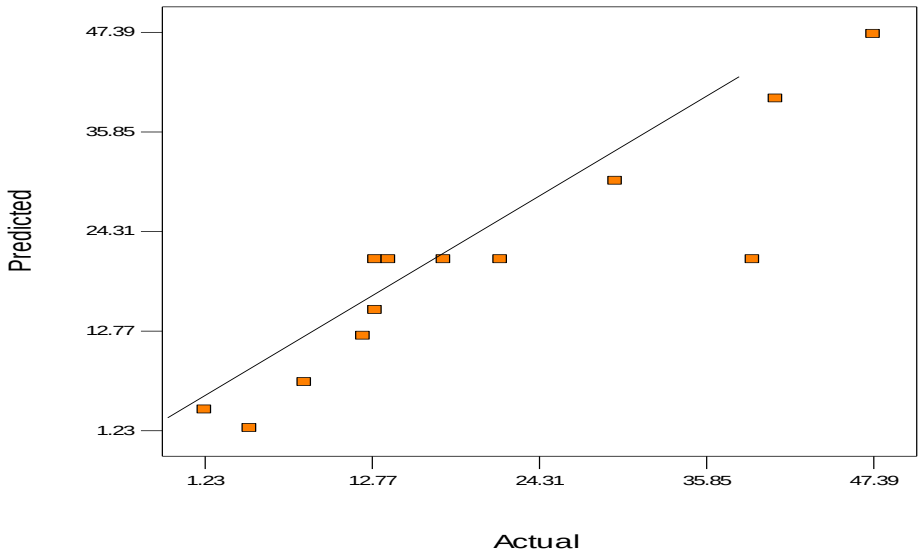


Figure: 4.18:Parity plot of the actual and predicted value of lead (II) ion adsorption on *E.tereticornis*barks (ETB) adsorbent

Parity plots of actual and predicted value of chromium (VI and lead (II) ions adsorption on *Eucalyptus tereticornis* barks from simulated wastewater shown in Figures 4.17 and 4.18 proved that the predicted responses from the empirical model are in agreement with the observed ones

Figures 4.19 and 4.20 demonstrate the effect of contact time and adsorbent dose on the responses of adsorption capacities of Cr (VI) and Pb (II) ions from simulated wastewater using *Eucalyptus tereticornis* barks adsorbent at constant pH and room temperature.

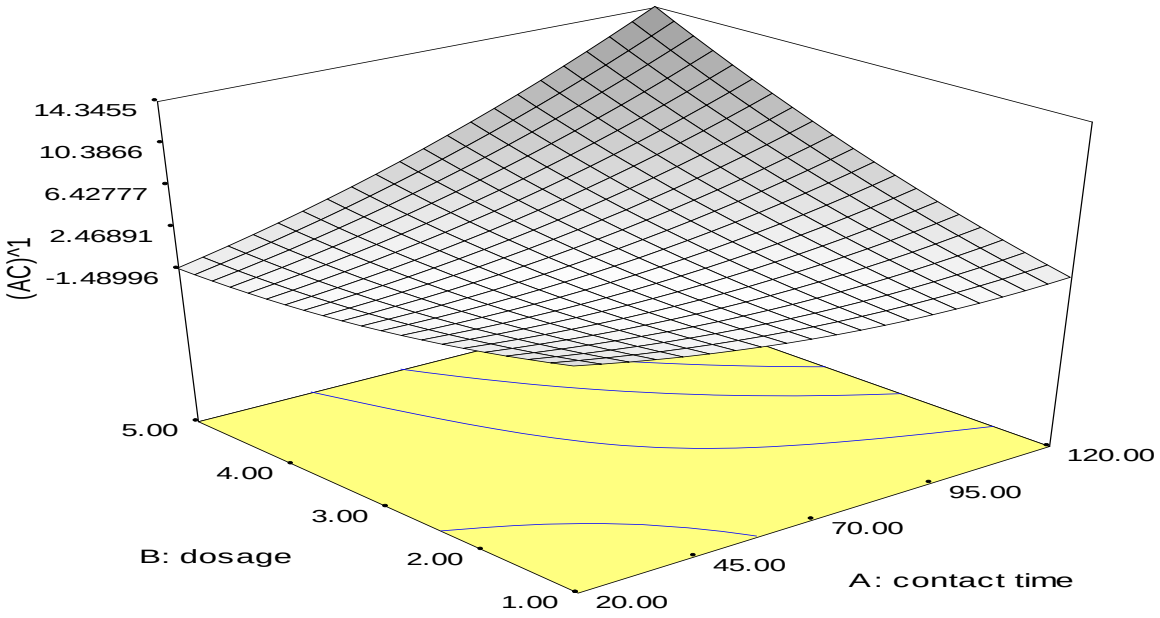


Figure 4.19: 3D Response surface plots of chromium (VI) ion adsorption on *E. tereticornis* barks (ETB) adsorbent.

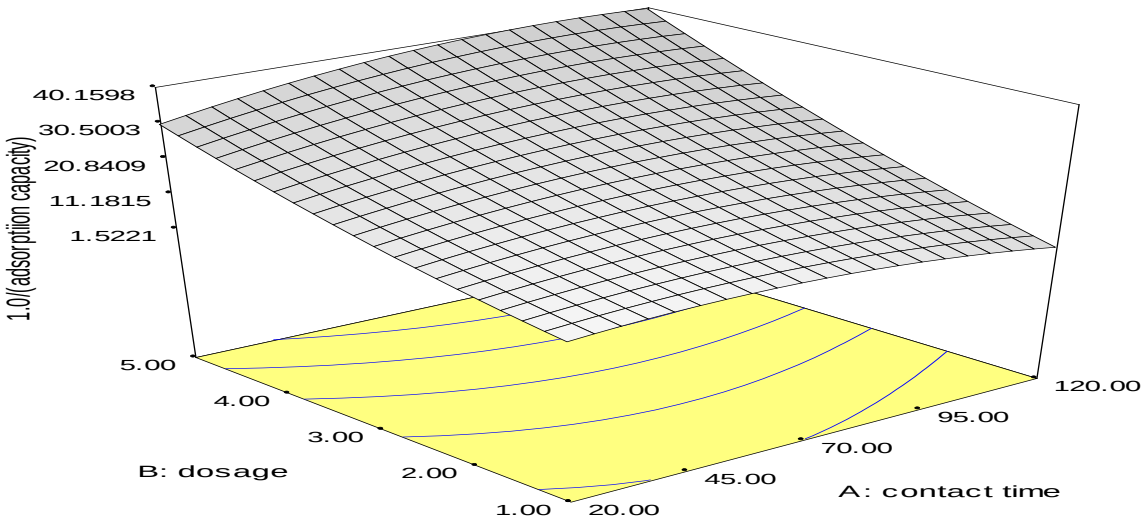


Figure 4.20: 3D Responsesurface plots of lead (II) ion adsorption on *E. tereticornis* barks (ETB) adsorbent.

The 3D response surface plots for adsorption of chromium (VI) and lead (II) ions are presented in Figures 4.19 and 4.20. These Figures demonstrate the effect of contact time and adsorbent dosage on the responses of chromium (VI) and lead (II) ions adsorption from simulated wastewater by keeping pH (5.5) and temperature (30^{o}C) constant. The curvature observed in the Figures 4.19 and 4.20 represents that, prominent effect of contact time and adsorbent dose on adsorption of chromium (VI) and lead (II) ions. From the plot, it reveals that the contact time and adsorbent is proportional with adsorption capacities.

The optimum values of the process parameters were obtained from numerical optimization of chromium (VI) and lead (II) ions adsorption on ETB using the optimization summary in Appendix D3 and D6. The desired goal of numerical optimization was to maximize the adsorption capacity. The optimum values contact time and adsorbent dosage predicted by the model were 120 min and 3.73g for chromium (VI) ion adsorption and 120min and 4.07g for lead (II) ion adsorption respectively. A desirability value of 1.000 was obtained after optimizing the both process parameters.

Composite of *Eucalpytus tereticornis* barks and leaves adsorbent for adsorption of chromium (VI) ion from simulated wastewater is presented in Table 4.9.

Table 4.9: Adsorptionof Chromium (VI) Ion on Composite of *Eucalpytus tereticornis* Barks and Leaves Adsorbent

Runs	Contact time(min)	Formulation ratio (g/g)	Adsorption capacity of Cr(VI) ion (mg/g))^1
1	20.000	0.10	50.0
2	120.00	0.10	59.0
3	20.000	0.90	8.89
4	120.00	0.90	14.0
5	0.7100	0.50	6.00
6	140.71	0.50	8.00
7	70.000	0.07	100
8	70.000	1.07	6.54
9	70.000	0.50	10.0
10	70.000	0.50	12.0
11	70.000	0.50	12.0
12	70.000	0.50	10.0
13	70.000	0.50	10.0

From the response data generated for adsorption of chromium (VI) ion, response ranges from 6 to 100, the ratio of maximum response to minimum was 16.667. A ratio greater than 10 usually indicates a transformation is required. The model was transformed using a power transformation.

Data generated in Table 4.9 were used to study the effect and interactions of contact time and adsorbent dose on adsorption of chromium (VI) ion (response) plotted in Figures 4.21 and 4.22.

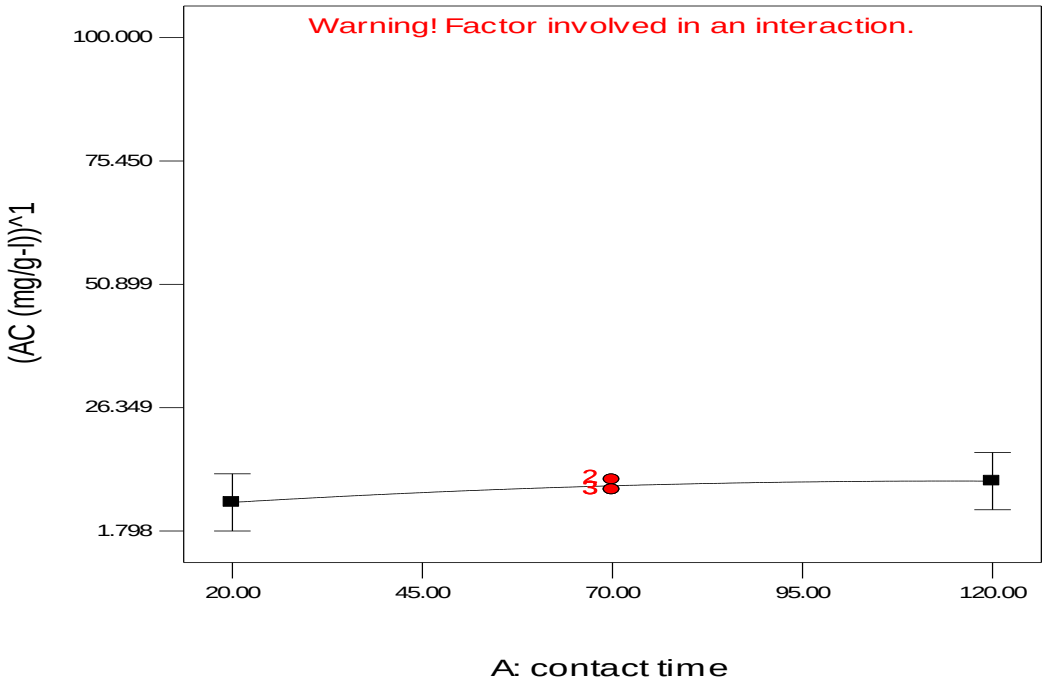


Figure 4.21: Effect of contact time against chromium (VI) ion adsorption on composite *Eucalyptus tereticornis* barks and leaves adsorbent

In order to explore the interaction of contact time and adsorbent dosage on the sorption capacity, the one factor plots of these two variables were presented in Figures 4.21 and 4.22.

From Figure 4.21, only a marginal change of sorption capacity with the variation of contact time was observed .This result implied that the contact time exhibits a less significant influence on the adsorption capacity (AC).

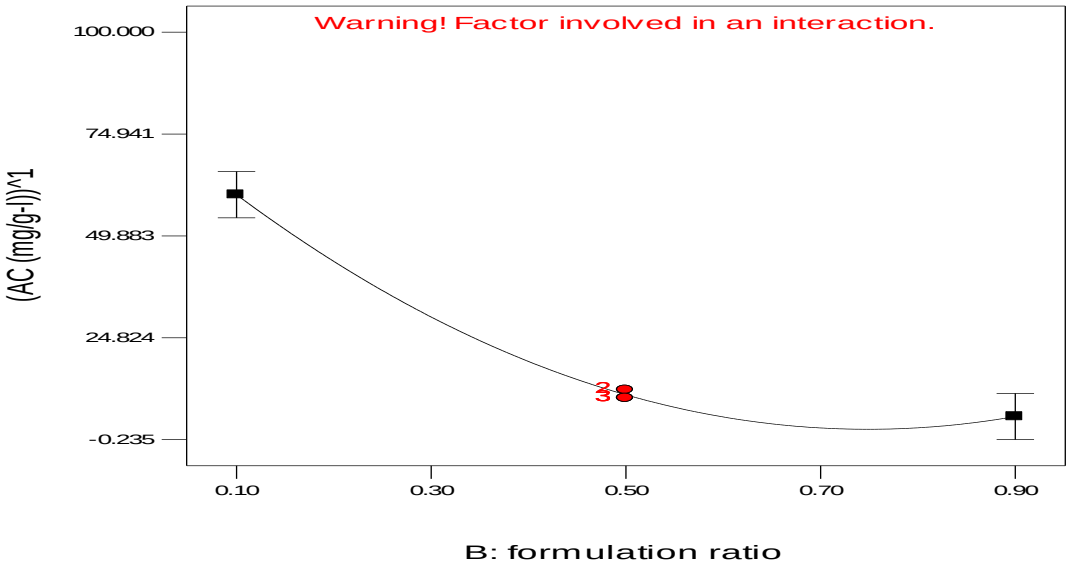


Figure: 4.22: Effect of formulation ratio against chromium (VI) ion adsorption on composite *Eucalyptus tereticornis*.

It normally expected that adsorption capacity should increase with increase in adsorbent dose but as it can be seen in Figure 4.21, adsorption capacity decreases with increased in adsorbent dose and this condition could be due to the aggregation or overlapping of adsorption sites caused by overcrowding of *Eucalyptus tereticornis* composite adsorbent. The decrease in total adsorbent surface available to the metal ion obtained in this study was similar to that reported by (Shukla *et al*., 2002). At high adsorbent dose, some adsorption sites remain unsaturated during the adsorption process because they are not accessible. .

Experimental data obtained for adsorption of lead (II) ion from simulated wastewater using composite of *Eucalpytus tereticornis* barks and leaves adsorbent is given in Table 4.10

Table 4.10: Adsorption of Lead (II) Ion on Composite of *Eucalpytus tereticornis* Barks and Leaves Adsorbent

Runs	Contact time (min)	Formulation ratio (g/g)	Adsorption capacity of lead (II) ion (mg/g)	Adsorption capacity of lead (II) ion $(mg/g)^{-1}$
1	20.000	0.10	19.2	0.052
2	120.00	0.10	19.2	0.052
3	20.000	0.90	1.11	0.990
4	120.00	0.90	1.56	0.640
5	0.7100	0.50	1.01	0.500
6	140.71	0.50	2.00	0.300
7	70.000	0.07	26.2	0.038
8	70.000	1.07	3.33	0.990
9	70.000	0.50	3.33	0.300
10	70.000	0.50	3.67	0.270
11	70.000	0.50	3.35	0.430
12	70.000	0.50	3.33	0.450
13	70.000	0.50	10.0	0.300

From the response data generated for adsorption of lead (II) ion, response ranges from 1.01 to 26.2, the ratio of maximum response to minimum of 25.9406. A ratio greater than 10 usually indicates a transformation is required. The model was transformed using inverse transformation and the data was used to plot the graphs in Figures 4.23 and 4.24 respectively.

Presented in Figures 4.23 and 4.24 demonstrated the combined effect of contact time and formulation ratio on the responses of chromium (VI) and lead (II) ion adsorption on composite of *Eucalpytus tereticornis* barks and leaves adsorbent from simulated wastewater.

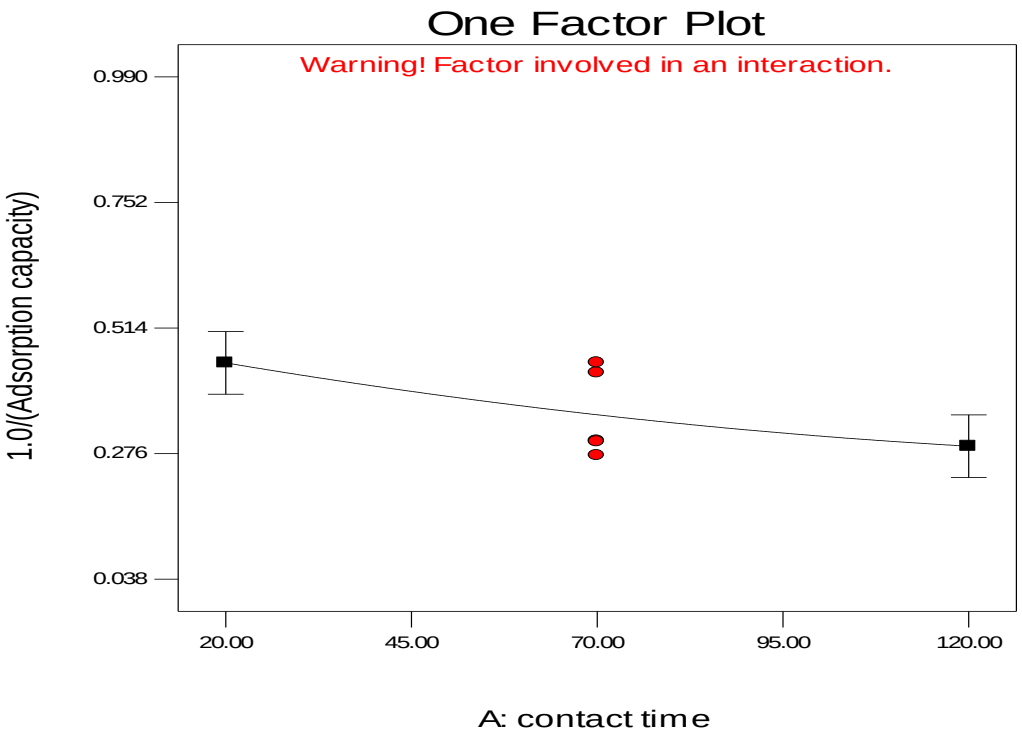


Figure 4.23: Effect of contact time against lead adsorption on composite of *Eucalyptus tereticornis* barks and leaves adsorbent

Adsorption of lead (II) ion was measured at given contact time ranges from 20-120 min, the plot revealed that Cr (VI) adsorption capacity was higher at the beginning. The rapid rate of adsorption process at the initial stage of adsorption could probably be due to larger surface area of the bark to leaves ratio being available at beginning for the adsorption of chromium (VI) ion reported by Senthil and Kirthika, (2009). Further increase in contact time led to progressive decrease in adsorption capacity due to the saturation of active site during the adsorption process.

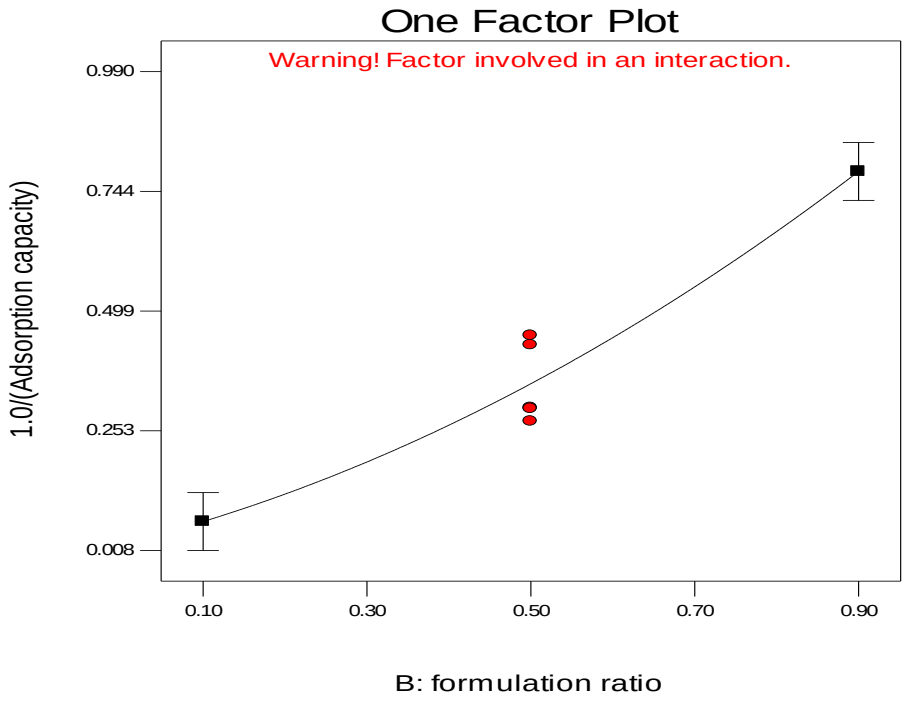


Figure 4.24: Effect of contact time against lead adsorption on composite of *Eucalyptus tereticornis* barks and leaves adsorbent

From Figure 4.24, it is apparent that the adsorption capacity of lead (II) ion increased as the adsorbent dosage increases from 0.008 g up to 0.990 g due to the limited availability of the number of adsorbing species for a relatively larger number of surface sites on the adsorbent at higher dosage of adsorbent. It is plausible that with higher dosage of adsorbent there would be greater availability of exchangeable sites from metal ions. Besides, literature suggested that the increase in adsorbent dosage in the suspension at a given metal concentration enhances the metal/adsorbent ratio, and thus increases the metal uptake per unit adsorbent, as long as the latter is not saturated (Chowdhury, *et al.*,2011).

Presented in Table 4.11 is the summary of analysis of variance for adsorption capacities of Cr (VI) and Pb (II) ions on *Eucalpytus tereticornis* composite (ETC) barks and leaves adsorbent from simulated wastewater.

Table 4.11: Summary of ANOVA Results for Adsorption Capacities of Cr (VI) and Pb (II) Ions on *Eucalpytus tereticornis* Composite (ETC) Barks and Leaves Adsorbent

Parameters	Chromium (VI) ion	Lead (II) ion
Model	< 0.0001	< 0.0001
Standard deviation, S.D	6.57	0.068
Coefficient of variances, C.V	27.87	16.75
Mean	23.57	0.41
R^2 squared	0.9691	0.9723
R^2 adjusted	0.9470	0.9526
Adeq. Precision	20.202	21.839

On the basis of the experimental data in Table 4.10, a second order response surface model fitting in the form of ANOVA is given in Table 4.11.In general, the probability value with less than 0.0500 is preferable. It can be seen from Table 4.11 that the P-value (P>F) obtained by the two model were less than 0.0001. It indicated the model terms are statistically significant. The P-values of the linear coefficient on the operating parameters were all less than 0.0001. It suggested that these two variables have significant influence on the sorption capacity.

$$qCr=+\ 72.19499 + 0.13333A - 201.96184B - 4.76250E - 004A^{2} + 137.1523B^{2}$$

$$0.048625AB \qquad 4.5$$

$$qPb=+\ 0.015863 - 4.80905E - 004A + 0.72614B + 7.74204E - 006A^{2} +$$

$$0.47717B - 4.36342E - 003AB \qquad 4.6$$

Parity plots of actual versus predicted values of chromium (VI) and lead (II) ions adsorption are presented in Figures 4.25 and 4.26respectively.

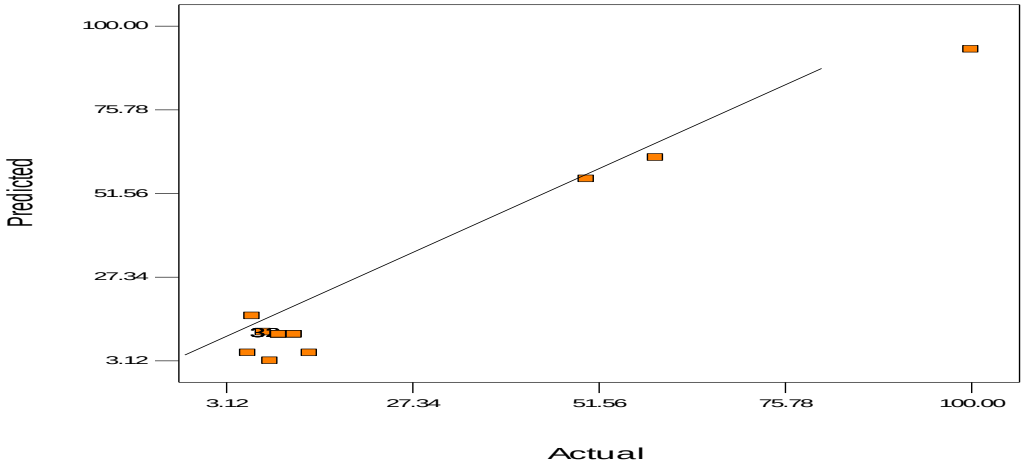


Figure: 4.25: Parity plots of actual and predicted value of chromium (VI) ion adsorption on composite of *Eucalpytus tereticornis* barks and leaves adsorbent

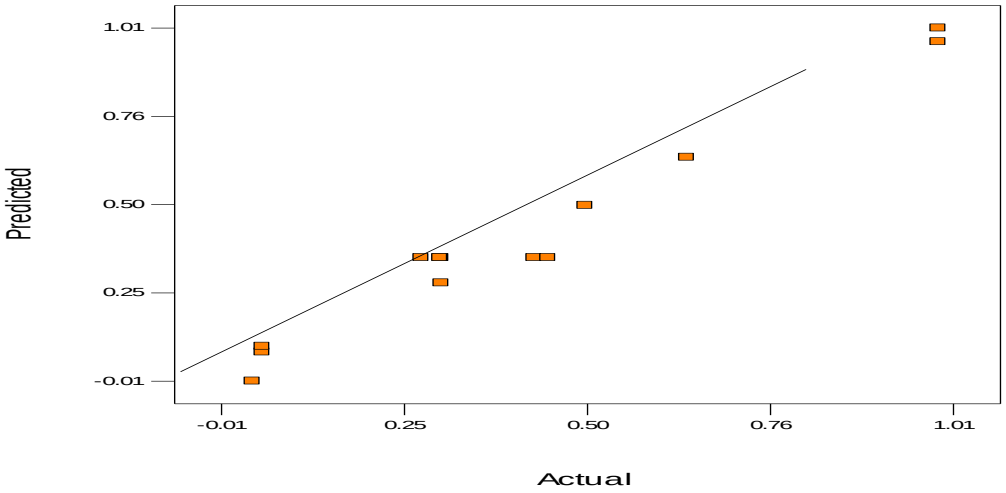


Figure 4.26: Parity plotsof the actual and predicted value of lead (II) ion adsorption on composite of *Eucalpytus tereticornis* barks and leaves adsorbent

The coefficient of determination (R^2) is a measure of goodness of fit. Its value varies from 0.0 to 1.0, with higher values being preferable. In this case, the value of R^2obtained for chromium (VI) and lead (II) ions adsorption are 0.9691 and 0.9723 as shown in Table 4.7. This result indicates that the fitted model could explain 97 % of the variability. The accuracy and general ability of the polynomial model were reliable. In addition, "Adeq Precision" measures the signal to noise ratio and a ratio is greater than 4.0 being desirable in a model. The ratio obtained was 20.202 and 21.839 as shown in Table 4.7.It indicated that an adequate signal was proved in this model. It also revealed

that this model could be used to navigate the design space. In summary, the ANOVA analysis demonstrated that the linear regression model could effectively predict the *E.tereticornis* composite for chromium (VI) and lead (II) ions adsorption.

Presented in Figures 4.27 and 4.28 are the 3D response surface of chromium (VI) and lead (II) ions adsorption on composite of *Eucalpytus tereticornis* barks and leaves adsorbent.

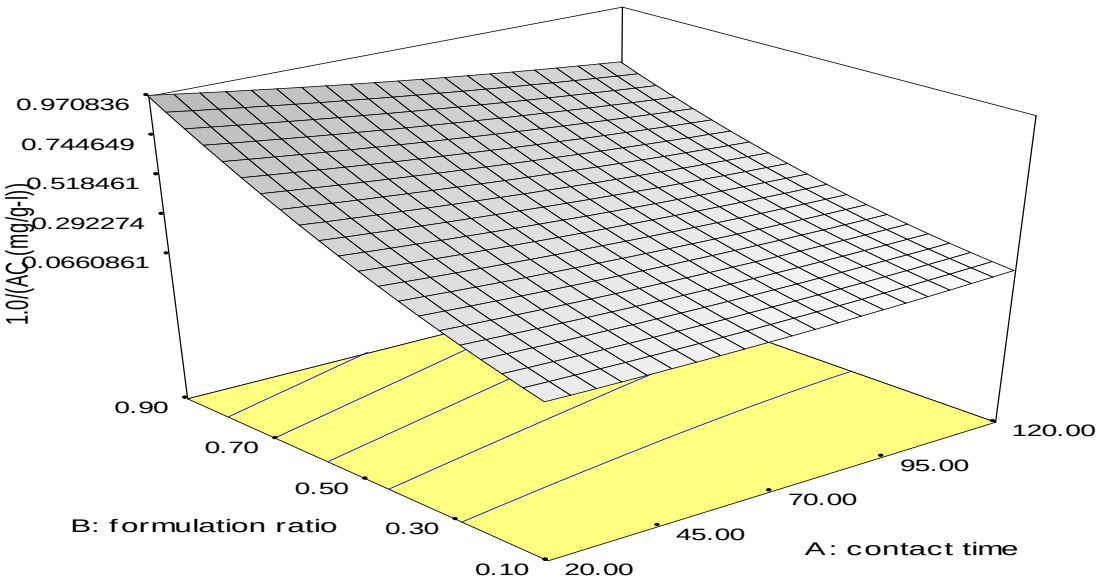


Figure 4.27: 3D Response surface plot of chromium(VI) ion adsorption on composite of *Eucalpytus tereticornis* barks and leaves adsorbent

Figure 4.26 and 4.27showing the variation in sorption capacity of the adsorbents with respect to process conditions. Regression equation of the model was analyzed using 3D response surface and one factor variables. The 3D response surface plots were obtained by plotting the response (adsorption capacity) on the Z-axis against any two variables while the other variables were kept at zero level.

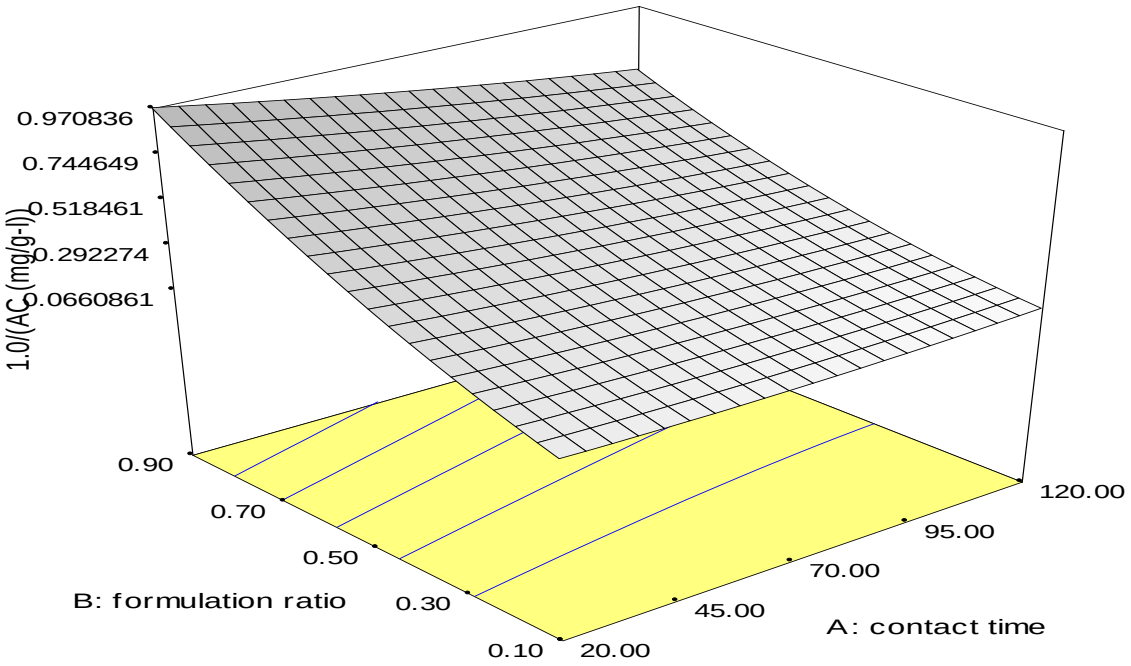


Figure 4.28: 3D Response surface plot of lead (II) ion adsorption on composite of *Eucalpytus tereticornis* barks and leaves adsorbent.

The optimum values of the process parameters were obtained from numerical optimization of chromium adsorption on ETC using the optimization summary in Appendix D15 and D18. The desired goal of numerical optimization was to maximize the adsorption capacity. The optimum values contact time and adsorbent dosage predicted by the model were 120 min and 0.10g for chromium adsorption and 120min and 0.90g for lead respectively. A desirability value of 0.771and 0.794 was obtained after optimizing the both process parameters.

4.3 Comparative Studies for Chromium (VI) and Lead (II) Ions Adsorption using *Eucalyptus tereticornis* Composite of Barks and Leaves Adsorbents

Adsorption chromium (VI) ion was compared with that of lead (II) ion at the same experimental conditions. Table 4.8 showed the experimental results obtained for chromium (VI) and lead (II) ions and the maximum adsorption capacity was measured

as 100mg/g and 26.2mg/g respectively. Chromium (VI) ion adsorption shows a higher adsorption capacity compared to lead (II) ion.

4.4 Adsorption Isotherm and Kinetic Modeling

4.4.1 Adsorption isotherm

In this study, three equilibrium models were analyzed to investigate the suitable adsorption isotherm and the detailed information of isotherm and kinetic parameters are presented in Appendix A-C

The equilibrium data were tested with the adsorption isotherms: Langmuir, Freundlich and Temkin isotherm. Figures 4.15, 4.16 and 4.17 show Langmuir, Freundlich and Temkin's chromium adsorption isotherm plot respectively.

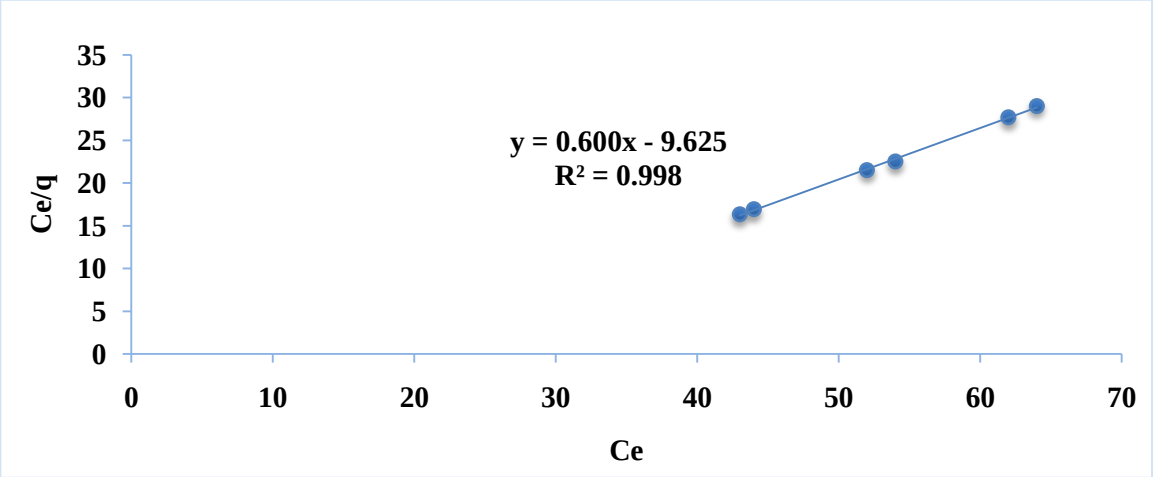


Figure 4.29: Chromium (VI) ion adsorption on *E.tereticornis* composite Langmuir plot

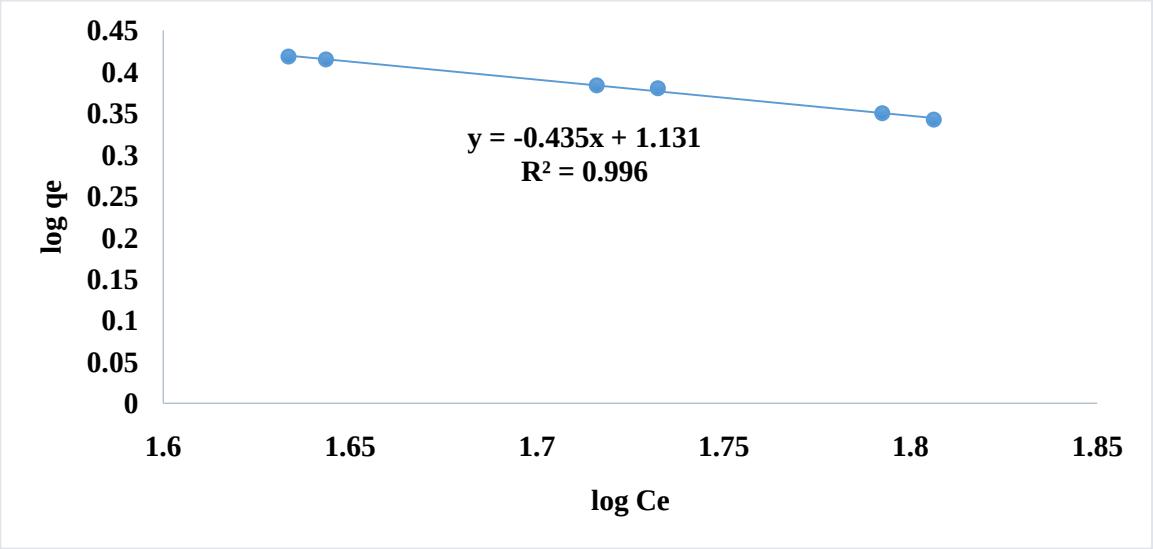


Figure 4.31: Chromium (VI) ion adsorption on composite of *E.tereticornis* Freundlich plot

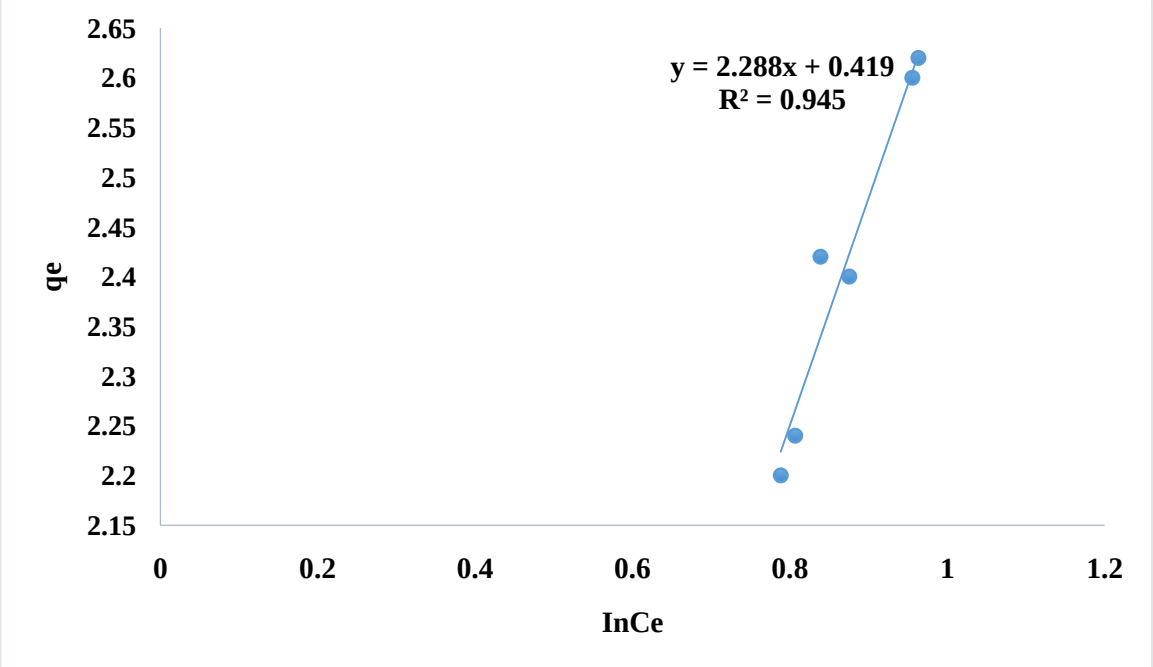


Figure 4.31: Chromium (VI) ion adsorption on composite of *E .tereticornis*Temkin plot

The constants of the plots are shown in Table 4.11 and the detailed calculations and Tables for the plots are given in Appendix A.

Langmuir adsorption isotherm best fit the adsorption with R-squared value of 0.9987. The heat of adsorption b_T value of1.082kJ/mol is very low signifying that it is physical adsorption. The Lagmuir R_L value is 0.0036 showing favourable adsorption isotherm

studies. R_L is vital dimensionless factor parameter. The value of R_L indicates the type of isotherm to be either unfavourable (R_L >1), linear (R_L =1) and favourable (0< R_L<1) or irreversible (R_L =0)

Table 4.12 presentsisotherm studies parametersfor chromium (VI) ion adsorption with their details calculation given in the Appendix A.

Table 4.12: Chromium (VI) Ion Adsorption Isotherm Parameter Values

Isotherm	Parameter	Value
Langmuir	B	16.0186
	R_L	0.0036
	R^2	0.9987
Freundlich	K_f	13.52
	1/n	-0.4346
	R^2	0.9961
Temkin	K_T	1.1607
	b_T	1.082
	R^2	0.9454

Figures 4.32, 4.33 and 4.34 present Langmuir, Freundlich and Temkin's lead (II) ion adsorption isotherm plot respectively.

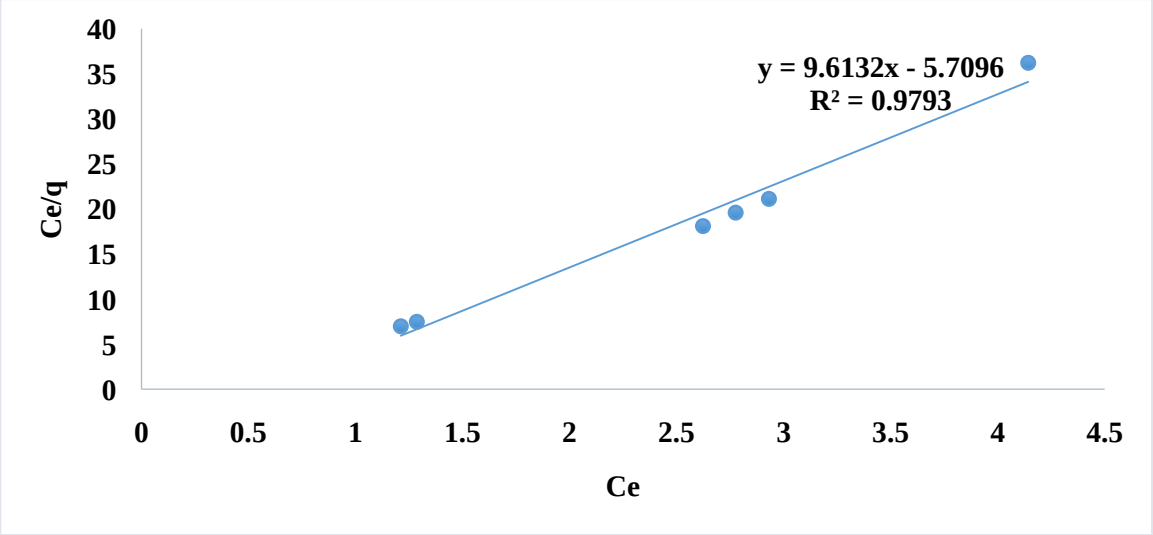


Figure 4.32: Lead (II) ion adsorption on composite of *E. terticornis* Langmuir plot

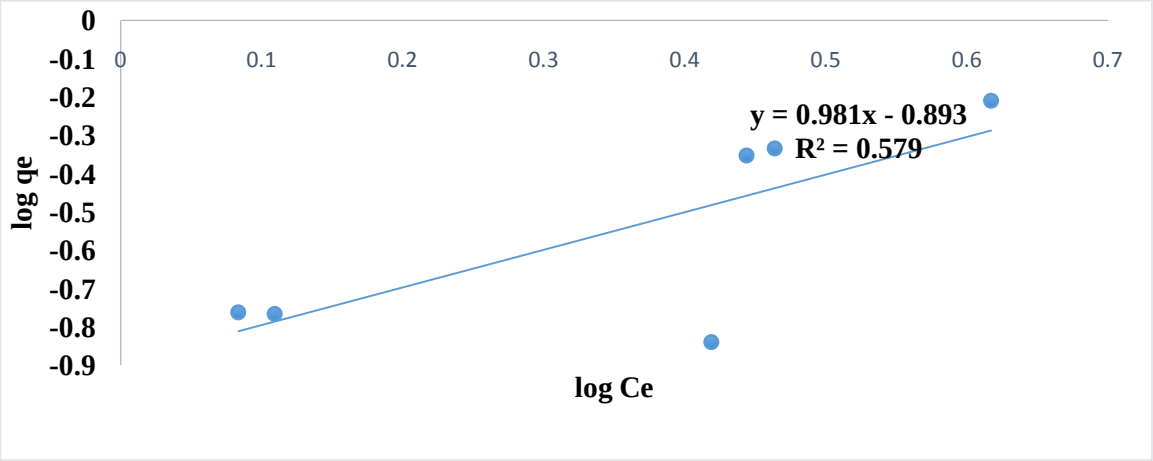


Figure 4.33: Lead (II) ion adsorption on composite of *E. tereticornis* barks and leaves adsorbent for Freundlich plot

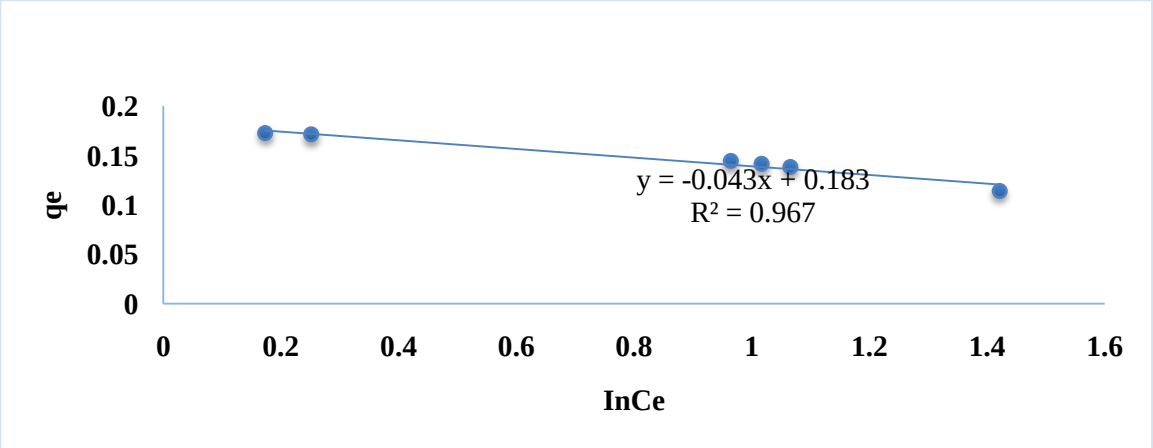


Figure 4.34:Lead (II) ion adsorption on of composite *E. tereticornis* barks and leaves adsorbent for Temkin plot

It can be seen from Figure 4.32-4.34 that the isotherm data fits the Langmuir Equation well (R^2=0.9793).The values of b(represents the degree of adsorption affinity of the adsorbate)andK_L(Langmuir constant)are determined from the Figure 4.34 and were found to be 0.1752 mg/g and 0.0328L/mg, respectively. The heat of adsorption from Temkin b_T value of 2.525 J/mol is very low signifying that it is physiosorption.

Table 4.13 presentsisotherm studies parameters for lead (II)ion adsorption with their details calculation given in the Appendix B.

Table 4.13: Lead (II) Ion Adsorption Isotherm Value

Isotherm	Parameter	Value
Langmuir	b	0.1752
	R_L	-0.0328
	R^2	0.9793
Freundlich	K_f	13.52
	1/n	-0.4352
	R^2	0.9961
Temkin	K_T	2.4434
	b_T	2.525
	R^2	0.5794

4.4.2 Kinetic Modeling

In order to predict the sorption kinetics, Pseudo second order, and second order and elovich Kinetic models were applied to the analyzed data. Three different kinetic models were used to test the best model in describing the kinetics of chromium and lead adsorption on *Eucalpytus tereticornis* composite. Figures 4.35-4.37 present pseudo-second order, second order and Elovich kinetic models for chromium (II) ion adsorption respectively.

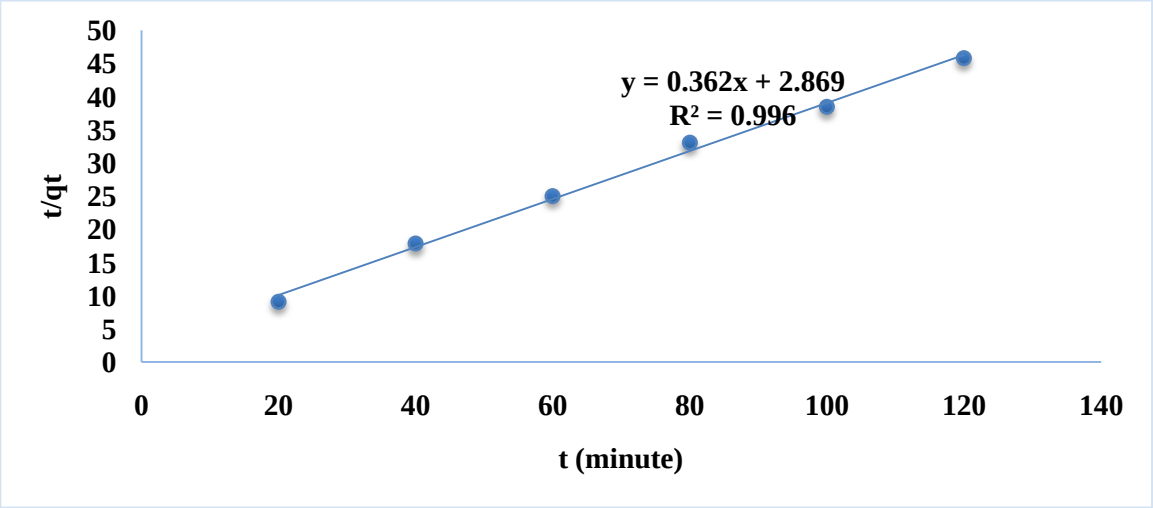


Figure 4.35: Chromium (VI) ion adsorption on composite of *E. tereticornis* barks and leaves adsorbent for pseudo second kinetic model

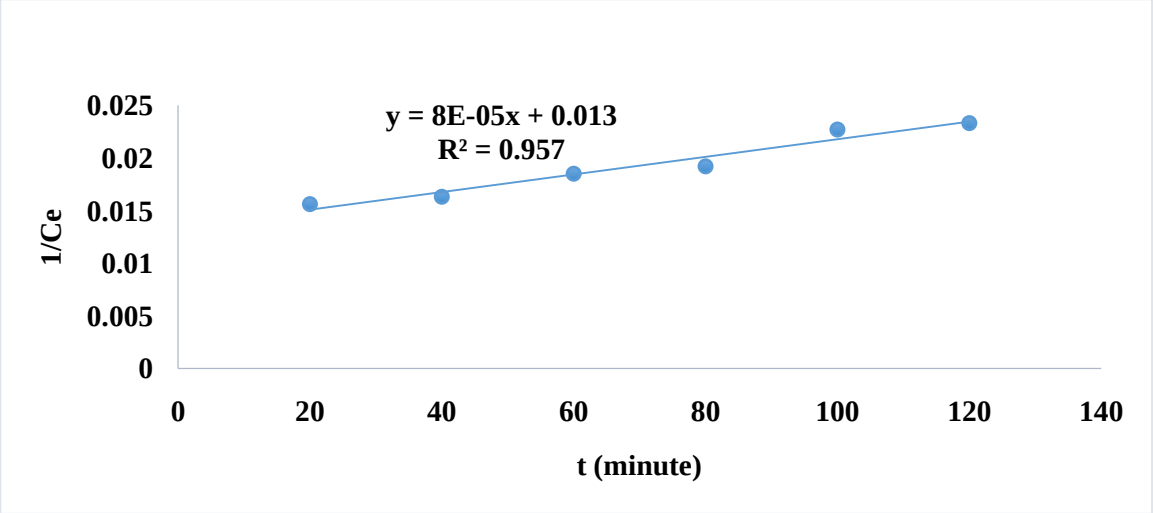


Figure 4.36: Chromium (VI) ion adsorption on composite of *E. terticornis* barks and leaves adsorbent for seconder kinetic model

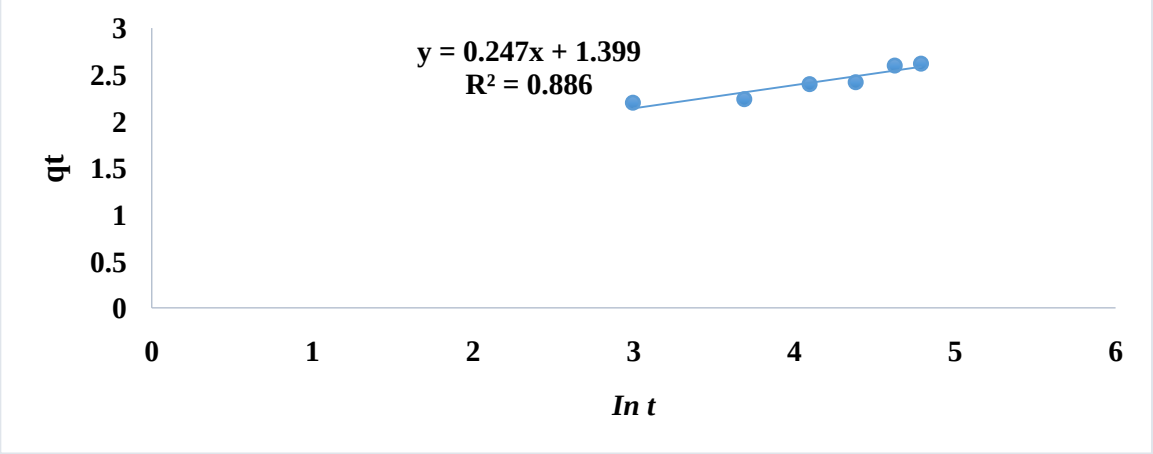


Figure 4.37: Chromium (VI) ion adsorption on composite of *E. tereticornis* barks and leaves adsorbent for elovich kinetics

Kinetic data best fitted into pseudo second order kinetic model with highest R-squared value of 0.9961. The calculations for the kinetic data and constants are given in the Appendix A.

Table 4.14: Evaluated Constants Obtained from the Tested Kinetic Model for Chromium (VI) Ion Adsorption

Kinetic model	R^2	Slope	Intercept	K	Other constants
Pseudo second order	0.9961	0.362	0.8691	22.745	Co=74.53
Second order	0.9573	0.00008	0.0134	0.00008	qe=0.3485
Elovich	0.8866	0.2477	1.399	b=4.0371	a=−10.6227

The result obtained in Table 4.14 indicated that pseudo-second order kinetic model is predominant with R^2 value of 0.9961 and that film diffusion might be the rate limiting step that control the adsorption process Althogh due to the nature of the adsorbent used in this study , pore diffusion and surface adsorption is expected but not contributing to the rate determining step because the linear portions of the curve for Cr(VI) ion adsorption on *Eucalpytus tereticorn* composite barks and leaves adsorbent do not pass through the origin as can be seen in Figures4.35-4.37.The finding in this study is complete agreement with the kinetic model developed by (Azizian *et al*., 2004.; Ho and McKay, 1999).

Meanwhile, Figures 4.38-4.39present pseudo second order, second order and Elovich kinetic models for lead (II) ion adsorption.

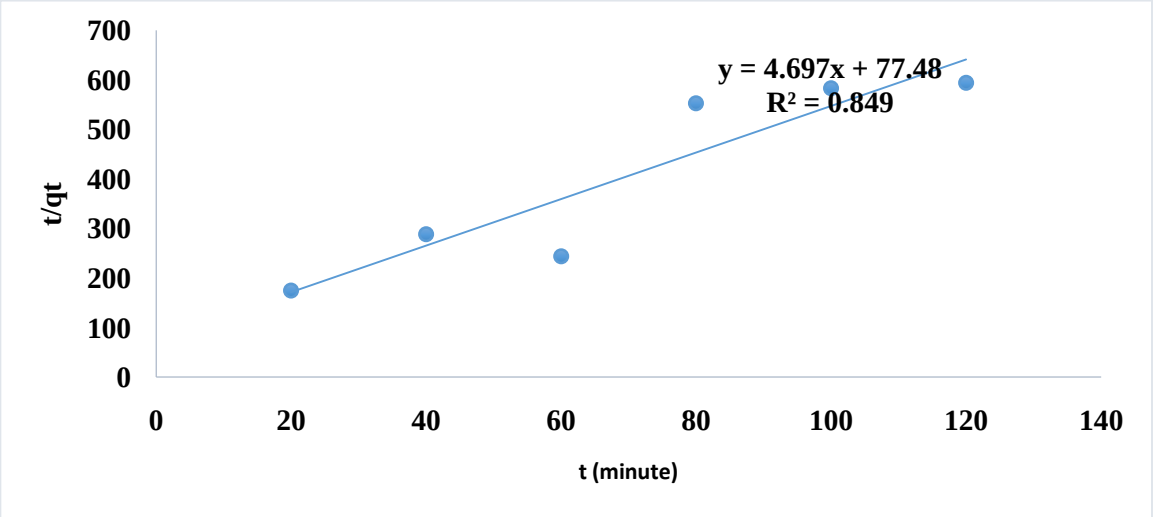


Figure 4.38: Lead (II) ion adsorption on composite of *E. tereticornis* barks and leaves adsorbent for pseudo second order kinetics

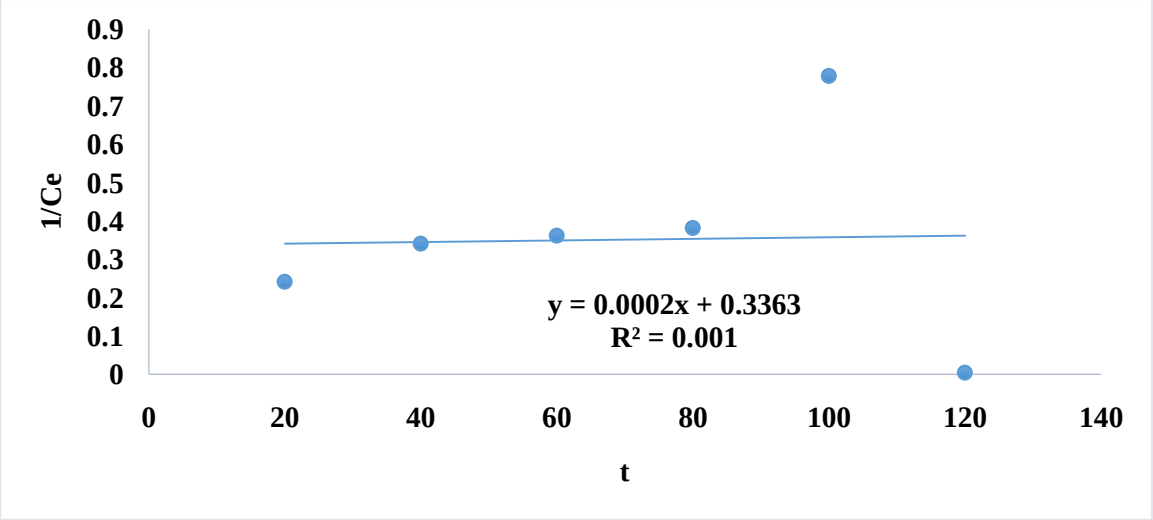


Figure 4.39: Lead (II) ion adsorption on composite of *E.tereticornis* barks and leaves for second order kinetics

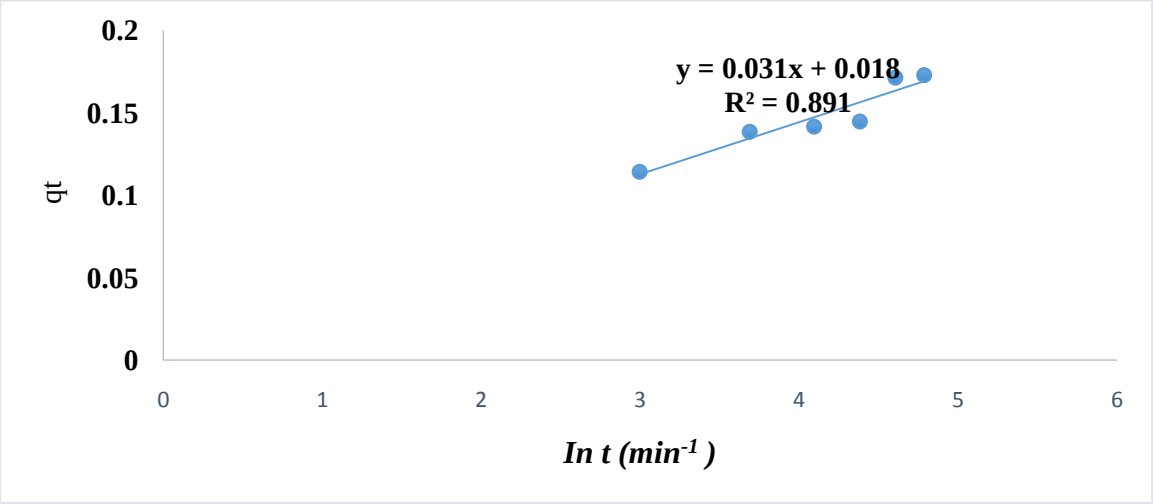


Figure 4.40:Lead (II) ion adsorption on composite of *E .tereticornis* barks and leaves adsorbent for second order kinetics

Kinetic data best fitted into elovich kinetic model with highest R-squared value of 0.8914. The calculations for the kinetic data and constants are given in the Appendix A.

Table 4.15: Evaluated Constants Obtained from the Tested Kinetic Model for Composite

Kinetic model	R^2	Slope	Intercept	k	Other constants
First order	0.8495	4.6976	0.0369	0.0002899	Co=2.9735
Second order	0.001	0.0002	0.3363	0.0002	qe=50.7614
Elovich	0. 8914	0.0315	0.0184	b=31.75	a=-2.7547

CHAPTER FIVE

CONCLUSION AND RECOMMENDATIONS

5.1 Conclusions

Based on the data from the present investigation, the following conclusions are made:

I. Low cost adsorbents prepared from plant wastes (*Eucalyptus tereticornis* bark and leave) were successfully used to adsorbed chromium (VI) and lead (II) ions from simulated wastewater and the maximum adsorption capacity found was arranged in sequential order: ETC (100mg/g) >ETL (28.6 mg/g)>ETB (21.90 mg/g) for chromium (VI) ion and for lead (II) ion, ETB > (54.05 mg/g) ETL (47.39 mg/g) >ETC (26.2 mg/g).

II. The derived statistical model equations were satisfactory in predicting the adsorption capacities. Hence, they could be used to directly predict the adsorption capacity under variable conditions with respect to adsorbent dosage and contact time.

III. Equilibrium data for both chromium (VI) and lead (II) ions adsorption were well fitted by Langmuir isotherm model with R^2 = 0.9987 for chromium (VI)ion and R^2= 0.9793 for lead (II) ion respectively. Also, adsorption of chromium ion followed pseudo first order kinetics with (R^2=0.9961) suggesting physiosorption due to the sharing of electrons between the adsorbent surface while lead (II) ion follows elovich kinetic model with R^2=0.8914. The maximum adsorption capacity was obtained for chromium (VI) ion adsorption with the application of Langmuir isotherm model as 16.02 mg/g.

IV. The results obtained in this study can be helpful in the design of an appropriate environmental management strategy to minimize the adverse impacts caused by heavy metals in industrial wastewater.

5.2 Recommendations

I. Although, the experiments were carried out at laboratory scale, the cost of preparing low cost adsorbents needs to be determined in further studies since cost is an important parameter for comparing the sorbent materials.

II. Studies on the effects of other process parameters such as temperature, particle size, concentration and ionic strength can also be an interesting area of future study.

III. It could also be of particular interest to study the adsorption performance of *Eucalyptus* plant from different sources.

IV. In addition, Inducible couple plasma (ICP) should be used instead of atomic adsorption spectrophotometer (AAS) to analyse the sample concentration simultaneously and yield a better result.

V. Finally, in order to widen the applicability of the studied adsorbent, they must be tested using the real industrial wastewater.

REFERENCES

Abdel-Ghani, N.T., Hefny, M.M and El-Chaghaby. (2008). G.A. Removal of Metal Ions from Synthetic Wastewater by Adsorption onto Eucalyptus *camaldulenis* Tree Leaves.*Journal ChileanChemical Society. Volume 53, pages 1585-1587.*

Abia, A.A., Horsfall, M. and Junior D.O. (2003). The use of chemically modified and unmodified cassava waste for the removal of Cd, Cu and Zn ions from aqueous solution. Bioresource Technology.

Ajmal, M.,Khan, A.H., Ahmad, S., andAhmad, A. (1998).*Water Resource.* 32, 3085-3091

Ajmal, M., Rao, Ra., Ahmad, R and Ahmad, J. (2000). Adsorption Studies on Citrus Reticulata (Fruit Peel of Orange): Removal and Recovery of Ni (II) from Electroplating Wastewater. *Journal of Hazard Mater.*117-31.

Alhaji, N. M. I. and Tajun, K. M. (2015). Optimization and Kinetic Study for the Removal ofChromium (VI) Ions by Acid Treated Sawdust Chitosan Composite Beads. *International Research Journal of Pure &Applied Chemistry.*

Ali, M., Mohammmad, A., Rehana, Y. and Anees A. (1997).Adsorption of Cu(II) from Wastewater on the Seed and Seed Shell of Mangifera Indica (Mango).*Indian Journal of Chemical Technology*. Volume. 4, pages 223-227.

Aziz, H.A., Adlan, M.N., and Ariffin, K.S. (2008). Heavy metals (Cd, Pb, Zn, Ni, Cu and Cr (III)) removal from water in Malaysia: post treatment by high quality limestone. Bioresour. Technol. 99, 1578– 1583.

Azizian, S. (2004). Kinetic models of sorption: A theoretical analysis.*Journal of Colloid and Interface Science*, 276(1), 47-52.

Babarinde, N.A.A., Oyebamiji Babalola, J., Adebowale and Sanni, R. (2006).Biosorption of lead ions from aqueous solution by maize leaf. *International Journal of Physical Science.* 1, 23–26.

Babel, S., Kurniawan, and T.A. (2003). Low-cost adsorbents for heavy metals uptake from contaminated water: A review. *Journal of Hazardous Materials* (97): 219– 243.

Babel, S., and Kurniawan, T.A. (2004). Cr (VI) removal from synthetic wastewater using coconut shell charcoal and commercial activated carbon modified with oxidizing agents and/or chitosan. Chemosphere 54 (7), 951–967.

Bailey, S.E., Olin, T.J., Bricka, R.M., and Adrian, D.D. (1999). A review of potentially low-cost sorbents for heavy metals. Water Res. 33, 2469–2479.

Barakat, M.A., Chen, Y.T., and Huang, C.P. (2004). Removal of toxic cyanide and Cu (II) ions from water by illuminated TiO_2 catalyst. *J. Appl. Catal. B: Environ. 53, 13–20*.

Baş, D. and Boyaci, İ.H. (2007) Modeling and optimization: Usability of response resurfaces methodology. *Journal of Food Engineering*, 78, 836-845.

Basha, S., Murphy, Z.V.P., and Jha, B. (2008). Sorption of Hg (II) from aqueous solutions onto *Carica papaya*: Application of Isotherms, *Industrial and Engineering Chemistry Research* (47): 980-986.

Basha, S., Murphy, Z.V.P., and Jha, B. (2009). Removal of Cu(II) and Ni(II) from Industrial Effluents by Brown Seaweed, *Cystoseira indica*, *Industrial and Engineering Chemistry Research* (48): 961–975.

Bhatia, S., Wong, C.T., and Abdullah, A.Z. (2009). Optimization of air-borne butyl acetate adsorption on dual-function Ag–Y adsorbent-catalyst using response surface methodology, *Journal of Hazardous Materials* (164): 1110-1117.

Bhattacharya, A.K., Mandal, S.N., and Das, S.K. (2006). Adsorption of Zn (II) from aqueous solution by using different adsorbents. *Chemical Engineering Journa*l. (123): 43–51.

Bhattacharya, A.K., Naiya, T.K., Mandal, S.N and Das, S.K. (2008). Adsorption, kinetics and equilibrium studies on removal of Cr (VI) from aqueous solutions using different low-cost adsorbents, *Chemical Engineering Journal* (137): 529- 541.

Bhatti, M.S., Reddy, A.S., Kalia, R.K and. Thukral.A.K. (2011). Modeling and optimization of voltage and treatment time for electrocoagulation removal of hexavalent chromium. Desalination 269:157–162.

Biswajit, D., Naba, K. M., Palas,R., and Soumya ,C.(2013).Application of Response Surface Methodology for Hexavalent Chromium Adsorption onto Alluvial Soil of Indian Origin, *International Journal of Environmental Pollution and Solutions.*

Chen, G.H. (2004). Electrochemicals Technologies in Wastewater Treatment. Separation Purification Technology. 38 (1), 11–41. Crini, G., 2005. Recent developments in polysaccharide-based materials used as adsorbents in wastewater treatment. Prog. Polym. Sci. 30, 38–70.

Chowdhury, Z.Z., S.M. Zain, A.K. Rashid and A.A. Ahmed. (2011). Equilibrium Kinetics and Isotherm Studies of Cu (II) Adsorption from Wastewater onto Alkali Activated Oil Palm Ash. *American Journalof Applied. Science*: 8(3): 230-237.

Deepa, C. N. and Suresha, S. (2014) .Biosorption of Lead (II) from Aqueous Solution and Industrial Effluent By using Leaves of *Araucaria Cookii*: Application of Response Surface Methodology. *Journal of Environmental Science, Toxicology and Food Technology (JESTFT): Volume 8, PP 67-79*

Florence, T.M. (1998).Trace Element Speciation in Biological Systems". Element Speciation: Analytical Methods and Problems. 319-338.

Gaballah , I., Kibertus G. (1994). Elimination of As Hg and Zn from Synthetic Solution and Industrial Effluents using Modified Barks. In Misra , M. Edition. Separation Process. Heavy Metals, Ions and Minerals. The Minerals, Metals and Materials Society.

Gaballah, I. and Kilbertus G. (1997). Recovery of Heavy Metal Ions through Decontamination of Synthetic Solutions and Industrial Effluents using Modified Barks.

Gadd, G.M. (1988). Heavy Metal and Radionuclide by Fungi and Yeasts. 197-204

Gupta, V. K., Jain, C. K., Ali, I., Sharma, M., and Saini, V. K. (2003). Removal Of Cadmium and Nickel from Wastewater using Bagasse Fly Ash—A Sugar Industry Waste," *Water Research*, vol. 37, no. 16, pp. 4038–4044.

Hamadi, N. K., Chen, X. D., Farid, M. M. and Lu, M. G. Q. (2001).Adsorption Kinetics for the Removal Of Chromium (VI) from Aqueous Solution by Adsorbents Derived from used Tyres and Sawdust. *Chemical Engineering Journal*.84, 95.

Herrmann, J.M. (1999). Heterogeneous Photocatalysis: Fundamentals and Applications to the Removal of Various Types of Aqueous Pollutants. Catal. Today 53, 115–129.

Ho,Y.S. and Mckay, G. (1999). Pseudo-Second Order Model for Sorption Processes. Process Biochemistry, 34: 451-465.

Ho, Y.S.and Wang, C.C., (2004). Pseudo-Isotherms for the Sorption of Cadmium Ion onto Tree Fern. Process Biochem. 39, 759–763.

Ho, Y.S., (2006). Review of Second-Order Models for Adsorption Systems, *Journal of Hazardous Materials.*136: 681-689.

Horsfall Jr. M., And Abia, A.A. (2003).Sorption of Cadmium (II) and Zinc (II) Ions from Aqueous Solutions by Cassava Waste Biomass (Manihot sculenta Cranz),"*Water Research*, vol. 37, no. 20, pp. 4913–4923.

Indu Sharma and Dinesh Goyal, (2011). Chromium Removal from Industrial Effluent by*Eucalyptus tereticornis* Bark: Asian Journal. Experimental. Science. Vol. 25, No. 1, p. 29-35

Johnson, P.D., Watson, M.A., Brown, J., and Jefcoat, I.A. (2002). Peanut Hull Pellets as a Single Use Sorbent for the Capture of Cu (II) From Wastewater. Waste Manage. 22, 471–480.

Kadirvelu, K., Thamaraiselvi, K., and Namasivayam, C. (2001). Removal of Heavy Metal from Industrial Wastewaters by Adsorption onto Activated Carbon Prepared from an Agricultural Solid Waste. Bioresource. Technol. 76, 63–65.

Kajitvichyanukula, P., Ananpattarachaia, J., andPongpom, S., (2005). Sol– Gel Preparation and Properties Study of Tio2 Thin Film for Photocatalytic Reduction of Chromium (VI) in Photocatalysis Process. Sci. Technol. Adv. Mater. 6, 352–358.

Karimaian K.A., Amrane A., Kazemian H.,Panahi R., AndZarrabi M. (2013). Retention of Phosphorous Ions on Natural and Engineered Waste Pumice: Characterization, Equilibrium, Competing Ions, Regeneration, Kinetic, Equilibriumand Thermodynamic Study. *Appl. Surf. Sci.* ***284****, 419.*

Karunasagar, D., Balarama Krishna, M.V., Rao, S.V.,and Arunachalam, J. (2005). Removal of Pre Concentration of Inorganic and Methyl Mercury from Aqueous Media using a Sorbent Prepared from the Plant Coriandrum Sativum. J. Hazard. Mater. B 118, 133–139.

Kratochvil, David; Pimentel, Patricia and Volesky, Bohumil. (1998).Removal of Trivalent and Hexavalent Chromium by Seaweed Biosorbent. *Environmental Science and Technology*, Vol. 32, No. 18, P. 2693-2698.

Kumar U., and Bandyopadhyay, M. (2006). Sorption of Cadmium from Aqueous Solution using Pretreated Rice Husk," *Bioresource Technology*, vol. 97, no. 1, pp. 104–109.

Kumara, P. S. Ramalingamb, S. Kiruphac, S. D. Murugesanc, A. Vidhyadevic, T. and Sivanesan, S. (2011). Adsorption Behavior of Nickel (II) onto Cashew Nut Shell: Equilibrium, Thermodynamics, Kinetics, Mechanism and Process Design. *Chemical Engineering Journal* Volume167, Page: 122-131.

Kurniawan, T.A., Chan, G.Y.S., Lo, W.H. and Babel, S. (2006). Physicochemical Treatment Techniques for Wastewater Laden with Heavy Metals. Chemical Engineering Journal. 118, 83–98.

Lee, J., Ye, L., Landen,W.O. and R.R. Eitenmillcr.(2000).Optimization of an Extraction Procedure for the Quantification of Vitamin E in Tomato and Broccoli using Response Surface Methodology. *Journal of Food Composition Analysis,* 13: 45-57.

Liu, X.D., Liu, S., Tokura, N., Nishi, N. and Sakairi (2003).A Novel Method for Immobilization of Chitosan onto Non-Porous Glass Beads through a 1,3 Thiazolidine Linker Polymer , Volume 44,Page 1021-1026.

Mashitah, M. D., Zulfadhly, Z. and Bhatia, S. (1999). Ability of Pycnoporoussanguineus to Remove Copper Ions from Aqueous Solution. Artificial Cells, Blood Substitues and Immobilized Biotechnology, 27 (5&6), 429-433.

Mohammadi, T., Mohebb, A., Sadrzadeh, M.,and Razmi, A. (2005). Modeling of Metal Ion Removal from Wastewater by Electrodialysis. Seperation Purification Technology. 41, 73–82.

Mohanty, K., Jha, M.,Biswas, M.N. and Meikap, B.C.(2005). Removal of Chromium (VI) from Dilute Aqueous Solutions by Activated Carbon Developed from Terminalia Arjuna Nuts Activated with Zinc Chloride. *Chemical Engineering Science*, Vol. 60, No. 11, P. 3049-3059.

Montgomery, D.C., 1997. Design and Analysis ofExperiments: Chapter 13, 4th Edition. John Wiley &Sons, USA.

Nakajima, A. and Sakaguchi, T. (1990). Recovery and Removal of Uranium by using Plant Wastes. Biomass 21, 55–63.

Oliveria, E. A., Montanher, S. F., Andrader, A. D.,Nobrega, J. A. and Rollemberg, M. C. (2005).Equilibrium Studies for the Sorption of Chromium and Nickel from Aqueous Solution using Rice Bran.Process Biochemistry, 40, 3485.

Ozturk,N. And Kavak,D. (2005) Adsorption of Boron from Aqueous Solutions using Fly Ash: Batch and Column Studies, *Journal of Hazard Mater*., 127 81–88.

Phussadee Patnukao., Apipreeya Kongsuwan., and Prasert Pavasant,(2008). Batch Studies of Adsorption of Copper and Lead on Activated Carbon from *Eucalyptus Camaldulensis Dehn. Bark, Journal of Environmental Sciences,* 20, 1028-1034.

Quek, S.Y., Wase, D.A.J. and Forster, C.F. (1998). The use of Sago Waste for the Sorption of Lead and Copper. Water SA 24, 251–256.

Rafatullah, M., O. Sulaiman, R. Hashim and Blazque. A. A. (2009). Adsorption of Copper (II), Chromium (III), Nickel (II) and Lead (II) Ions from Aqueous Solutions by Meranti Sawdust. *Journal of Hazardous Materials*, 170: 969-977.

Saeed, A., Waheed Akhter, M. AndIqbal, M.(2005). Removal and Recovery of Heavy Metals from Aqueous Solution using Papaya Wood as a New Biosorbent. SeperationPurificationTechnology. 45, 25–31.

Sharma, Y.C. (2003). Cr (VI) Removal from Industrial Effluents by Adsorption on an Indigenous Low-Cost Material. *Colloids and Surfaces A: Physicochemical and Engineering Aspects*, Vol. 215, No. 1-3, P. 155-162.

Sari A. and Tuzen M. (2009). Kinetic and Equilibrium Studies of Pb(II) and Cd(II) Removal from Aqueous Solution onto Colemanite Ore Waste. *Desalination* ***249****, (1), 260.*

Satya, V., Yadla, S.V., Chandana, M.V., and Lakshmi, V. (2003). A Review on Adsorption of Heavy Metals from Aqueous Solution, *International Journal of Chemical, Biological and Physical Sciences.*

Sawalha, M.F., Peralta-Videa, J.R., Romero-Gonza´lez, J., Duarte-Gardea, M., and Gardea-Torresdey, J.L. (2007). Thermodynamic and Isotherm Studies of the Biosorption of Cu (II), Pb(II), and Zn(II) by Leaves of Saltbush (Atriplex Canescens). *Journalof ChemicalThermodynamic.* 39, 488–492.

Senthil, P.K and Kithira .K.(2009). Equilibrium and Kinetic Study of Adsorption of Nickel from Aqueous Solution onto Bael Tree Leaf Powder.*Journal of Engineering Science and Technology*,Volume 4, No, 351 - 363

Shukla, S.S. (2002). The Role of Sawdust in the Removal of Unwanted Materials from Water, *Journal ofHazardous Materials* (B95): 137–152.

Site, A.D. (2000). Factors Affecting Sorption of Organic Compounds in Natural Sorbent/Water Systems and Sorption Coefficients for Selected Pollutants: A Review, *Journal of Physical and Chemical Reference Data* (30): 187-439.

Siti, N.A. A; Mohd, H. and Shah, I. (2013). A Review Adsorption Process of Heavy Metals by Low-Cost Adsorbent: *World Applied Sciences Journal 28 (11): 1518-1530,*

Srivastava, S. K., Singh, A. K. and Sharma, A.(1994). "Studies on the uptake of lead and zinc by lignin obtained from black liquor paper industry waste material, *"Environmental Technology*, vol. 15, no. 4, pp. 353–361.

Sudaryanto, Y., Hartono, S.B., Irawaty, W. Hindarso, H. and Ismadji, S. (2006). High Surface Area Activated Carbon Prepared from Cassava Peel by Chemical Activation. Biresource. Technology .97: 734-739.

Suleman, Q., Anwar, R., Saleemi and Muhammad M. A. (2007). Heavy Metal Uptake by Agro Based Waste Materials.*Electronic Journal of Biotechnology* .Volume,10 Number, 3.

Suleman, Q., Anwar, R. andSaleemi, M.U. (2009). Biosorption of Lead (II) and Chromium (VI) on Groundnut Hull: Equilibrium Kinetics and Thermodynamics Study. *Electronic Journal and Biotechnolgy,* 12 (4).

Swayampakula, K. Boddu, V. MNadavala., S. K.and Abburi, K. (2009). Competitive Adsorption of Cu (II), Co (II) and Ni (II) from their Binary and Tertiary Aqueous Solutions using Chitosan-Coated Perlite Beads as Biosorbent, *Journal Of Hazardous Materials*170, 680–689.

Tatycostodes, V. C., Fauduet, H., Porte, C. AndDelacroix, A. (2003). Removal of Cd (II) and Pb(II) Ions, from Aqueous Solutions by Adsorption onto Sawdust of Pinus Sylvestris," *Journal of Hazardous Materials*, Vol. 105, No. 1–3, Pp. 121–142.

Temkin, M. and Pyzhev, J. A. V. (1940). Kinetics of Ammonia Synthesis on Promoted Iron Catalysts. Acta Physiochim12: 217-222.

Thakur, (2006) Environmental Biotechnology Basic Concepts and Applications Treatment Processes, vol. 3. Humana Press, New Jersey, pp. 635–676.

Vigneswaran, S., Ngo, H.H., Chaudhary, D.S. and Hung, Y.T. (2004). Physico-Chemical Treatment Processes for Water Reuse.

Wang, L., Wang, N., Zhu, L., Yu, H. and Tang, H. (2008).Photocalytic Reduction of Cr (VI) over Different Tio_2Photocatalysts and the Effect of Dissolved Organic Species. *Journal of Hazard Matter*, Volume 152, Page 93-99

APPENDICES

This section covers the tabulated FTIR spectra, Design of Experiment, adsorption isotherm parameter and kinetic modelling

Appendix A

The amount of heavy metal adsorbed into the adsorbent is designated by q in mg/l of the adsorbent and given by the formula $q = \frac{V}{W}(C_o - C_e)$ ……..…… (A.1)

Where C_o and C_e (g/mL) are the concentration of heavy metal at initial and equilibrium respectively, W is the weight of the adsorbent used in grams and V is the volume of the solution in liters. The optimum adsorbent dosage of 5.0 grams were used throughout each stage of adsorption isotherm and kinetic studies test. Initial concentration for chromium was 174mg/l and that of lead was 0.987mg/l

They were calculated and tabulated in Table A.1 and A.2 to obtain the adsorption isotherm plots.

Table A.1: Adsorption Isotherm and Kinetic Parameters of Chromium (VI) ion Adsorption on *Eucalpytus tereticornis* Composite (ETC)

Time Min	Ce mg/l	Qe mg/g	Ce/qe	Log Ce	Log qe	InCe	Int	qt mg/g	t/qt	1/Ce
20	64	2.20	29.09	1.8062	0.3424	0.7885	2.9957	2.20	9.0909	0.0156
40	62	2.24	27.68	1.7924	0.3502	0.8065	3.6889	2.24	17.8571	0.0163
60	54	2.40	22.50	1.7324	0.3802	0.8387	4.0943	2.40	25.000	0.0185
80	52	2.42	21.49	1.7160	0.3838	0.8838	4.3820	2.42	33.0578	0.0192
100	44	2.6	16.92	1.6435	0.4149	0.9555	4.6052	2.60	38.4615	0.0227
120	43	2.62	16.33	1.6335	0.4183	0.9632	4.7875	2.62	45.8015	0.0233

Table A.2:Adsorption Isotherm and Kinetic Parameters of Lead (II) ion Adsorption on *Eucalpytus tereticornis Composite* (ETC)

Time Min	Ce mg/l	Qe mg/g	Ce/qe	Log Ce	Log qe	InCe	Int	Qt	t/qt	1/Ce
20	4.143	0.1143	36.25	0.6173	-0.2095	1.4214	2.9957	0.1143	174.98	0.2413
40	2.9309	0.1385	21.16	0.4637	-0.3338	1.0657	3.6889	0.1385	288.81	0.3403
60	2.7765	0.1416	19.61	0.4439	-0.3527	1.0170	4.0943	0.1416	243.73	0.3617
80	2.6237	0.1447	18.13	0.4189	-0.8395	0.9646	4.3820	0.1447	552.43	0.3811
100	1.286	0.1714	7.503	0.1092	-0.7659	0.2515	4.6052	0.1714	583.87	0.7776
120	1.2121	0.1729	7.010	0.0835	0.7622	0.1924	4.7875	0.1729	694.04	0.0471

APPENDIX B

B.1: Composite for Chromium (VI) Ion Adsorption Isotherm

Langmuir Isotherm

The Langmuir isotherm equation is given as:

$$\frac{C_e}{q_e} = \frac{1}{K_L b} + \frac{C_e}{K_L} \quad \text{(B1)}$$

R^2=0.9987

Slope=$\frac{1}{K_L}$=0.6009

K_L=1.6642

Intercept= =$\frac{1}{K_L b}$ b= 16.0186

$R_L = \frac{1}{1+bC_0}$*Where Co is initial concentration*=174mg/l

R_L =0.003604

Freundlich Isotherm constants

$$\text{Log}\, q_e = \frac{1}{n}\log C_e + logK_F \quad \text{(B2)}$$

R^2=0.9961

$\frac{1}{n} = -0.4356 = Slope$, n= -2.2957

Intercept=1.1311

$logK_F = 1.1311$,

$$K_F = 13.5$$

Temkin Isotherm constant

$$q_e = \frac{RT}{b_T} InCe + \frac{RT}{b_T} InK_T \quad \text{(B3)}$$

$$\frac{RT}{b_T} = Constant\ related\ to\ heat\ of\ adsorption\ J/mol$$

R^2=0.9454

$$\frac{RT}{b_T} = 2.2888 J/mol = Slope$$

$$b_T = \frac{8.314 * 298}{2.2888} = 1082 j/mol$$

$Intercept$=0.419

$$Intercept = In(K_T)$$

In (K_T) =In (0.149)

$$K_T = 1.1607$$

B.2: Composite for Lead (II) Ion Adsorption Isotherm

Langmuir Isotherm equation is given as:

$$\frac{C_e}{q_e} = \frac{1}{K_L b} + \frac{C_e}{K_L} \quad \text{(B.4)}$$

R^2=0.9793

Slope=$\frac{1}{K_L}$=9.6132

K_L=0.1040

Intercept= =$\frac{1}{K_L b}$ = -5.7069 b= -0.1752

$R_L = \frac{1}{1+bC_0}$ *Where Co is initial concentration*=174mg/l

$R_L = -0.0328$

Freundlich Isotherm constants

$$\text{Log } q_e = \frac{1}{n}\log C_e + logK_F \quad \text{(B.5)}$$

R^2=0.9961

$\frac{1}{n} = -0.4356 = Slope$, n= -2.2957

Intercept=1.1311

$logK_F = 1.1311,$

$K_F = 13.52$

Temkin Isotherm constant

$$q_e = \frac{RT}{b_T} InCe + \frac{RT}{b_T} InK_T \quad \text{(B6)}$$

$\frac{RT}{b_T} = Constant\ related\ to\ heat\ of\ adsorption\ J/mol$

R^2=0.5794

$\frac{RT}{b_T} = 0.9813 J/mol = Slope$

$b_T = \frac{8.314 * 298}{0.9813} = 2525 j/mol$

$Intercept$=0.8934

$Intercept = In(K_T)$

In (K_T)=In(0.8934) and $K_T = 2.4434$

APPENDIX C

C.1:Chromium (VI) IonAdsorption on ETC for Kinetic Studies Data Calculations

Pseudo-second order kinetic

From figure

$R^2 = 0.9961$

$Intercept = \frac{1}{q_e} = 2.8691, \qquad q_e = 0.3485 g/l$

$$Slope = \frac{1}{q^2{}_e k} = 0.362 \qquad k = \frac{22.745 l}{g min}$$

Second-order kinetics

From Figure 4.28

$R^2 = 0.9573$, slope= $k = 0.00008/gmin$

$$Intercept = \frac{1}{C_0} = 0.0134/gC_0 = 74.63 g/l$$

Elovich kinetic model

From Figure 4.29

$R^2 = 0.8866$

$slope = \frac{1}{b} = 0.2477, \qquad b = 4.0371$

$Intercept = \frac{1}{b} In(ab) = 1.399 \quad substituting\ b = 4.0371,$

$$a = -10.6227$$

C.2: Lead (II) Ion Adsorptionon ETC forKinetic Studies Data Calculations

Pseudo-second order

From Figure 4.36,

$R^2 = 0.8495$

$$Intercept = \frac{1}{q_e} = 0.0369, \qquad q_e = 27.1003 g/l$$

$$Slope = \frac{1}{q^2{}_e k} = 4.6976 \qquad k = \frac{0.0002899 l}{gmin}$$

Second-order kinetics

From Figure 4.35

$$slope = k = 0.0002/gmin$$

$$Intercept = \frac{1}{C_0} = 0.3363/gC_0 = 2.9735 g/l$$

$R^2 = 0.001$

Elovich kinetic model

$$slope = \frac{1}{b} = 0.0315, \qquad b = 31.75$$

$$Intercept = \frac{1}{b} In(ab) = 0.0184, \quad substituting\ b = 31.75, \quad a = -2.7547$$

$R^2 = 0.8914$

APPENDIX D

This appendix D presented the Design Expert 6.06 predicted and experimental value of chromium and lead adsorption on *Eucalpytus tereticornis* parts.

Table D.1:Experimental and Predicted Values of Chromium (VI) Ion Adsorption on *Eucalpytus tereticornis* Barks adsorbent.

Runs order	Experimental value	Predicted Value
1	1.53	1.52
2	1.57	1.52
3	0.84	0.34
4	1.05	7.06
5	2.33	3.99
6	3.07	0.15
7	21.90	14.35
8	2.22	8.62
9	1.47	1.52
10	1.19	1.49
11	1.51	1.52
12	1.51	1.52
13	0.80	0.68

Table D.2:ANOVA Result of a Quadratic Model for Chromium (VI) Ion Adsorption using *Eucalpytus Tereticornis* Barks Adsorbent

Source	Sum of square	DF	Mean square	F –value	Prob.>F (p-value)
Model	1230.89	5	48.18	2.09	0.0180
A	68.45	1	68.45	3.10	0.1218
B	40.67	1	40.47	1.84	0.2170
A2	15.23	1	15.23	0.69	0.4337
B2	9.61	1	9.61	0.43	0.5306
AB	99.70	1	99.70	4.51	0.0713
Residual	154.65	7	22.09		
Lack of fit	154.65	3	51.55	39051.98	*0.1818*
Pure error	*5.280E-003*	4	1.320E-003		
Cor. Total	385.54	12			

Table D.3: Optimization Design Summary for Chromium (VI) ion adsorption on *Eucalpytus tereticornis* Barks Adsorbent

Name	Goal	Lower limit	Upper Limit
Contact time	Is in range	20	120
Adsorbent dose	Is in range	1	5
Adsorption capacity	Maximize	1.22745	50.0541

Table D.4 Experimental and Predicted Values of Lead (II) Ion Adsorption on *Eucalpytus tereticornis* Barks Adsorbent

Runs order	Experimental value	Predicted value
1	32.47	29.78
2	37.88	43.21
3	19.49	18.68
4	19.69	18.68
5	15.24	18.68
6	19.49	18.68
7	1.230	2.170
8	13.00	13.42
9	21.65	29.95
10	54.05	47.35
11	19.49	18.68
12	2.290	5.690
13	22.94	28.92

Table D.5:ANOVA Resultfor a Quadratic Model for Lead (II) ion adsorption Using *Eucalpytus tereticornis* Barks Adsorbent

Source	Sum of square	DF	Mean square	F -value	Prob.>F (p-value)
Model	1988.88	5	397.78	19.17	0.0006
A	48.48	1	48.48	2.34	*0.1702*
B	*1683.80*	1	1683.80	*81.15*	<0.0001
A2	79.23	1	79.23	3.82	*0.0916*
B2	*27.94*	1	27.94	*1.35*	0.2840
AB	160.09	1	160.09	7.72	*0.0274*
Residual	145.24	7	20.75		
Lack of fit	130.44	3	*43.48*	11.75	0.0188
Pure error	14.80	4	3.70		
Cor. Total	2134.12	12			

Table C.6:Optimization Design Summary for Lead (II) Ion adsorption on *Eucalpytus tereticornis* Barks Adsorbent

Name	Goal	Lower Limit	Upper Limit
Contact time (min)	Is in range	20	120
Adsorbent dose (g)	Is in range	1	5
Adsorption capacity (mg/g)	Maximize		

Table D.7:Experimental and Predicted Values of Chromium (VI) ion Adsorption Capacity (mg/g) on *Eucalpytus Tereticornis* Leaves Adsorbent

Runs order	Experimental value	Predicted value
1	0.93	0.86
2	1.01	0.98
3	0.70	0.72
4	0.67	0.72
5	0.75	0.72
6	0.74	0.72
7	0.035	0.26
8	0.88	0.63
9	0.63	0.82
10	0.92	0.98
11	0.74	0.72
12	0.33	0.21
13	0.62	0.61

Table D.8:ANOVA Results for a Quadratic Model for Chromium (VI) ion adsorption using*Eucalpytus tereticornis* Leaves Adsorbent

Source	Sum of square	DF	Mean square	F –value	Prob.>F (p-value)
Model	*0.073*	5	0.13	4.82	0.0314
A	0.043	1	0.043	1.61	0.2447
B	0.51	1	0.51	19.09	0.0033
A2	*4.168E-006*	1	*4.168E-006*	*1.559E-004*	0.9904
B2	0.017	1	0.017	0.65	0.4454
AB	0.073	1	0.073	2.75	0.1413
Residual	0.19	7	0.027		
Lack of fit	0.18	3	0.061	59.23	0.0009
Pure error	*4.119E-003*	4	*1.030E-003*		
Cor. total	0.83	12			

Table D.9:Optimization Design Summary for Chromium (VI) Ion Adsorption on *Eucalpytus tereticornis* Leaves Adsorbent

Name	Goal	Lower Limit	Upper Limit
Contact time(min)	Is in range	20	120
Adsorbent dose (g)	Is in range	1	5
Adsorption capacity (mg/g)	Maximize	0.034965	1.0101

Table D.10:Experimental and Predicted Values of Lead (II)Ion Adsorptionon*Eucalpytus tereticornis* Leaves Adsorbent.

Runs order	Experimental value	Predicted value
1	29.59	30.17
2	47.39	47.18
3	17.73	21.07
4	13.93	21.07
5	13.00	21.07
6	39.06	21.07
7	1.230	3.660
8	8.120	6.840
9	12.18	12.21
10	40.65	39.71
11	21.65	21.07
12	4.330	1.520
13	13.00	15.20

Table D.11: ANOVA Results for a Quadratic Model for Lead (II) Ion Adsorption Using *Eucalpytus tereticornis* Leaves Adsorbent

Source	Sum of square	DF	Mean square	F –value	Prob.>F (p-value)
Model	2101.69	5	420.34	6.22	0.0164
A	8.90	1	8.90	0.13	0.7273
B	1893.29	1	1893.29	28.03	0.0011
AD	94.45	1	94.45	1.40	0.2756
B^2	32.85	1	32.85	0.49	0.5081
AB	55.17	1	55.17	0.82	0.3962
Residual	472.83	7	67.55		
Lack of fit	21.54	3	7.18	0.064	0.9764
Pure error	451.29	4	112.82		
Cor. Total	2574.53	12			

Table D.12:Optimization Design Summary for Lead (II) Adsorption on *Eucalpytus tereticornis* Leaves Adsorbent

Name	Goal	Lower Limit	Upper limit
Contact time (min)	Is in range	20	120
Adsorbent dose (g)	Is in range	1	5
Adsorption capacity (mg/g)	Maximize	1.22745	47.3934

Table D.13:Experimental and Predicted Values of Lead (II) Ion Adsorption on *Eucalpytus tereticornis* Composite (Barks and Leaves) Adsorbent

Runs order	Experimental value	Predicted value
1	50.00	55.75
2	59.00	61.93
3	8.90	3.12
4	14.00	5.41
5	6.00	5.42
6	8.00	11.41
7	100.00	93.28
8	6.54	16.10
9	10.00	10.80
10	12.00	10.80
11	12.00	10.80
12	10.00	10.80
13	10.00	10.80

Table D.14 ANOVA Results for a Quadratic Model for Chromium (VI) Ion Adsorption using *Eucalpytus tereticornis* Composite (Barks and Leaves) Adsorbent

Source	Sum of square	DF	Mean square	F –value	Prob.>F (p-value)
Model	9461.75	5	1892.35	43.86	< 0.0001
A	35.86	1	35.86	0.83	0.3922
B	5955.90	1	5955.90	138.04	*< 0.0001*
A^2	9.86	1	9.86	0.23	0.6472
B^2	3349.95	1	3349.95	77.64	*< 0.0001*
AB	3.78	1	3.78	0.088	0.7757
Residual	302.03	7	43.15		
Lack of fit	297.23	3	*99.08*	82.56	0.0005
Pure error	4.80	4	1.20		
Cor. Total	9763.78	12			

Table D.15:Optimization Design Summary for Chromium (VI) Ion on *Eucalpytus tereticornis* Composite (Barks and Leaves) Adsorbent

Name	Goal	Lower Limit	Upper Limit
Contact time (min)	Is in range	20	120
Adsorbent dose (g)	Is in range	1	9
Adsorption capacity (mg/g)	Maximize	6.0	100

Table D.16:Experimental and Predicted Values of Lead (II) Ion Adsorption on *Eucalpytus tereticornis* Composite (barks and Leaves) Adsorbent

Runs order	Experimental value	Predicted value
1	0.052	0.078
2	0.052	0.095
3	0.99	0.97
4	0.64	0.64
5	0.50	0.50
6	0.30	0.28
7	0.038	5.439E-003
8	0.99	1.01
9	0.30	0.35
10	0.27	0.35
11	0.43	0.35
12	0.45	0.35
13	0.30	0.35

Table D.17:ANOVA Results for a Quadratic Model for Lead (II) Ion Adsorption Using *Eucalpytus tereticornis* Composite (Barks and Leaves) Adsorbent

Source	Sum of square	DF	Mean square	F –value	Prob.>F (p-value)
Model	1.15	5	0.23	49.21	< 0.0001
A	0.050	1	0.050	10.63	*0.0138*
B	1.03	1	1.03	220.12	*< 0.0001*
A2	*2.606E-003*	1	*2.606E-003*	0.56	0.4802
B^2	0.041	1	0.041	8.65	*0.0217*
AB	0.030	1	0.030	6.50	*0.0381*
Residual	0.033	7	4.688E-003		*0.8369*
Lack of fit	*5.726E-003*	3	*5.726E-003*	0.28	
Pure error	0.027	4	*6.772E-003*		
Cor. total	1.19	12			

Table D.18:Optimization Design Summary for Lead (II) Ion Adsorption on *Eucalpytus tereticornis* Composite (Barks and Leaves) Adsorbent

Name	Goal	Lower Limit	Upper Limit
Contact time (min)	Is in range	20	120
Adsorbent dose (gram)	Is in range	1	9
Adsorption capacity(mg/g)	Maximize	0.0381679	0.990099

APPENDIX E

CHARACTERISTIC INFRARED ABSORPTION BANDS OF FUNCTIONAL GROUPS

Class of Compounds	Absorption, cm^{-1}	Intensity	Assignment
Alkanes and	2850-3000	s	C-H stretch
Alkyls	1450-1470	s	C-H bend
	1370-1390	m	CH_3 C-H bend
	1365 + 1395 (two bands)	m	$-CH(CH_3)_2$ or $-(CH_3)_3$ bend
	715-725	w	$-(CH_2)_n$ bend
Alkenes	3020-3140	w-m	=C-H stretch
	1640-1670	vw-m	C=C stretch
$RCH=CH_2$	910 + 990 (two bands)	m + s	=C-H bend
$RR'C=CH_2$	885-895	s	=C-H bend
cis-RCH=CHR'	665-730	m-s, broad	=C-H bend
trans-RCH=CHR'	960-980	s	=C-H bend
RCH=CR'R"	790-840	s	=C-H bend
Alkynes			
R-C≡C-H	3265-3335	s, sharp	≡C-H stretch
	2100-2140	m	C≡C stretch
	610-700	s, broad	≡C-H bend
R-C≡C-R'	2190-2260	vw-w	C≡C stretch
Alkyl halides			
R-F	1000-1350	vs	C-F stretch
R-Cl	750-850	s	C-Cl stretch
R-Br	500-680	s	C-Br stretch
R-I	200-500	s	C-I stretch
Alcohols	3300-3400	s, broad	O-H stretch
C=C-CH_2-OH	1035-1050	m-s	C-O stretch
R-CH_2-OH (1^o) or C=C-CH(R)-OH	1050-1085	m-s	C-O stretch
RR'CH-OH (2^o) or C=C-CRR'-OH	1085-1125	m-s	C-O stretch
RR'R"C-OH (3^o)	1125-1205	m-s	C-O stretch
Ar-O-H	1180-1260	m-s	C-O stretch
Ethers			
R-O-R'	1085-1150	s	C-O-C stretch
Ar-O-R	1020-1075 and 1200-1275 (two band)	m-s	=C-O-C sym. & asym. stretch
Aldehydes	2700-2725	m	H-C=O stretch
R-CH=O	1720-1740	s	C=O stretch
C=C-CH=O or Ar-CH=O	1685-1710	s	C=O stretch
Ketones			
RR'C=O	1710-1720	s	C=O stretch
C=C-C(O)-R	1665-1685	s	C=O stretch
Ar-C(O)-R	1675-1695	s	C=O stretch
four member cyclic	1770-1780	s	C=O stretch
five member cyclic	1740-1755	s	C=O stretch
six member cyclic	1710-1720	s	C=O stretch

Class of Compounds	Absorption, cm^{-1}	Intensity	Assignment
Carboxylic Acids	2500-3500	s, broad	O-H stretch
R-C(O)-OH	1710-1715	s, broad	C=O stretch
C=C-C(O)-OH or Ar-C(O)-OH	1680-1710	s	C=O stretch
Esters	aliphatic 1160-1210 acetates ~1240 aromatic 1250-1310	s-vs	O=C-O-C stretch
R-C(O)-O-R	1735-1750	s	C=O stretch
C=C-C(O)-O-R or Ar-C(O)-O-R	1715-1730	s	C=O stretch
R-C(O)-O-Ar	1760-1790	s	C=O stretch
Acyl Chlorides			
R-C(O)-Cl	1785-1815	s	C=O stretch
Ar-C(O)-Cl	1770-1800	s	C=O stretch
Anhydrides			
R-C(O)-O-C(O)-R	~1750 + ~1815	s,s	C=O symmetric
Ar-C(O)-O-C(O)-Ar	~1720 + ~1775 (both two bands)	s,s	& asym. stretch
Nitriles			
R-C≡N	2240-2260	m-s	C≡N stretch
C=C-C≡N or Ar-C≡N	2220-2240	s	C≡N stretch
Amines			
$R-NH_2$	~3400 + ~3500 (two bands)	w	N-H symmetric & asym. stretch
	1580-1650	w-m	N-H bend
RR'N-H	3310-33350	w	N-H stretch
Amides			
$R-C(O)-NH_2$	3200-3400 and 3400-3500 (two bands)	w-m	N-H symmetric & asym. stretch
	1650-1690	s, broad	C=O stretch
	1590-1655	m-s	N-H bend
R-C(O)-NH-R	3400-3500	w-m	N-H stretch
	1640-1690	s, broad	C=O stretch
	1510-1560	m-s	N-H bend
R-C(O)-NR'R"	1630-1680	m-s	C=O stretch
Nitro Compounds			
$R-NO_2$	~1550 and ~1370	s	N-O symmetric & asym. stretch
C=C-NO_2 or Ar-NO_2	~1525 and ~1335 (both two bands)	s	N-O symmetric & asym. stretch
Aromatic Compounds	3010-3100	m	Ar C-H stretch
	1450-1600 (two to four bands)	m-s sharp	ring C=C stretch
monosubstituted	730-770 and 690-710 (two bands)	s	C-H bend
		s	C-H bend
o-disubstituted	735-770	s	C-H bend
m-disubstituted	750-810 and 690-710	s	C-H bend
		s	C-H bend
p-disubstituted	810-840	s	C-H bend

Intensity abbreviations: vw = very weak, w = weak, m = medium, s = strong, vs = very strong